School of Physics, Engineering, and Technology

MSc Project Report

2022/2023

Student Name: Sinuo Feng

Project Title: Analysing the acoustics of a forest environment with an acoustic scale model

Supervisors: Dr Frank Stevens

Prof Andy Hunt

School of Physics, Engineering, and Technology

University of York

Heslington

York

YO10 5DD

Abstract

Trees are a key component of our surroundings, and hold great symbolic, ecological, and functional significance. This is particularly true where multiple trees comprise a forest environment, which human beings have interacted with and within for millennia. An understanding of the acoustic properties of these environments is of great importance to many fields, including noise propagation, soundscape evaluation, and sound design. There is existing literature focussing on different aspects of forest acoustics, but work remains to be done in developing a full understanding of how the different physical characteristics of a forest (the layout, numbers of trees, trunk diameters, bark material) combine and result in a particular acoustic. This report presents the results of a project making use of impulse response measurement in both a real forest, and in a scale model, to investigate these effects, particularly in the context of recent work simulating the acoustics of sparsely reflecting outdoor environments. Results from in situ and scale model forest impulse response measurements are presented and evaluated. These results allow for conclusion to be drawn regarding the effect of tree trunks on the acoustics of forest environments, the suitability of scale modelling as an approach to understanding these acoustics, and the validity of the approximation of tree trunks as rigid cylinders used.

"Nothing matters."

— Frank Stevens

Contents

List of Figures

List of Tables

Acknowledgements

I would like to thank all of those involved in this project work.

My greatest gratitude will go to Dr Frank Stevens for his trust in me for this project, and his sincere but poorly expressed encouragement. Thanks for all the discussion about the literature and the project work. Frank has managed to bear all of my weird ideas and sometimes my miserable thoughts throughout.

I would like to thank my second supervisor, Prof Andy Hunt, for his helpful advice during the project work, constant encouragement and enthusiasm when talking about my project.

To Mr Andrew Chadwick for all the discussion about the project and the help in MATLAB. Thanks for driving us to the forest three times and helping me build the forest scale model. The piece of installation art gave me a pleasing sense of happiness.

To Mr Richie Cully for finding that ideal forest and for all the help in the measurement work.

Chapter 1

Introduction

The aim of this project is to gain a better understanding of the acoustic properties of forest environments where tree trunks are particularly prominent, and to validate the method of modelling a forest environment using an acoustic scale model.

The majority of research on outdoor acoustics typically focusses on the problem of noise pollution caused by traffic in urban areas, and its impact on people's well-being [1]. It has been discovered that forests have an acoustic property of sound attenuation, and green infrastructure has been implemented to decrease noise levels in urban environments [2]. The form and layout of a forest and the scattering phenomena caused by trees are key factors influencing sound attenuation in a forest [3]. Previous research has mostly examined the acoustic properties of foliage, branches, or trees as a whole, with little attention addressed to the role of tree trunks. However, a review of existing literature suggests that tree trunks have a substantial role in mid-frequency sound propagation, with the diameter of tree trunks having a major impact on the acoustic properties of forests [4]. Therefore, studying the impact of layout among tree trunks can provide a more comprehensive understanding of the acoustic properties within forest environments.

Furthermore, previous developments have been made in the field of modelling forest acoustics. To examine reverberation in forest environments, Spratt and Abel developed a *Treeverb* algorithm that models the tree trunk as a rigid cylinder to simulate the scattering of sound waves among

trees [5]. Additionally, Stevens et al. introduced the *Waveguide Web* (*WGW*) algorithm for modelling the acoustics of outdoor environments with sparse reflections. This algorithm combines the approach proposed by Spratt and Abel with a further *Scattering Delay Network* (*SDN*) reverberator to improve the simulation accuracy [1]. These approaches have significantly contributed to understanding the acoustic properties of tree trunks in forest environments. However, it is required to carry out tests in real forest environments to validate this modelling method.

Acoustic scale modelling has been used in the acoustic design of concert halls and opera theatres [6]. A three-dimensional scale model allows for predicting the acoustic properties of the full-scale space as it captures complex waves such as reflections and diffusion [7]. The acoustic model primarily focusses on the sound absorption of halls within a reverberation chamber [8]. This modelling method has also been used to investigate sound propagation of outdoor environments within an anechoic chamber, such as Stonehenge [9]. The existing literature on modelling an outdoor space using a scale model remains limited, so it is required to examine the validity and effectiveness of this modelling method by comparing the scale model with a real world outdoor space. This research aims to evaluate this research question using a forest scale model.

1.1 Research questions

The following research questions encapsulate the aim of the work:

1. What are the acoustic properties of tree trunks in a forest environment?
2. Is an acoustic scale model a good approach to studying forest acoustics?
3. Are the assumptions made in the *Treeverb* and *WGW* valid?

This thesis will address these research questions in Chapter 7.

1.2 Structure of the thesis

Chapter 2 presents a review of academic literature in areas relevant to the project work. Section 2.1 covers acoustic impulse responses, and the measurement method used in the project. Section 2.2 presents a review of previous studies conducted in forest acoustics. Section 2.3 reviews the work in modelling forest acoustics, which provides the modelling method for this project. Section 2.4 reviews acoustic scale modelling methods. The completion of this literature review then allows for a clear definition of project objectives.

Chapter 3 documents the impulse response (IR) measurement conducted in the forest environment, including the details of the site and the recording process. The measurement and analysis of sound attenuation in a forest and an open field are then presented.

Chapter 4 contains the forest IR analysis. This is presented by the analysis of each IR, including time and frequency feature analysis, the calculation of ISO 3382 acoustic parameters, SIRR analysis and auralisation. The IRs are then compared with one another. These results allow for the investigation of the acoustic characteristics of a forest environment.

Chapter 5 documents the IR measurement work conducted in the acoustic scale model. It covers the design of the scale model, including: the scale factor, materials used, recording space, and subsequent construction of the model. The scale model IR recording process is then presented.

Chapter 6 presents the scale model IR analysis. This consists of the same analysis as in Chapter 4, baring the SIRR analysis and auralisation. This chapter also covers the comparisons with the results from the *WGW* and from the Stonehenge scale model. It concludes with a comparison of the scale model IRs with the real world forest IR.

Chapter 7 concludes the report with a summary of the project work, and the extent to which the research questions have been answered. It concludes a list of the contributions of this work to the field. The chapter then further with a description of future work, an evaluation of the project management, and a personal reflection.

Chapter 2

Background Theory

This Chapter presents a review of the literature covering various topics relevant to this project. In Section 2.1, acoustic impulse response will be covered, this can provide an understanding of room acoustics. Section 2.2 will present different characteristics of forest acoustics. In Section 2.3, relevant modelling forest acoustics methods will be covered, with a focus on the key element of tree trunks in a forest environment. The acoustic scale model will be explained in Section 2.4, providing the methodology of this modelling method.

2.1 Acoustics

Acoustics is the science of sound, considering the behaviour of sound waves including: refraction, absorption, reflection, diffraction and scattering [10]. Within the field of acoustics, room acoustics is the study of the behaviour of sound in indoor spaces.

In this section, a brief overview of room acoustics will be presented. This will be achieved through the study of acoustic impulse responses, their measurement, and their analysis.

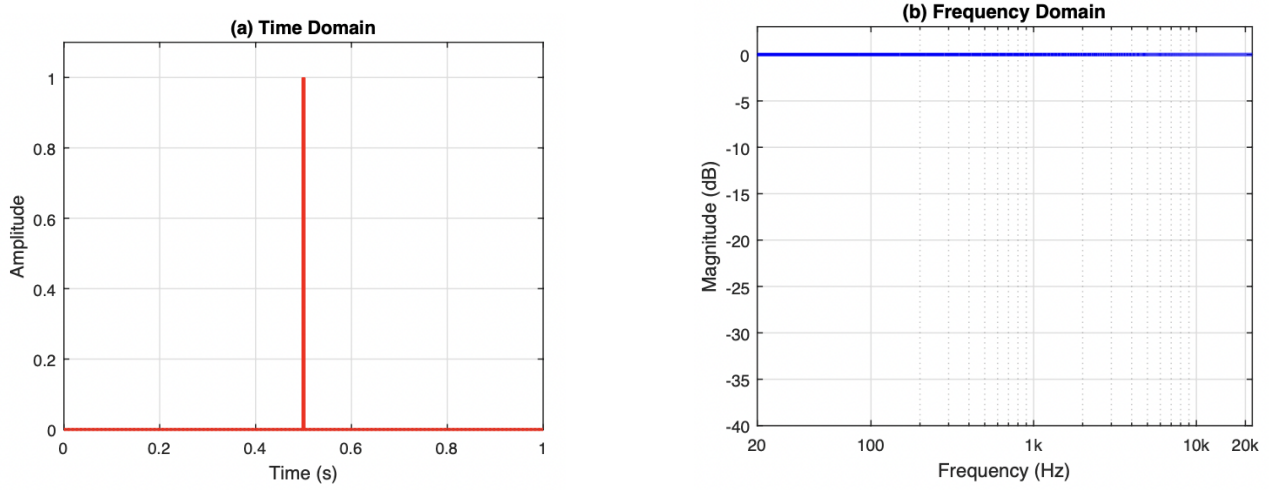

(A) Unit impulse in time domain (B) Unit impulse in frequency domain

FIGURE 2.1: Unit impulse plots in time and frequency domains. From [12].

2.1.1 Acoustic impulse responses

An impulse response (IR) is an *acoustic fingerprint* of a space, it can be used to analyse the acoustic characteristics of a space, such as reverberation [3]. As the name suggests, IR captures the way in which a room responds to an impulse. An impulse is defined as a δ-function:

$$\delta(t) = \begin{cases} \infty, t = 0 \\ 0, t \neq 0 \end{cases} \tag{2.1}$$

where t is time, Eq. 2.1 illustrates an infinitely short impulse with an infinitely large amplitude. Fig. 2.1 shows the unit impulse plots in the time and frequency domains, demonstrating the impulse has a unit amplitude at 0.5 s. The impulse shows an excitation in the time domain and a flat magnitude across frequency in the spectrum. This perfect impulse is desired in IR measurement because this can excite the room equally in the whole frequency range [11]. Although it is difficult to reproduce this impulse perfectly, it can be approximated with impulsive sounds (e.g. a start pistol), or alternative methods (e.g. sine weep methods). These methods will be covered in Section 2.1.3 in detail.

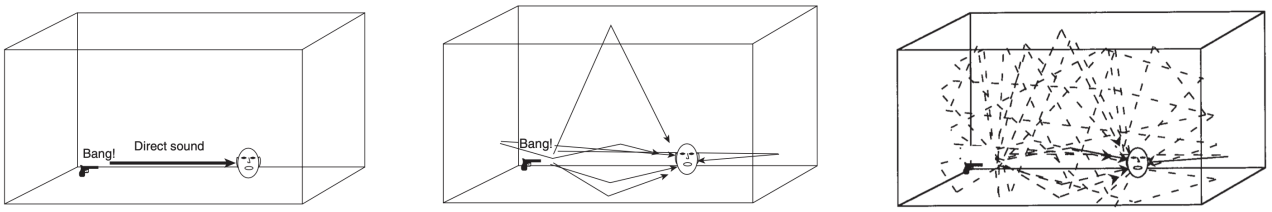

(A) Direct sound (B) Early reflection (C) Reverberation

FIGURE 2.2: Sound behaviour in response to a starter pistol in an idealised room. From [13].

An impulse response can be conceptualised in three stages, as shown in Fig. 2.2. Here, a gunshot represents an impulse, which emits sound into the space. There is a direct path between the source and the receiver, followed by distinct early reflections by the surfaces [13]. The sound waves then continue to move around the space, resulting in multiple low-level and interfering reflections that are no longer distinct echoes. This is known as reverberation. Fig. 2.3 shows a representation of the IR signal at the receiver.

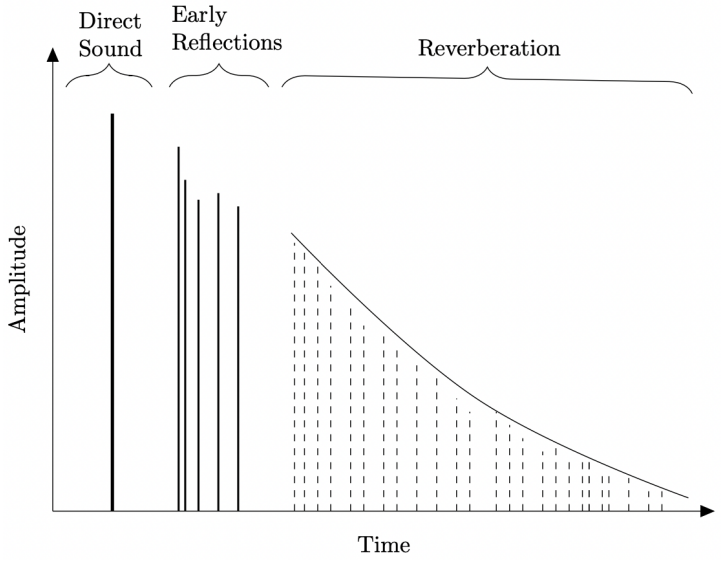

FIGURE 2.3: Impulse response in a time domain plot. From [12].

2.1.2 Sound absorption coefficient

When the sound waves interact with the surface, some energy is reflected, and some is absorbed. The acoustic absorption properties of the surface materials can be defined as the sound absorption coefficient α. The value of α represents the proportion of the sound energy at different frequency octave bands being absorbed by the incident wave, which is between 0 to 1 [12]. The α equals

1 correlates to sound energy being absorbed, which can be understood as sound lost through an idealised open window. While α equals 0 correlates to sound energy being all reflected. The α value is influenced by different factors, including the thickness of the material and its porousness.

2.1.3 Impulse response measurement

There are two types of methods for impulse response measurements, including impulsive methods and signal processing methods.

Impulsive methods have been used balloon pops and starter pistols as an impulse to excite the room [14–16]. These methods are not repeatable, the acoustic properties of these impulses would have an impact on the results, and affect the analysis of measured space. However, a previous study has indicated that the use of a starter pistol is potentially useful for measurement, especially in outdoor environments [17].

There are signal processing methods for impulse response measurement, including maximum length sequence (MLS) and sine sweep methods. MLS reproduces every binary sequence that can be generated by the shift registers, which can produce a flat frequency spectrum and have good correlation properties [18]. A time aliasing error may occur in this measurement method due to the continuous repetition of the signal and a circular deconvolution process [19]. The linear sine sweep (LSS) method utilises a continuous sine wave signal that sweeps linearly across a specified frequency range. The generated impulse response is obtained by convolution of the measured signal with the inverse filter. This method is sensitive to distortion introduced by loudspeakers, and pulsive noise during recording [20].

The exponential sine sweep (ESS) method utilises a continuous sine wave signal that sweeps logarithmically across a specified frequency range typically ranging from 20 Hz to 20 kHz. The ESS equation is given by:

$$s(t) = \sin\left[\frac{w_1 \cdot T}{\ln(\frac{w_2}{w_1})} \cdot \left(e^{\frac{t}{T} \cdot \ln(\frac{w_2}{w_1})} - 1\right)\right] \tag{2.2}$$

where T is the length of the sweep, w_1 is the start of the frequency, and w_2 is the end of the frequency. The use of the linear deconvolution technique, instead of the circular one, is based on convolution in the time domain using an inverse filter, which allows for the removal of harmonic distortion products [19, 20]. This method provides increased low-frequency energy, hence, an envelope was applied in the inverse filter to reduce the amplitude for compensating. This can provide a better signal-to-noise ratio at low frequencies than the LSS method. Similar to the LSS method, the ESS method is sensitive to abrupt impulsive noise during the recording, which results in the reverse IR.

It's desirable to use an omnidirectional source in the measurement according to ISO 3382, which can excite the space equally in all directions [11]. Although an omnidirectional source is expensive, an alternative method is to rotate the source to approximate this directivity, which will be discussed in Section 2.2. Additionally, an omnidirectional receiver is also desirable for the measurement.

2.1.4 Impulse response analysis

An IR can capture the behaviour of sound in space (i.e. the effect that the surfaces, shape, and geometry of the space have on the sound produced in that space). These IRs can be used for auralisation, where convolution can be used to place a sound source virtually in the IR recording space. They can also be analysed to derive acoustic parameter values.

The analysis of IR can use ISO 3382 to gain room acoustic parameters, for which an energy decay curve (Schroeder curve) must be calculated [11]. The decay curve equation is given by:

$$E(t) = \int_{\infty}^{t} p^2(\tau) d(-\tau) \tag{2.3}$$

where p is the sound pressure, and E is the energy across time. This is derived from reverse-time integrated squared impulse response, representing the sound pressure level (SPL) as a function of time after the sound source stops graphically [11].

Several acoustic parameters are defined in ISO 3382 for acoustic analysis, such as early decay time (EDT), clarity, and definition. Additionally, the IRs should be filtered into octave bands to obtain acoustic parameters for different frequency ranges.

The Schroeder curve was developed for the calculation of reverberation time (RT_{60}). This can be estimated from T30, which can be extrapolated from the linear regression of the energy decay curve between -5 dB and -35 dB at -60 dB point [11]. The source level has to provide 45 dB above the background level for the T30 value measurement. T20 measurement evaluates the range from -5 dB to -25 dB, and the required source level is at least 35 dB above the background level.

Similarly, the EDT parameter can be extrapolated from the linear regression of the energy decay curve from the first 10 dB at the -60 dB point. EDT has been shown as a more comprehensive perceived reverberation parameter compared to T30, as it takes into account the initial section of IRs.

Definition (D50) is a measure of speech intelligibility, defined by the early-to-total energy ratio, where the early time considers the first 50 ms. D50 is expressed in percentage and the calculation is given in Eq. 2.4.

$$D50 = \frac{\int_0^{0.05} p^2(t)dt}{\int_0^{\infty} p^2(t)dt} \tag{2.4}$$

2.1.5 Spatial analysis

B-format recordings have four channels (W, X, Y and Z), which capture the directional information. This can be used to investigate the spatial characteristics of an impulse response, by calculating the instantaneous intensity vector, **I** [21]. The B-format signals are divided into discrete time frames, and then a short-time Fourier transform (STFT) is performed on each channel of the recordings. The **I** vector can then be estimated in the resultant frequency domain signals using:

$$\mathbf{I}(\omega) = \frac{\sqrt{2}}{Z_0}\Re\{W^*(\omega)U(\omega)\} \tag{2.5}$$

where U(ω) is vector [X(ω), Y(ω), Z(ω)], Z_0 is the characteristic acoustic impedance of air, and * denotes the complex conjugate [3]. The calculation of **I** is part of the analysis method used in Spatial Impulse Response Rendering (SIRR) [22]. Fig. 2.4 shows an example of the SIRR analysis plot of a forest environment, where each arrow is a time-frequency distribution of **I** vector. The arrow pointing at the right corresponds to the direct sound from the source to the receiver, and the arrow pointing up corresponds to the sound coming from the right of the receiver, respectively. It can be observed that the **I** vector is overlaid on a spectrogram of the W-channel recording, this allows the concurrent analysis of the magnitude and direction of arriving acoustic energy [21].

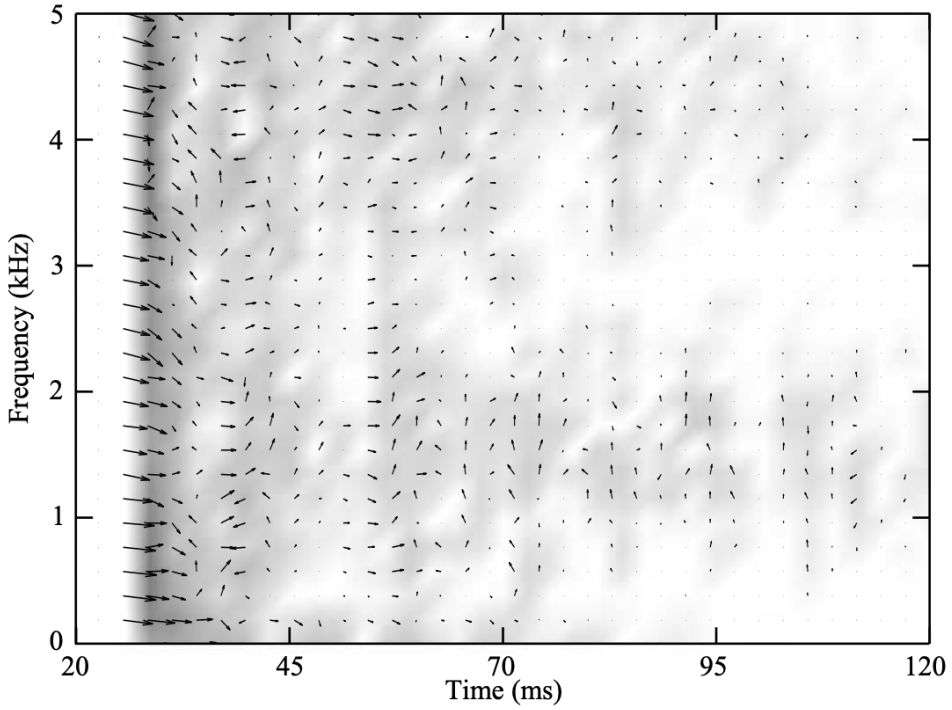

FIGURE 2.4: An example of SIRR analysis plot of a forest environment in Koli National Park. From [21].

2.1.6 Summary

This section evaluates the acoustic IR measurement and IR analysis. By evaluating the acoustic properties captured in the IRs, the acoustic characteristics of a space can be studied. Section 2.2 will review the studies of the acoustic properties of a forest, and investigate how different factors in a forest will affect the behaviour of sound.

2.2 Forest Acoustics

In this section, a review of relevant literature in forest acoustics will be presented, which will examine the main factors that affect sound propagation in a forest environment, such as a forest layout, scattering among the trees, tree bark sound absorption, ground effects [4]. By evaluating these factors, a better understanding of the acoustic properties of a forest, including noise reduction capabilities and reverberation properties, can be attained.

2.2.1 Impulse response measurement in a forest environment

A B-format impulse response measurement was using a B-format microphone and a single speaker conducted in the forest at Koli National Park in Finland [3]. The height of the recording equipment was 1.5 m from the ground and the source used was a 30 s exponential sine sweep, with the frequency ranging from 22 Hz to 20 kHz. This process was repeated four times with the loudspeaker pointing at four different orientations. Fig. 2.5 shows the source orientation in the measurement. The measurement at 0° was defined where the source directly pointed at the receiver, then each time rotated the source 90° to approximate an omnidirectional point source in the horizontal plane. The omnidirectional IR was generated by summing the IRs of four angles. Fig. 2.6 shows the IR results at 0° (upper plot) and summing IR results (lower plot), where the summing results show a greater amplitude as it boosted the reverberated sound. As introduced in Section 2.1, ISO 3382 is the standard for indoor measurement. However, considering the principle of the IR measurement and the reverberation would be of interest, ISO 3382 was used in the analysis. The analysis of this forest will be introduced in Section 2.2.3.

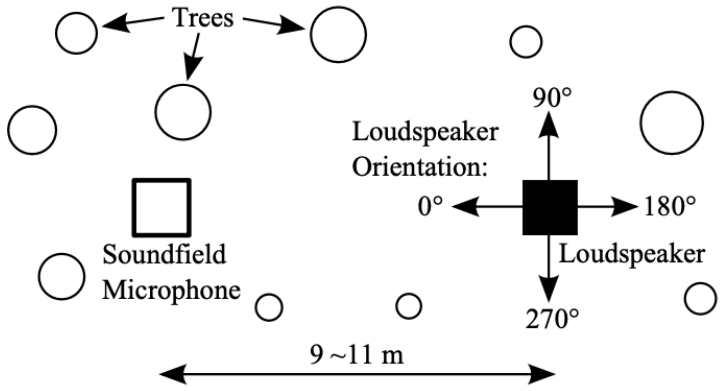

FIGURE 2.5: The equipment for the Koli forest IR measurement, showing the four speaker source orientations. From [3].

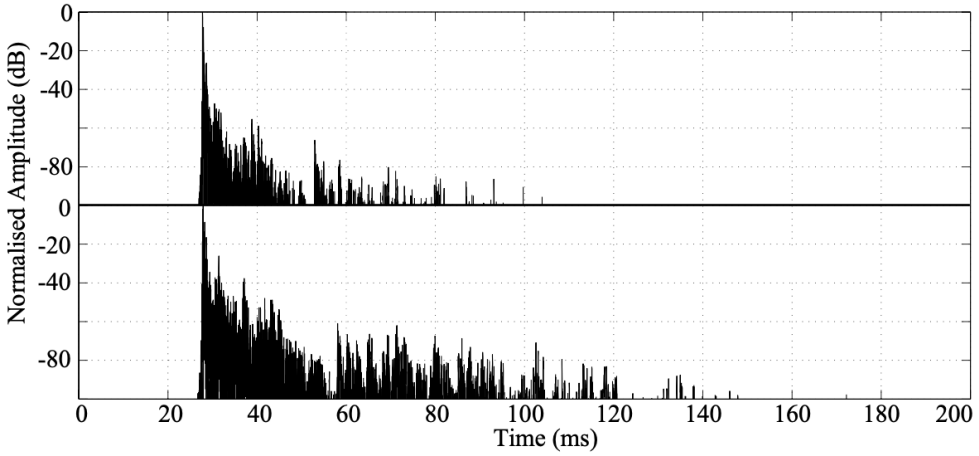

FIGURE 2.6: IR measured in Koli forest. The upper plot shows the IR recorded with source directly pointing at the receiver; The lower plot shows the summing IR of four source orientations. From [3].

It's noted that there are very few impulse response measurements conducted in forest environments, but that there is a wealth of research about the acoustics of the forests.

2.2.2 Form and layout in a forest

Sound attenuation by vegetation has been investigated since at least 1946, when Eyring investigated the acoustic properties of a Panamanian jungle [23]. It has been proposed trees can be used as noise barriers near sources such as highways and railroad tracks [24, 25]. The form and layout of a forest have been indicated as important properties in determining the

sound attenuation [26, 27]. To investigate these properties, a study was conducted to assess the impact of visibility, width, height, and length in 35 evergreen tree belts [2].

To simulate a noise source condition, the measurement was conducted with the source placed 1 m outside the tree belt and the source was edited traffic noise [2]. The excess attenuation of each site was attained by comparing the difference in sound level between the tree belt and the open ground [28]. Fig. A.1 shows the positions that were measured in a tree belt. Additionally, the width and length of a tree belt were determined in Fig. A.1a, and the height of the tree belt was determined in Fig. A.1b. The visibility represents the property of the density of the tree belts, where the lower the visibility, the higher the density.

The results indicated a negative association between relative attenuation and visibility, whereas a positive association was found with the width, length, and height of the tree belts [2]. The sequence of the importance of the factors is visibility, width, height and length, where visibility and width have a relatively greater impact than the others.

Low visibility can result in great noise attenuation due to the sound energy reduction and scattering effects by branches and foliage [25]. Additionally, shrubs were found to have the greatest noise reduction of all the tree belts. Width corresponds to the distance between the source and receiver. A wider tree belt allows for more possible acoustic pathways among trees, resulting in increased absorption and diffusion [26]. Additionally, a longer tree belt can result in greater disturbance of acoustic waves, indicating increased diffraction. Trees with greater height can provide a larger surface area for the diffusion and absorption of sound waves [29].

The visibility, width, height and length correspond to the layout and form of a tree belt, which significantly contributes to sound attenuation. This is related to the interaction of various acoustic phenomena in a forest environment, such as diffraction, diffusion and absorption by trees.

2.2.3 Scattering among trees

The effect of sound propagation in a forest environment is highly frequency dependent [30]. A study of the sound attenuation at frequency octave bands in a forest was conducted by

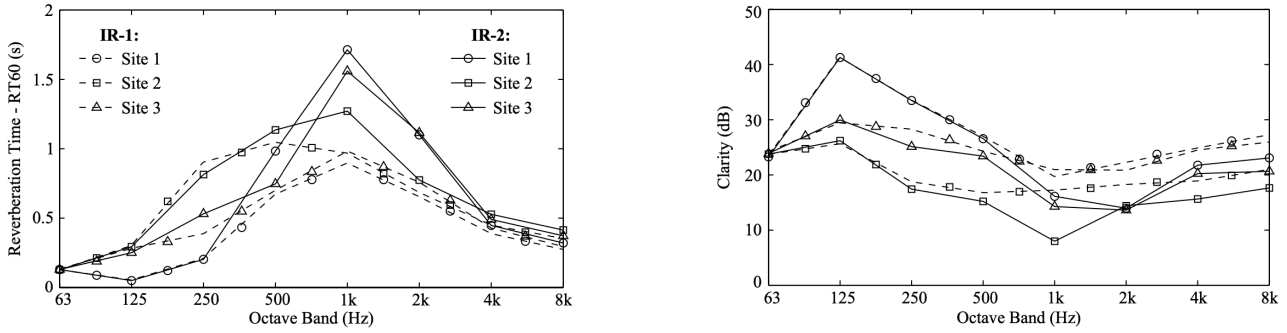

(A) Reverberation Time (T30) (B) Clarity (C50)

FIGURE 2.7: Acoustic parameters calculated for the Koli forest IRs from octave bands 63 Hz to 8 kHz. From [3].

comparing it with the open ground [27]. The results show that the difference in the attenuation of both environments in a frequency range between 1 and 2 kHz is relatively small. This indicates that the vegetation has little effect on sound propagation in this frequency range which may be due to scattering by the trees. A similar reduction in attenuation was also observed in Kragh's study, indicating that vegetation has minimal impact on sound attenuation between frequencies 500 Hz and 2 kHz [31].

As mentioned in Section 2.2.1, a B-Format acoustic impulse response (IR) measurement was conducted in a forest [3]. The analysis of the acoustic parameters, including reverberation time (T30) and clarity (C50), has indicated reverberation in a forest environment. Fig. 2.7 shows the T30 and C50 values obtained from IRs at the sites.

It's indicated that the reverberation time and clarity in three sites with different densities and diameters have similar frequency dependent properties [3]. In Fig. 2.7a, it can be observed that the reverberant time is mostly concentrated around the 1 kHz octave band, which is between 1.3 s and 1.7 s. This range of reverberation time is similar to that of a concert hall [32]. Additionally, T30 is relatively low in other octave bands, which matches the results that sound attenuation in a forest is predominantly present outside the mid-frequency range. In Fig. 2.7b, C50 values indicate a high ratio between the early and late energy, which indicates good speech intelligibility. The lowest C50 can be observed at the 1 kHz octave band, suggesting relatively greater late energy is suggested in the forest.

The distinctive reverberant sound energy at mid-frequency indicates the scattering mainly

by tree trunks, as it relates to the diameter of the tree trunks which ranges from 0.1 m to 0.6 m [3]. Chobeau determined that the scattering due to tree trunks is dependent on trunk apparent diameter and the relationship between the diameter and the frequency present in the incident sound [4]. Generally, the diameters of the tree trunk scatter frequency of sound with wavelengths equal to or smaller than the diameter of the tree trunk [30].

Previous studies have also indicated that tree trunk is the key factor in sound scattering above 1 kHz in a forest environment [28, 30, 33, 34]. A similar reverberation time of 1.5 s at a frequency range above 1 kHz was observed in a bamboo forest [33]. In this environment, the tree trunks would act as a main factor in sound propagation because the bamboo has a rigid surface, and hollow tube structure and is mostly uniform in diameter (about 0.13 m). Additionally, Padgham conducted a modelling forest acoustics work and analysed simulated decay curves to assess reverberation time [34]. Forests with smaller tree trunk diameters were found to have a higher reverberation time than forests with the same trunk locations but with larger tree trunk diameters.

A study has been conducted to evaluate the scattering effect in the branches and foliage [16]. It's found that branch is a larger factor in sound scattering by trees compared to foliage. The branches with a larger size can produce greater sound scattering as they can provide longer acoustic path lengths. The study indicates the foliage scatter sound at higher frequencies, which is typically above 4 kHz [16].

The interaction of sound waves with branches, foliage and tree trunks caused scattering and absorption in a forest environment. Consequently, acoustic waves propagating at certain frequency bands could cause an increase in reverberation time due to multiple reflections [4]. Additionally, sound scattering through these elements could result in various possible acoustic pathways, and the effects lead to sound attenuation in a forest environment.

2.2.4 Sound absorption by tree bark

It's also indicated that the absorption of the tree trunks has an impact on the sound propagation in a forest [35]. However, it is worth mentioning that only a limited number of studies have

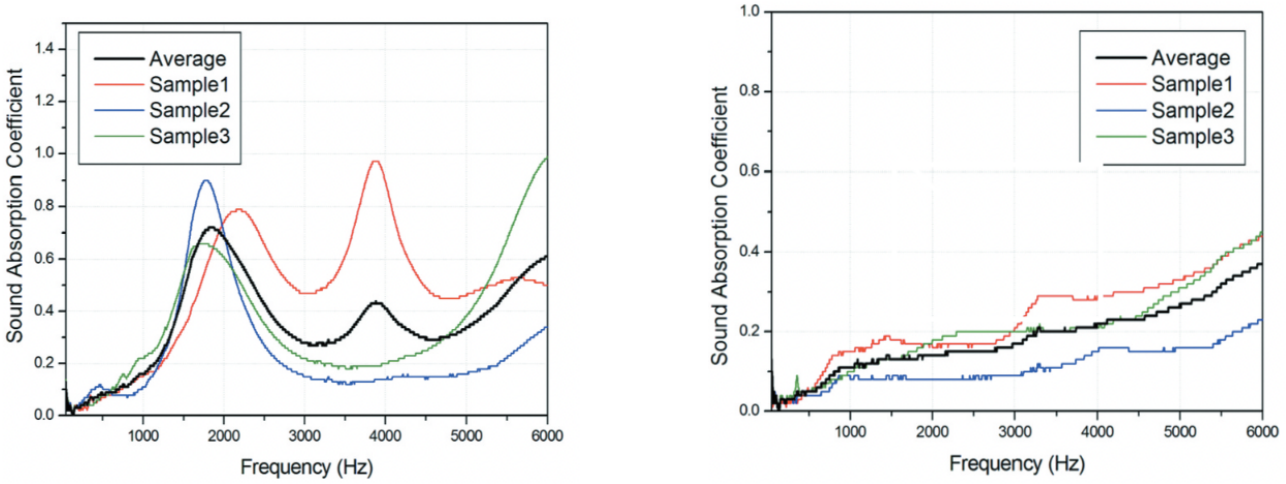

(A) SACs of *stone pine*

(B) SACs of *maritime pine*

FIGURE 2.8: Sound absorption coefficient from 50 Hz to 6 kHz of two coniferous species. Each species was measured with three samples, whose SACs are labelled as *Sample*, and the average SACs of these results are labelled as *Average*. From [38].

investigated the specific sound absorption properties of tree trunks. Li et al. accessed the sound absorption coefficient (SAC) of the tree bark, where tree bark can be defined as the tissues of the stems that are outside of the cambium cell layer [36]. The results indicate that bark is the dominant factor in the sound absorption of a tree trunk. The SACs for the measured tree trunk were generally lower than 0.1 below 1.6 kHz, which aligns with the findings found in Reethof's study [37]. Additionally, the roughness of the tree bark has an impact on sound absorption. The moss grown barks would have higher SACs due to the relatively soft surface of the moss compared to the bark itself.

A study measured the SACs on deciduous and coniferous species in the frequency range of between 50 Hz and 6 kHz using an impedance tube [38]. Fig. 2.8 shows the results of SACs of two coniferous species. Each species was measured with three samples, whose SACs are labelled as *Sample* in Fig. 2.8, and the average SACs of these results are labelled as *Average*. It's interesting to note that even trees of the same species can have varying sound absorption properties. It can be observed that each species shows different SACs at different frequency ranges. For stone pine, the average SAC at around 2 kHz reaches 0.7, which indicates a relatively good sound absorption property. For maritime pine, the average SACs can be observed an increase with increasing frequency. Additionally, the study indicates that the sound absorption by tree bark correlates to the tree species, trunk diameter, bark shape and fibrous structure.

2.2.5 Ground interference

It appears that the interference of the ground can affect the sound attenuation. Ground interference can be determined by the interference between the direct and ground reflected sound [27]. The interference from the ground can be constructive and destructive, it depends on the path length difference between the direct and reflected sound, the impedance of the ground and the coherence of the direct and reflected sound [27]. It's indicated that if the forest floor is acoustically soft, sound attenuation may occur at low frequencies due to deconstructive interference [30]. If the forest floor is acoustically hard, sound energy may be increased due to constructive interference. The coherence of the path corresponds to the plantation between the direct and reflected sound, in the case of the presence of vegetation, interference would be disrupted as the sound waves may diffuse. It's indicated that ground interference affects sound propagation between direct sound and reflected sound mainly below 500 Hz, where the impact of sound scattering from trees remains relatively insignificant [16, 27, 28, 33].

2.2.6 Atmospheric effects

Atmospheric effects such as humidity, wind and temperature can have an impact on sound propagation in a forest environment. Humidity and temperature can affect air absorption. It's indicated that air absorption would have a greater impact on a higher frequency range [27, 39]. Wind can cause turbulence and generate fluctuations in air pressure. These fluctuations can interfere with the propagation of sound waves, leading to sound diffusion. Additionally, wind conditions in a forest environment can cause background noise and leaves rustling [16]. It's indicated that these atmospheric gradients are negligible in a forest environment, however, for a longer distance, these elements should be taken into consideration in sound attenuation [4].

2.2.7 Summary

This section has presented a review of the previous work in forest acoustic, examining the noise reduction property in a forest environment. It's indicated that the scattering among trees,

sound absorption by trees and ground interference affect sound propagation within the forest [27]. The ground interference effect depends on the ground impedance and source and receiver position, which appear to have a greater impact at low frequencies [16]. Scattering by trees including trunks, branches and foliage attributes to sound attenuation at higher frequencies [28]. However, in the mid-frequency range, the influence of vegetation on sound attenuation appears to be relatively minor [31]. The studies have also indicated reverberation in this frequency range, with tree trunk playing a crucial role in scattering due to their diameter seen by the acoustic waves [3]. Additionally, the layout and form of a forest have a significant impact on sound propagation, relating to factors such as tree distribution, density, and spatial arrangement [2].

These research findings provide an insight into the acoustic in the forest environment. However, research specifically focusing on the acoustic properties of tree trunks in forest environments remains limited. Additionally, computer simulations and modelling methods have been employed to investigate the acoustic properties of tree trunks and will be introduced in the next section.

2.3 Modelling Forest Acoustics

As discussed in Section 2.2, tree trunks are the key factors in mid-frequency sound attenuation in forest environments. Previous studies in modelling forest acoustics have addressed this property and have adopted the approach of modelling tree trunks as rigid cylinders which will be reviewed in this section.

2.3.1 Treeverb digital reverberator

Treeverb is a digital reverberator, an algorithm used to simulate acoustic reverberation in a forest environment. It was designed to model the scattering of acoustic waves among trees in an idealised forest for implementation of the designed model [5].

As discussed in Section 2.2, branches and foliage scatter sparsely the high frequencies, whereas the sound scattering caused by tree trunks is of interest. Hence, trees are simplified as tree

trunks that have no branches and foliage. Additionally, the modelled tree trunk is characterised by its diameter and surface impedance [40]. Due to its shape and characteristics of being acoustically hard, in this *Treeverb* model, trees are modelled as rigid cylinders and the surface of the cylinders absorbs no energy [5].

Another assumption made in the *Treeverb* model is the absence of ground within the idealized forest [5]. Additionally, the locations of the source, receiver and trees are on one plane, which can be interpreted to be 2.5-dimensional geometry, taking into account the presence of ground reflections [1]. Fig. A.2 shows the forest layout which was simulated in this study. This forest consists of 25 trees, each with a radii of 0.5 m, and randomly spaced 6 m apart from one another.

In this study, a digital waveguide network was introduced to simulate sound propagation. The network structure consists of interconnected delay lines and nodes. As the modelled forest is considered as a two-dimensional geometry, the network establishes the connected paths between each node, source, and receiver. Each delay line within the network represents a connected path and incorporates time delays and spreading loss. Each node represents a tree that is modelled as a rigid cylinder [1]. Fig. 2.9 shows a simple example of the waveguide network, where T1, T2, and T3 are the interconnected tree-nodes, S is the source and R is the receiver. The source and receiver are connected to the tree-nodes with unidirectional delay lines. The tree-nodes are connected with bidirectional delay lines, which represent the sound wave incidents on a tree-node that can propagate to other tree-nodes or a receiver, or reflect back along the path of the incident wave.

As the trees are assumed to be spaced far enough from other trees, the sound wave that encounters a tree can be considered as a plane wave [5]. Based on this approximation, Morse's solution to the acoustic scattering of a plane wave incident on a rigid cylinder was implemented at each tree-node [41]. With this solution, the scattering occurring at each tree takes place in a frequency dependent manner. When a plane wave encounters a rigid cylinder, it results in two arrivals that are separated by a delay. Fig. 2.10 shows the incident wave encounters with a modelled tree trunk, T, and θ represents the interested angle of the scattered wave. The resulting waves transmit around two paths, which in this example, are D1 (clockwise) and D2 (anticlockwise) [1].

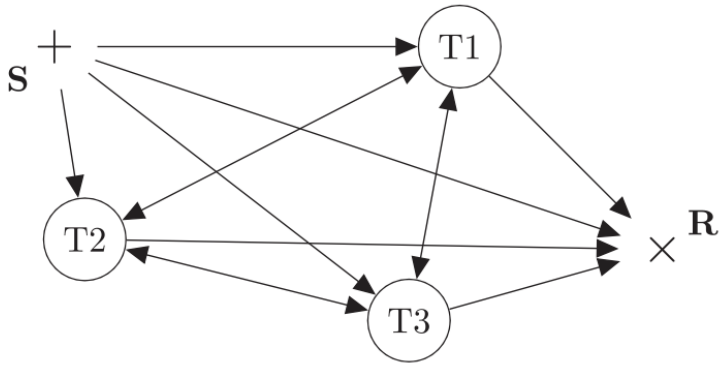

FIGURE 2.9: An example of *Treeverb* waveguide network for modelling forest acoustics. It consists of three tree-nodes, T1, T2, T3, and a source, S, and a receiver, R. The source and receiver are connected to the tree-nodes with unidirectional delay lines. The tree-nodes are connected with bidirectional delay lines. Each delay line within the network represents a connected path and incorporates time delays and spreading loss. Each node represents a tree that is modelled as a rigid cylinder. From [1].

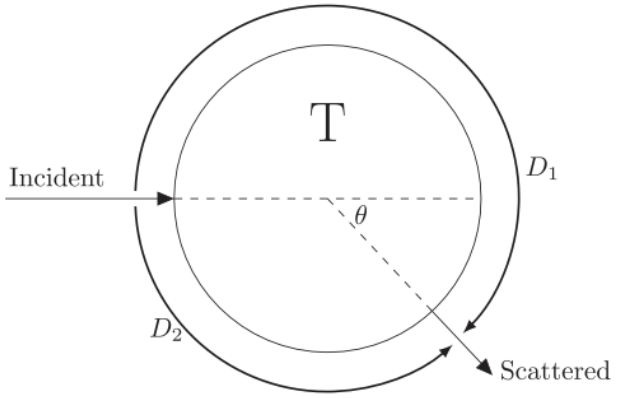

FIGURE 2.10: Incident wave encounters a tree trunk, T, modelled as a rigid cylinder. The resultant scattered wave around the tree at angle θ is formed by two paths, D_1 and D_2. From [1].

For a shorter path, the scattering wave has a high-pass characteristic for all scattering angles. For a longer path, the scattering wave has a high-pass characteristic for smaller scattering angles and a low-pass characteristic for larger scattering angles [5]. Therefore, a digital scattering filter model using low-order IIR filters was designed. Fig. 2.11 shows the filter design in the block diagram of tree-node scattering. $z^{-\tau_\theta}$ represents the sample delay between the two paths, α_1(z) represents the filtering action related to the shorter path and α_2(z) represents the filtering related to the longer path [1].

In summary, *Treeverb* reverberator enables selecting the position of the source, receiver, and

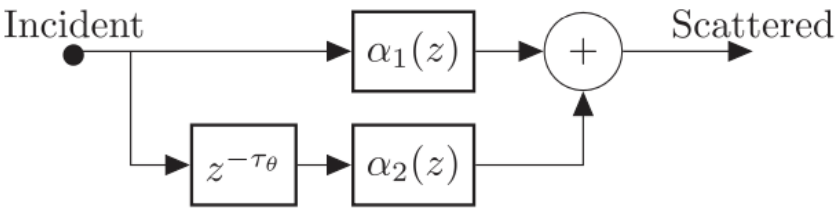

FIGURE 2.11: The filter design in the block diagram of tree-node scattering. From [1].

trees, while using waveguide delay lines to compute sound propagation loss. Morse's solution and the digital scattering filter model are implemented at the tree-nodes to approximate tree trunk scattering. However, when simulating multiple trees using this waveguide model, the computational time increases significantly [5]. To address this, an alternative image-source method was implemented. By using this method, a simulated impulse response was generated using a forest layout, as shown in Fig. A.2. The result of the impulse response is shown in Fig. 2.12.

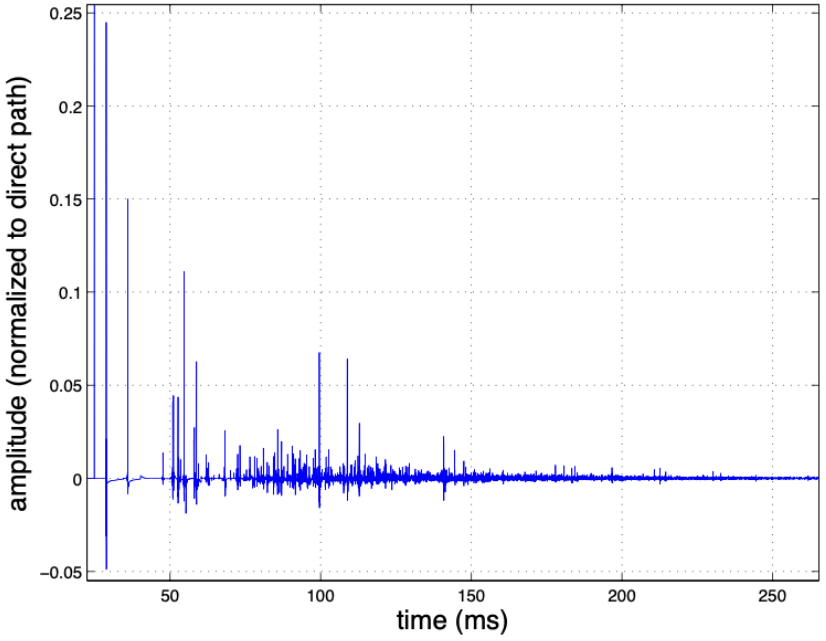

FIGURE 2.12: Simulated impulse response of a forest environment using *Treeverb* reverberator. The forest layout is shown in Fig. A.2. From [5].

Fig. 2.12 indicates that the impulse response from a forest environment is fairly sparse in the early reflections although the higher-order scatterings also show relatively high amplitude around 100 ms [5]. The image-source implementation provides a more efficient computation

and a relatively sparse impulse response result in the *Treeverb* study, whilst it's a good attempt of introducing the waveguide method.

2.3.2 Waveguide Web digital reverberator

Waveguide Web (*WGW*) is a digital reverberator designed for modelling the acoustics of outdoor environments with sparse reflections. It's a waveguide method that is an extension of the *scattering delay network* (*SDN*) reverberator which enables accurate simulation of first-order reflections. The network structure of the *WGW* is similar to the *SDN*, using delay lines and interconnected nodes to model space. Whilst, the *WGW* developed the simulation that allows precise attenuation of second-order reflections by implementing directionally dependent filtering at each node [1]. Hence, Morse's solution and the scattering filter model can be implemented to simulate forest acoustics, which is also an extension of *Treeverb* using the proposed waveguide method.

The *WGW* algorithm, similar to the *Treeverb* reverberator, incorporates first-order Infinite Impulse Response (IIR) filters to approximate the scattering characteristic around the cylinders of both paths at different angles [1]. Fig. 2.13 shows comparison plots between the simulated impulse responses obtained from Morse's solution and the *WGW* algorithm in the time and frequency domains, with a condition of radius equal to 0.2 m and a reflection angle of 60°. *WGW* approach demonstrates a relatively good match between the *WGW* approach and Morse's solution at high frequencies, while some discrepancies appear below 100 Hz in the spectrum. Additionally, the time domain plot shows two scattered wave impulse responses separated by delay with amplitude difference which also agrees well with the result obtained from Morse's solution. To improve the accuracy of this IIR filter, the development of the *WGW* method, which incorporates generating filter coefficients from Morse's solution for the frequency dependent scattering nodes, was examined in Brooks-Park's study [42].

WGW further evaluates the generated IR results with the *Treeverb* reverberator by comparing them with a similar forest configuration. The forest consists of 25 trees with varying radii between 0.2 to 0.5 m, randomly distributed within a 30×30 m area (shown in Fig. A.3). The generated IR results are shown in Fig. 2.14. In Fig. 2.14a, *Treeverb* method shows a

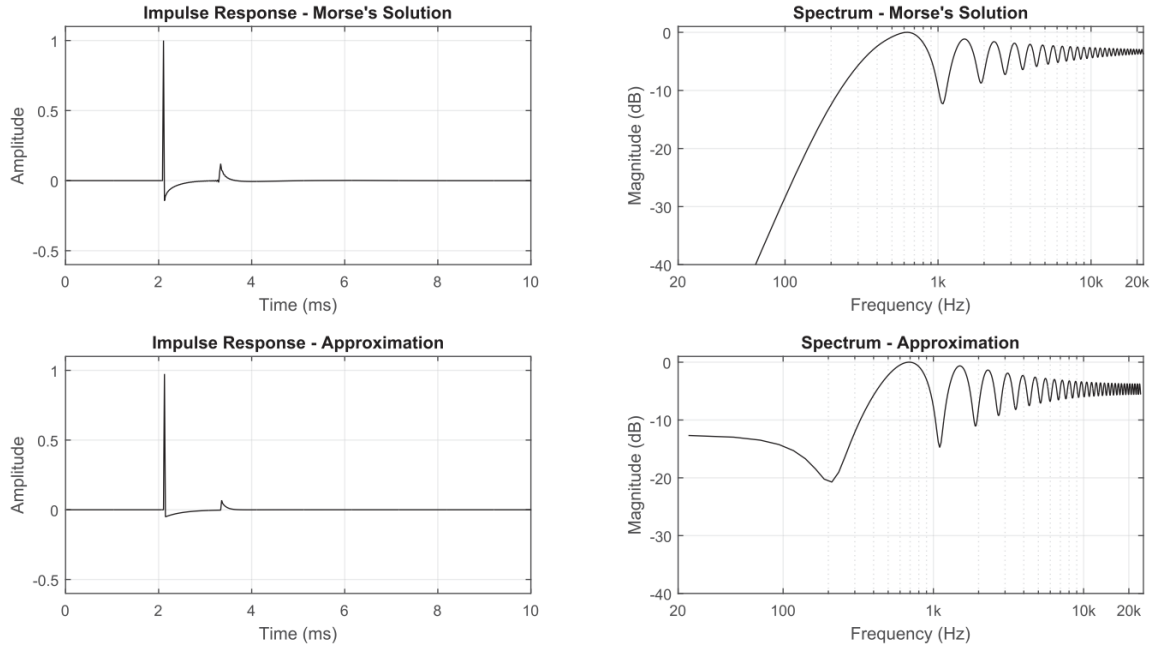

FIGURE 2.13: Comparison plots of Morse'solution to scattering from a rigid cylinder with the approximation of the filter model used in the WGW algorithm. The condition is $r = 0.2$m, $\theta = 60°$. From [1].

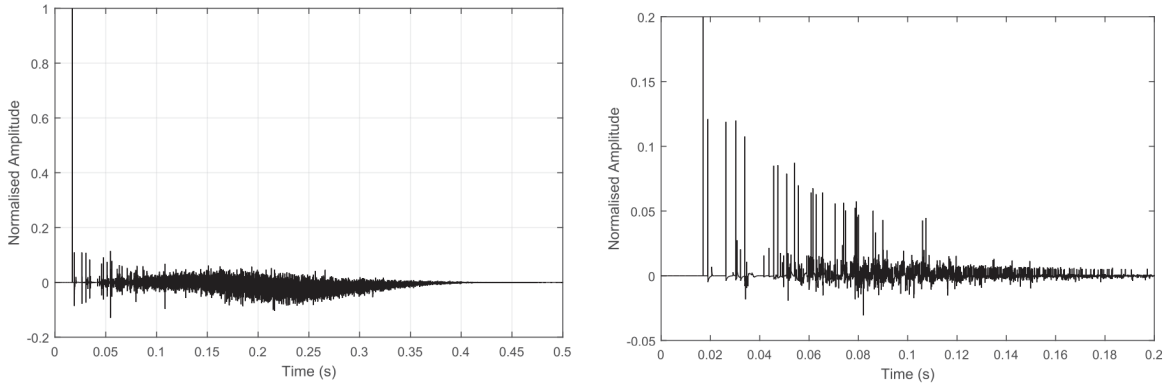

(A) IR generated using Treeverb methodology.

(B) IR generated using WGW methodology.

FIGURE 2.14: Comparison plots of generated IR for the same forest layout. From [1].

relatively long reverberant tail and a cluster of dense results after the early reflections; In Fig. 2.14b, *WGW* method shows distinct initial reflections followed by sparse reflections and a less reverberant tail. Additionally, the IR measured in Koli national park (shown in Fig. 2.6) clearly indicates sparse responses with a relatively short reverberation tail, which agrees well with the *WGW* method results. Hence, the impulse response generated by *WGW* appears to be more plausible.

2.3.3 Summary

Both the *Treeverb* and *WGW* algorithms consider tree trunks as the main factor that affects sound attenuation in a forest environment and model the tree trunk as a rigid cylinder. This approach effectively simulates the impulse response of a forest environment. However, this method needs to be further validated. Part of the project work is to create an acoustic scale model to physically evaluate this modelling method, where tree trunks are modelled as rigid cylinders. The details of the scale model will be discussed in the next section.

2.4 Acoustic Scale Modelling

Section 2.3 reviewed the computer simulations of forest reverberation. Another approach to acoustic modelling is to create an acoustic scale model, which has been used in the design of concert halls and opera theatres [6]. This method will be reviewed in this section.

2.4.1 Acoustic scale modelling of rooms

The acoustic scale modelling method was first introduced in the 1930s to study room acoustics using a three-dimensional model [43]. This modelling method allows for predicting the acoustic properties of the full-scale space as it captures the complex wave effects, such as diffusion, diffraction and ground interference [8, 9]. In Spandöck's study, the scale model factor was 1:5, and the measuring method was to record a sound signal in the model using a wax drum at a high speed and playback five times slower [6]. This establishes the principle of scale modelling techniques that the dimension of the physical space and the wavelengths of the test signals are reduced by the scale. Therefore, the frequency of sound waves is increased by the scale, which Eq. 2.6 demonstrates the relationship.

$$f_r = k \times f_s \tag{2.6}$$

where f_r is the frequency of the sound wave in the full scale, f_s is the frequency of the test signal in the scale model, and k is the scale factor. For instance, considering a scale factor of 1:10, which can be expressed as 0.1. In this case, the acoustic properties of a test signal frequency at 20 kHz in the scale model correspond to the acoustic properties at a frequency of 2 kHz in the real scale. Additionally, the materials used in the model should closely approximate sound absorption coefficients (SACs) at the scaled frequencies [44]. For instance, considering a scale factor of 1:10, SAC of the model material at 20 kHz needs to approximate that of the real material at 2 kHz.

In 2009, Jeon et al. investigated the effectiveness of a scale model in reproducing the absorptive properties of a multi-purpose hall [8]. The scale factor was 1:10, and the main reflecting surfaces and absorptive elements including audience, seating and absorption banner were modelled and measured in a reverberation chamber. It's interesting to note that the audience is a major factor in sound absorption in a hall due to their impedance and their clothing. Fig. A.4 shows the scale model of Gimhae Arts Hall (GAH). It's suggested that the scale factor should be as large as possible as the air absorption is greater at higher frequencies [45]. Therefore, the measurement was conducted by filling the reverberation chamber with nitrogen gas. The absorption coefficients of the scale model elements were chosen to be as close as possible to the actual hall, especially at frequencies that significantly influence sound propagation. Several SACs of medium-density fiberboard (MDF) with different treatments were examined for the reflecting surfaces. It's suggested that the timber has considerable sound absorption at ultrasonic frequencies, which can be reduced by varnishing the surface [46]. Despite the better fit of the SACs for three-times-lacquered MDF, lacquered MDF with putty was selected for the model due to its easiness of workability, in which putty is a mixed material effective for filling gaps.

2.4.2 Acoustic scale modelling of outdoor spaces

Scale modelling method has also been used in studying sound propagation in outdoor spaces. An investigation of sound scattering from building facades using a scale model was conducted [7]. It's suggested in this study that the choice of scale factor is a compromise between the

capabilities of the measuring equipment and the size of the available test space. The smaller the test space, the higher ultrasonic frequencies are required for the measurements.

In a recent study conducted by Cox et al., the acoustic properties of Stonehenge were examined using an acoustic scale model [9]. The research chose a scale factor of 1:12, which was the largest model that could fit in the semi-anechoic chamber. Considering that stones have a relatively low SAC, in which the typical range is from 0.01 to 0.02, the model stones were made to have minimal sound absorption. Some of the model stones were cast in polymer-modified plaster, and others were 3D printed hollow and filled with heavy material. Additionally, cellulose car spray paint was used to seal the stones to minimize sound absorption. For the model grassland, the unvarnished MDF was chosen as the modelling material. The SACs of this material match better with the grassland at a scaled frequency range of from 125 Hz to 1 kHz. Fig. 2.15 shows the scale model of Stonehenge constructed in a semi-anechoic chamber.

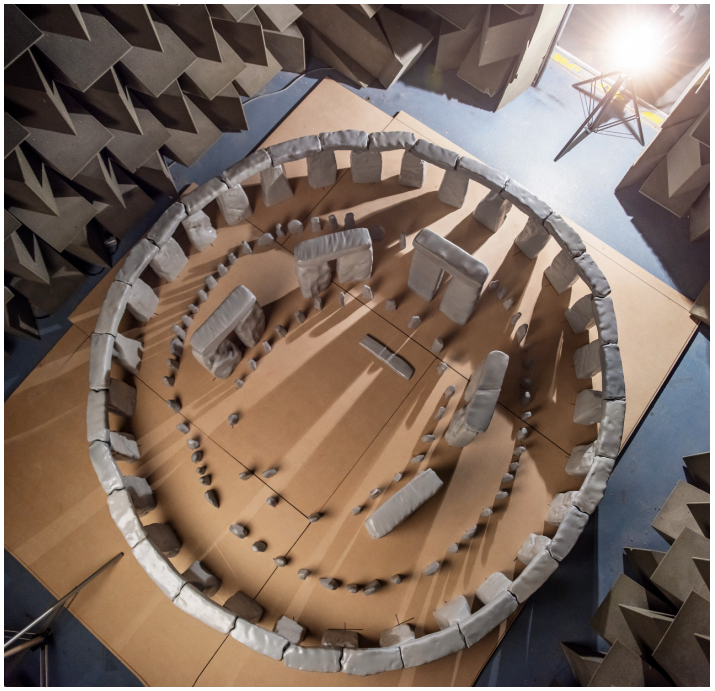

FIGURE 2.15: Scale model of the Stonehenge in the semi-anechoic chamber. From [47].

The measurement was using the ESS method, with frequencies ranging from 800 Hz to 96 kHz, enabling the analysis of acoustic properties from 125 Hz to 4 kHz octave bands [9]. The recording equipment used therefore had to be capable of producing and capturing this frequency range, as well as being suitably sized to represent scale source and receiver positions. Ideally,

omnidirectional sources and receivers should be used in impulse response (IR) measurement [11]. However, ultrasonic, compact, and omnidirectional loudspeakers were not available, so four tweeters were arranged in a square configuration to approximate omnidirectionality in the horizontal plane. A free field microphone was used, positioned upwards to capture the omnidirectional response. To absorb reflections, the equipment in the chamber was covered with foam. Fig. A.5 shows the microphone and the speaker used in the measurement. Additionally, due to the electric noise at higher frequencies from the microphone and the preamplifier, the measurements were conducted by repeating the sine sweep 128 times.

IR analysis was then conducted in accordance with ISO 3382 [9]. T_{30}, an estimation of RT_{60} and early decay time (EDT) were used to examine the reverberation time, while the Definition (D_{50}) was used to investigate speech intelligibility within Stonehenge.

Acoustic scale models have been used to study forest acoustics since the 1980s. Sound propagation through vegetation was investigated by modelling trees and forest ground [30]. Trees were modelled as paper tubes 30 cm high and 2 cm in diameter. Two different conditions of the forest ground were considered: acoustically hard, modelled with hardboard, and acoustically soft, modelled with carpet. The measurement was conducted in the semi-anechoic chamber, with a filtered white noise in octave bands of about 4 kHz and 8 kHz used as the test signal. However, no specific scale factor was mentioned in the paper, and the measurements were found to be dissimilar to the results examined in the real forest environment.

Another study investigated the sound attenuation caused by the trees as the cylindrical scatterers [40]. In this work, two experiments were examined. The first experiment aimed to validate the method of modelling the trees as infinitely long cylindrical scatterers, as proposed by Embleton [48]. The model was constructed in a small anechoic chamber, where trees were modelled as wooden dowel rods. In order to simulate the infinitely long cylindrical condition, the rods were positioned to the ceiling using welded wire mesh, while on the chamber floor, they were supported by foam to maintain vertical orientation. The source used was a broadband random noise signal generated by the air jet, and a microphone capable of recording sound frequencies up to 100 kHz was used. Additionally, a tray of sand was used to model the ground in the second experiment, which aimed to investigate the sound attenuation caused by a set of

scatterers with a forest ground condition. However, the scale factor was also not given in this experiment.

2.4.3 Summary

The section reviewed the development of acoustic scale modelling, examining the application to forest acoustics. The key factors can be now addressed in summary. Firstly, the factor should ideally be as large as possible considering the air absorption at high frequencies [45]. But, it's a comprise between the available test space and the capability of the measuring equipment [7]. Secondly, the frequency of the test signal is increased by the scale to preserve the size of the element dimension and the corresponding sound wavelength [9]. Thirdly, the materials used in the model should closely approximate sound absorption coefficients (SACs) at the scaled frequencies, especially within the frequency range that significantly affects sound propagation. Ultrasonic, compact and omnidirectional loudspeakers and microphones are desired for the comprehensive assessment of the acoustic properties. The cost of creating the scale model, and the effort of constructing the model, should also be taken into consideration during the design process.

2.5 Project Objectives

This Chapter has presented a review of literature relevant to this project, including the study of acoustic impulse responses, forest acoustics, the simulation of forest acoustics, and acoustic scale modelling. In each of these sections of the literature review, key findings have been identified. These findings now allow for a set of objectives, outlining the steps to be completed to achieve the project aims, to be defined:

1. Record IRs in a real forest environment.

    - Find a suitable forest for IR measurement. For the aims of this research project, a suitable forest environment should ideally have relatively tall tree trunks, few branches

and foliage at ear's height, and a flat ground surface with few low plantations. It's ideal that this forest environment should be situated away from other plantations. But if this is not feasible, the measurement will consider certain radiations of the trees that mainly influence the sound propagation in the source and receiver range.

- Choose measurement range and the positions of source and receivers, then conduct forest IR measurements. The measurement method will use the ESS method. To approximate omnidirectional directivity, the method of rotating the source using one single speaker will be conducted.
- Conduct forest layout measurements, then convert the measurement data to coordinates. The measurements will document the diameters and relative positions of the tree trunks and the conversion will be conducted in SketchUp.
- Measure and analyse sound attenuation in a forest and an open field. The measurement equipment will use a starter pistol and a sound pressure level, and four different distances will be examined.

2. Analyse forest IRs. This will be conducted with the time and frequency domain analyses of each IR. The comparisons of the IR results allow for the investigation of the acoustic characteristics of tree trunks in a forest environment.

3. Record IRs in a forest scale model.

   - Design the scale model. The acoustic scale model will consist of a set of rigid cylinders and a flat ground surface. The design of the model includes the scale factor, modelling materials for the tree trunks and the ground, and recording space.
   - Construct the scale model. The model will use the same layout as the real world measured forest, the construction needs to mark the coordinates of each tree, source and receiver positions directly on the modelled ground. Then the dowelling method will be used to stabilise the modelled tree trunk on the ground.
   - Conduct scale model IR measurements. The ESS method and rotating the source will be used in the measurement.

4. Analyse scale model IR results and compare these results with the real forest IR results. Define the similarities and discrepancies of the IRs recorded in both environments and the effectiveness of the forest scale model can be further evaluated.

Chapter 3

Forest IR Measurement

This chapter will cover the forest IR measurement process and layout measurement process. Section 3.1 presents a description of the chosen recording site. The documentation of the IR measurement process is presented in Section 3.2. In Section 3.3, the process of the layout measurement will be covered, followed by the methodology of converting the layout measurement results to coordinates. The measurement and analysis of sound attenuation in a forest environment and an open field are then explained in Section 3.4.

3.1 Find a suitable forest for IR measurement

The ideal forest environment has been discussed in Section 2.5, and field investigations have been taken in Wheldrake Wood, Broad Hwy, York. Different locations have been considered, using a starter pistol as an impulse to record impulse responses of each spot. Fig. 3.1 shows two different spots investigated in Wheldrake Wood. Fig. 3.1a shows a forest environment that has relatively tall tree trunks with little foliage at ear's height, and there is no additional low plantation. However, the braches are at lower heights, and the ground surface is slightly bumpy. Fig .3.1b shows a forest environment that has tall tree trunks with little foliage and branches at ear's height and a relatively flat surface. The measurement should take place among these trees, however, there are additional low plantations.

(A) Spot 1 (B) Spot 2

FIGURE 3.1: Two possible IR measurement spots investigated in Wheldrake Wood.

Another possible location was found in the same wood (which is shown in Fig. 3.2). There is only one type of tree, *Abies grandis*, in this forest environment, where tree trunks are relatively tall, straight and cylindrical with different diameters. A canopy is formed by the foliage at the top of the trees. Most twigs are located above the height of the ear. The ground surface is relatively flat with no additional low plantation. In general, this forest environment is dominated by tree trunks, which is ideal for this research project. Although there are over 100 trees in this area, considering the time in actual layout measurement, and the effort and cost of recreating this environment as an acoustic scale model, it's more reasonable to measure certain radiation of the trees' position for this research project.

3.2 Forest IR measurement process

After deciding on the measurement spot, the actual measurements were taken on Thursday the 22nd of June 2023. The measurements were conducted with the help of Dr Frank Stevens, one of the associate lecturers in the Audio Lab, Mr Andrew Chadwick, one of the technicians in the

FIGURE 3.2: Chosen IR measurement spot in Wheldrake Wood.

Audio Lab, and Mr Richie Cully, one of the colleagues in the MSc course (The picture of the measurement team can be seen in Fig. A.6).

3.2.1 Choose measurement range and the positions of source and receivers

Before choosing the source and receiver positions, the first assignment was to draw the layout measurement range. This range later will be constructed as a scale model in the anechoic chamber, where the test space is slightly larger than 3.5 m^2. Considering the scale should be as large as possible as discussed in Section 2.4, the measurement range chosen for this project is a 20 m^2 square.

Starting from one standpoint, two approximately perpendicular tape measures with a length of 20 m were used to define the other two points, where the tape measures were not obstructed by the trees. Similarly, the final intersection point was defined by these two points and ensured a consistent distance of 20 m. Additionally, each standpoint was marked with a named flag. The naming method considered the actual directivity of the site, which are *NW* (Northwest),

NE (Northeast), *SE* (Southeast), and *SW* (Southwest) in a clockwise sequence. The *NE* flag is shown in Fig. A.7.

For the later conversion of the forest layout, a layout diagram was drawn representing the actual positions of 33 trees in this measurement range. Each tree was given a name with a unique alphabet which was marked on the diagram and directly on the tree itself. The diagram is shown in Fig. 3.3.

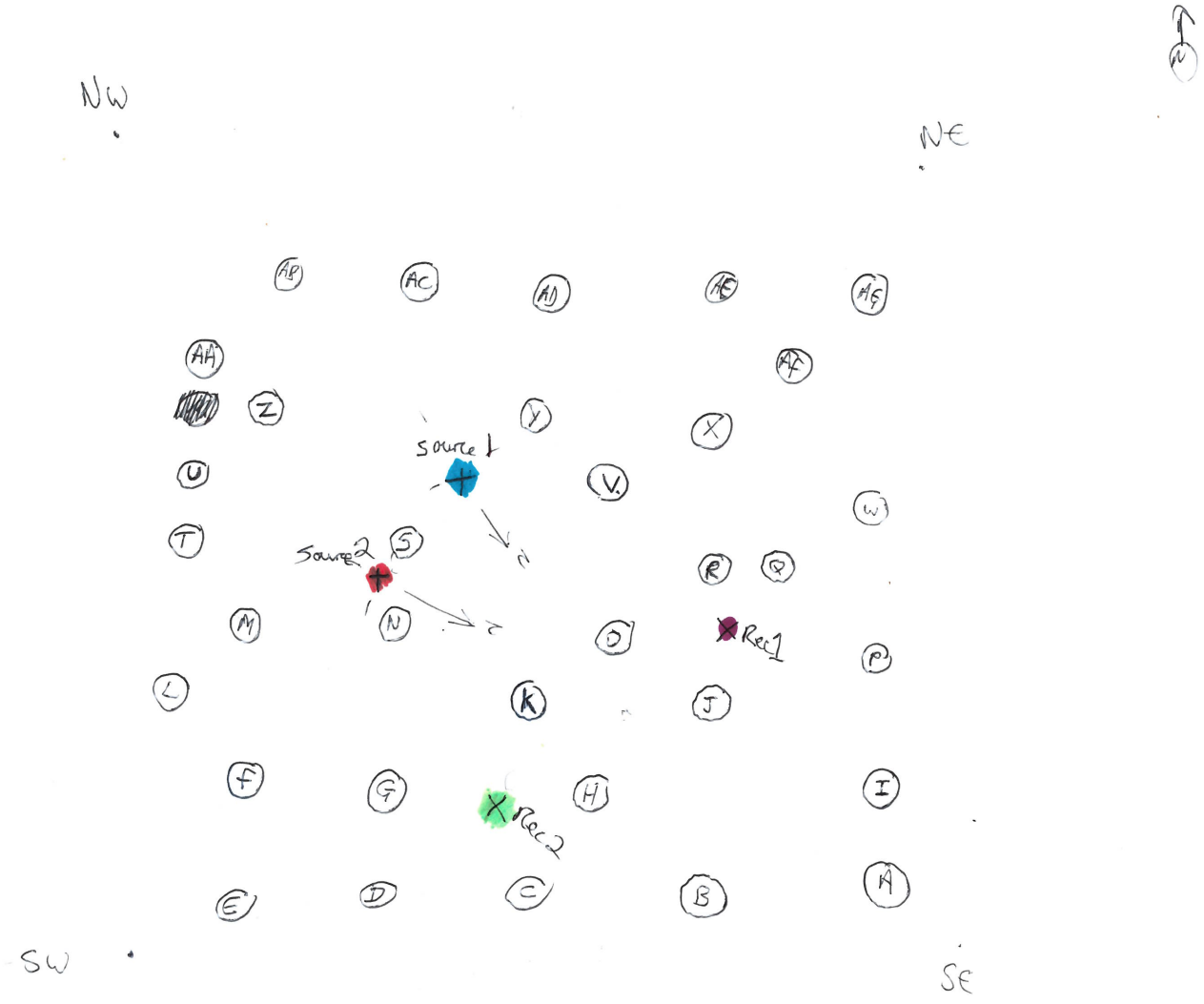

FIGURE 3.3: A hand-drawn diagram of the measured forest layout.

The source and receiver positions were then selected within this measurement range, including two sources and two receivers. All source and receiver positions were at least 1 m away from the trees close to them, and the distances between each source and receiver ranged from 7 m to 10 m to capture the impulse responses within this 20 m^2 range. *Source 1* was selected with

(A) The position of *Source 1* and two receivers.

(B) The position of *Source 2* and two receivers.

FIGURE 3.4: The layout of source and receiver positions.

clear sight to *Receiver 1* and *Receiver 2* (The layout is shown in Fig. 3.4a). *Source 2* was selected with a tree obstructed to both receivers: *Receiver 1* is impeded by *Tree O*; *Receiver 2* is impeded by *Tree N* (The layout is shown in Fig. 3.4b).

3.2.2 Conduct forest IR measurement

A Genelec 8130A digital loudspeaker was used in the recording. The loudspeaker was powered by a portable inverter generator which was placed on the ground and covered in a plastic bag to avoid water or electricity (Fig. A.8 shows the speaker and inverter covered in a bag on the site). Signals were recorded with two microphones. An Earthworks M30 omnidirectional measurement microphone was used to record mono signals, which have flat frequency responses and are good for acoustic parameters analysis (Fig. A.9a shows the M30 microphone). A Soundfield ST450 MkII was used to record B-Format signals, and the results can be used in auralisation and the SIRR analysis (Fig. A.9b shows the Soundfield microphone). The loudspeaker and microphones

were placed at a height of 1.5 m from the ground. To accurately determine this height, a tape measure was used. Additionally, a Zoom F8 multitrack field recorder was used to record two microphone signals and two Sony battery packs were used to power the Zoom recorder and the Soundfield kit (Fig. A.10 shows the Soundfield recorder and the Zoom recorder with battery supply).

In order to improve the signal-to-noise ratio (SNR), several methods were used for the forest IR measurements. The gain of the Soundfield recorder was driven to the maximum, with breakout leads connected to the Zoom recorder to reduce the gain. The level of the speaker was also driven as high as possible. A 15 s exponential sine sweep (ESS) was used, with frequency ranging from 60 Hz to 20 kHz at a sampling rate of 48 kHz. Considering the low frequency of the sweep vibrating greater, which might cause clipping, the recording started at the frequency of 60 Hz. Additionally, the sweep was repeated twice at each position which will be detailed in the following recording process.

Considering the IR of the starter pistol recorded at this site became silent approximately 3 s after the direct sound (waveform shows in Fig. A.11), the sweep was generated with the gap at the end of 6 s in MATLAB to ensure the reverberation is fully recorded. Reaper was used as DAW for the measurements (Fig. A.12 shows the forest recording in Reaper project). Time region was used for each sweep recording in Reaper to ensure the length of each recording was the same. For each source position, the speaker was rotated four times to approximate the omnidirectional directivity, which was the same method as the forest IR measurements in Koli National Park [3]. For this recording, *North* was defined as the source facing directly to *Receiver 1*. The source was rotated clockwise by approximately 90° for each subsequent direction. Therefore, the orientations were labelled as *East*, *South*, and *West*, respectively. Fig. A.13 shows the pictures taken on the site of four orientations of the loudspeaker. The sweep was played back through the speaker and simultaneously recorded by the two microphones positioned at two receiver positions to record efficiently. After recording four orientations, the two microphones were swapped between the receiver positions, and another set of four orientations was recorded. This recording process was repeated for each source position. A total of 32 recordings were taken for each microphone during the IR measurement process. The IRs were attained by deconvolving 8 sweeps at each position and then averaged out. The IRs

recorded with M30 microphone can be found in Appendix C.1.1; IRs recorded with SoundField microphone can be found in Appendix C.1.2.

During the measurement, some recordings were abandoned due to the noise of aeroplanes, birds, pigeons and strong wind. Although the recordings were trying to minimise the noise and improve SNR, these noises can not be avoided in the results.

3.3 Forest layout measurement and conversion

This section will present the process of the layout measurement, documenting the diameters and relative positions of the tree trunks. The process of converting these layout data to coordinates will then be explained.

3.3.1 Conduct forest layout measurements

In order to recreate this forest layout in an acoustic scale model, the circumference of each tree, the relative positions between the source and receiver, and between the sources/receivers and trees were measured, and the detail of converting these data to the forest layout will be detailed in Section 3.3.2.

The circumferences of 33 trees in this range were measured. Given that sound propagation significantly influences the horizontal plane in an outdoor environment, the circumference measurement height was the same as the IR measurement [21]. A taylor tape measure was used to note the circumference at the height of approximately 1.5 m. The measurement accuracy was to the nearest 0.005 m. Fig 3.5 shows the picture of the tree circumference measurement.

The positions of the two sources and two receivers were used as four standpoints to measure the relative position of each tree, as it also preserved the height of IR measurements. Therefore, the stands had not been moved since the positions were selected for the IR measurements. A laser measure was used to measure the distance and placed on the metal board, which was mounted on the stand. The starting point was approximately the centre of the stands, and the

FIGURE 3.5: The circumference measurement of *Tree H* was noted with a taylor tape measure.

endpoint was the centre of the apparent diameter of the tree. Fig. 3.6 shows the pictures of the laser measurement. This method allows for four measurement data to locate one tree position to minimise the error. For the tree, the standpoint had no clear sight, a tape measure was used to note the approximate data, which is shown in Fig. A.14. Similarly, the starting point was the centre of the stand, and the endpoint was the edge of the tree close to the standpoint, which was found by eye. The measurement accuracy of the laser measure and the tape measure was to the nearest 0.01 m. Additionally, the four standpoints' relative distances were also noted using the same measurement methods. The layout measurement data are shown in Table. B.1 and B.2.

It's worth noting that this forest layout can not be perfectly recreated since the measurement errors are made from some tree trunks are not straight, or not perfectly cylindrical, or the bumpy surface of the tree bark, or the centres of the tree trunks were found by eye, etc.

(A) A laser measure at the standpoint pointing at the tree.

(B) A laser point showing at the apparent centre of the tree trunk.

FIGURE 3.6: The relative tree position measurement was noted with a laser measure.

3.3.2 Convert the measurement data to coordinates

The process of converting measurement data to the forest layout was conducted in SketchUp. The method used was to define the four standpoints' positions, and then use these standpoints to define each tree's position based on the data from Table. B.2. The position of the tree is determined by the distance from each standpoint to the centre of the tree. Assume the trees are cylindrical, this data can be attained by adding the radius of the tree and the measured distance from the standpoint to the edge of the tree. The radius of the tree can be attained from the measured circumferences. The converted layout data is given in Table. B.3.

The source and receiver positions were defined using the close by trees measurement data. The start of the process was to define three positions using three measurement data, which include *Source 1*, *Receiver 1* and a close by tree, *K*. It's noted from the measurement that these positions have a clear line of sight to one another. Fig. 3.7 shows this process. First define *Source 1* and *Receiver 1* positions using their relative distance, then draw circles centred at

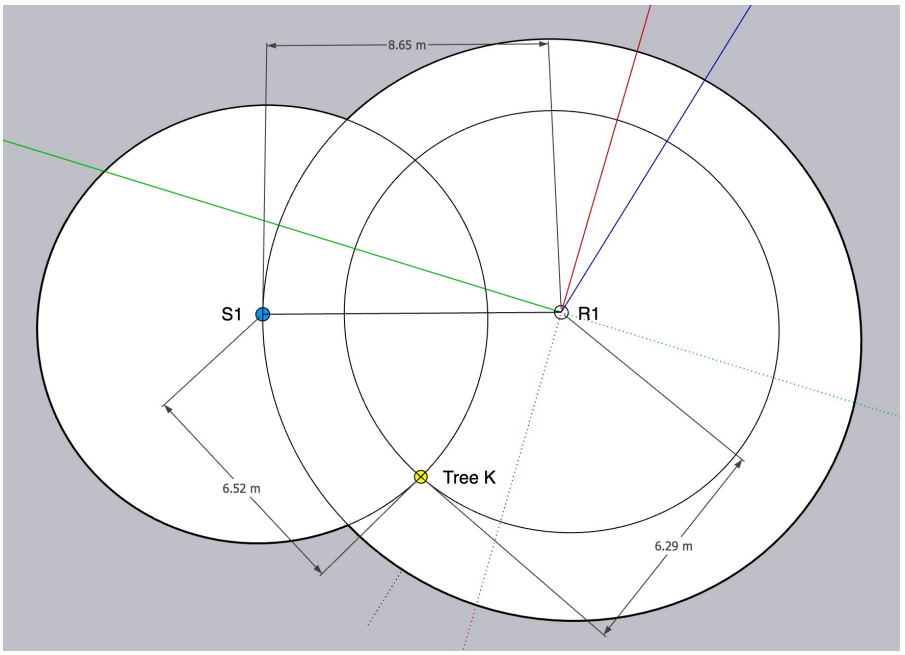

FIGURE 3.7: Determine positions of *Source 1*, *Reciever 1* and *Tree k*. *Source 1* and *Receiver 1* were defined using their relative position. Their positions were marked as circles, where the centre points were the actual locations. These two standpoints were then used to define *Tree K* position using their associated distance. *Tree K* was determined at one of the intersection points compared to the actual layout in Fig. 3.3, and the yellow circle represents the actual size of the tree.

these two standpoints with the radius of their associated distance to *Tree K*. It results in two intersection points, according to the actual layout diagram (shown in Fig. 3.3), *Tree K* can be determined at one position and marked as a circle with its associated radius. The same procedure was conducted to define another close by tree, *O* (Fig. A.15 shows the process). Similarly, using these two tree positions as standpoints, *Source 2* and *Receiver 2* positions can be determined by the distances from these two trees to each of these standpoints (Fig. A.16 shows the process of defining *Receiver 2*).

After defining these four standpoints, the tree positions can be determined starting with the trees that are close to the source or receiver. It should be noted that in this process, the laser measure data was used to determine the position, and the tape measure data was used as a reference to confirm the tree position. Fig. 3.8 shows the process of defining *Tree F* using three measurement data and one reference data. These three measurement data formed an intersection point, which Fig. 3.9 shows the zoom-in view of this point. It can be observed that the three circles determine the range of the tree location. An estimation was made to define the

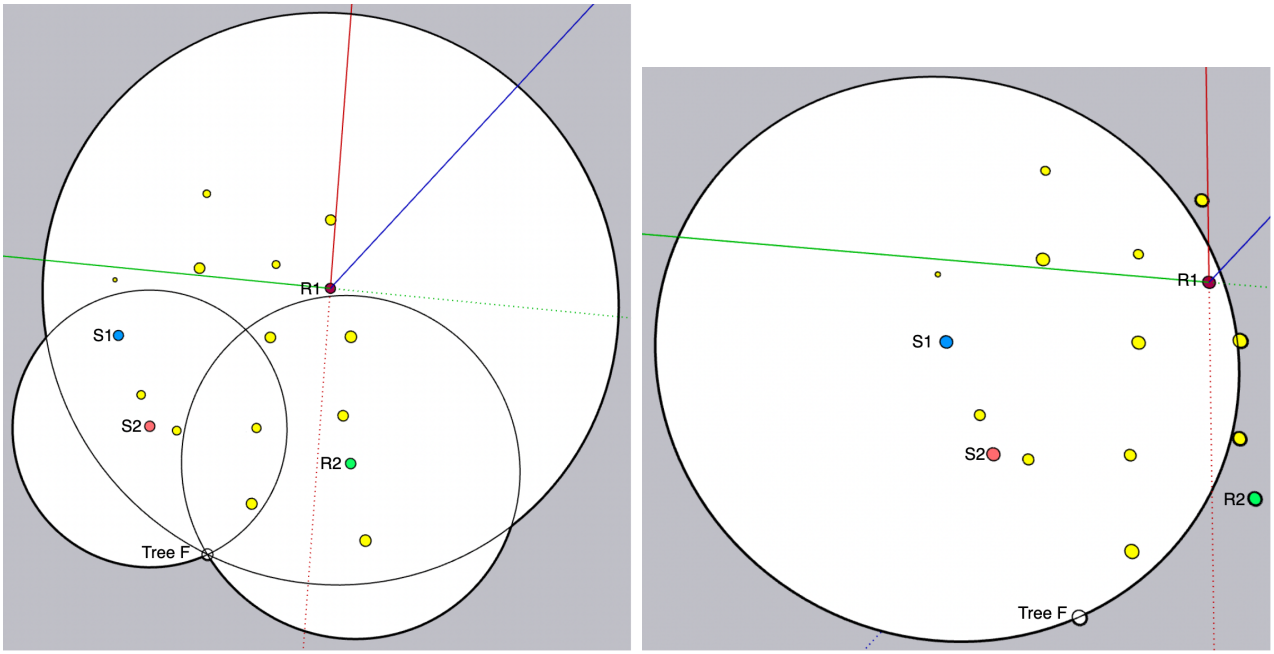

(A) Three laser measure data from *S2*, *R1* and *R2* were used to determine the position.

(B) One tape measure from *S1* was used to confirm the position.

FIGURE 3.8: Determine the centre position of *Tree F*.

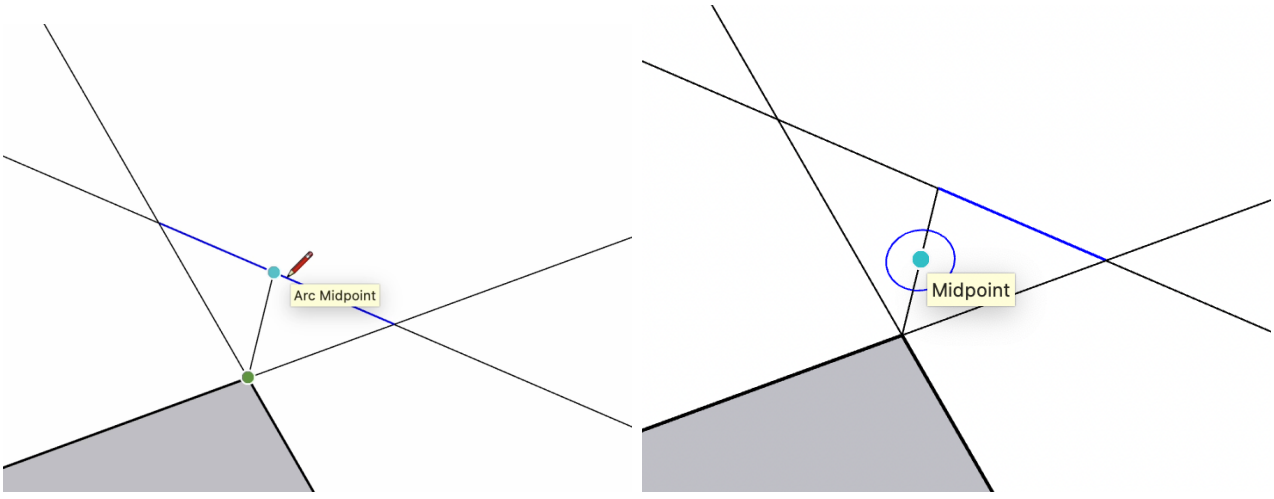

FIGURE 3.9: A zoom-in view of defining *Tree F* intersection point. The centre point was estimated by finding the centre point of the triangle-shaped range.

position by finding the centre point (midpoint) of the triangle-shaped range. Fig. A.17 shows the process of defining *Tree R* using four measurement data. In this example, one of the circles crosses the triangle-shaped range, where the midpoint of this crossed arc was determined as the centre point of *Tree R*. The same method was applied to define other trees. In order to convert this layout to coordinates, a 20×20 m square was drawn to confine this range and define the X and Y axis. Take the position of *Receiver 1* as the original point, the coordinates of each source, receiver and tree position can be measured (Fig. A.18 show this process). The results are shown in Table. B.4, and the layout was also generated in MATLAB shown in Fig. 3.10. This converted layout agrees well with the condition when there is no clear line of sight from one standpoint to the tree (Fig. A.19 shows *Tree V* is impeded by *Tree V* from *Receiver 1*).

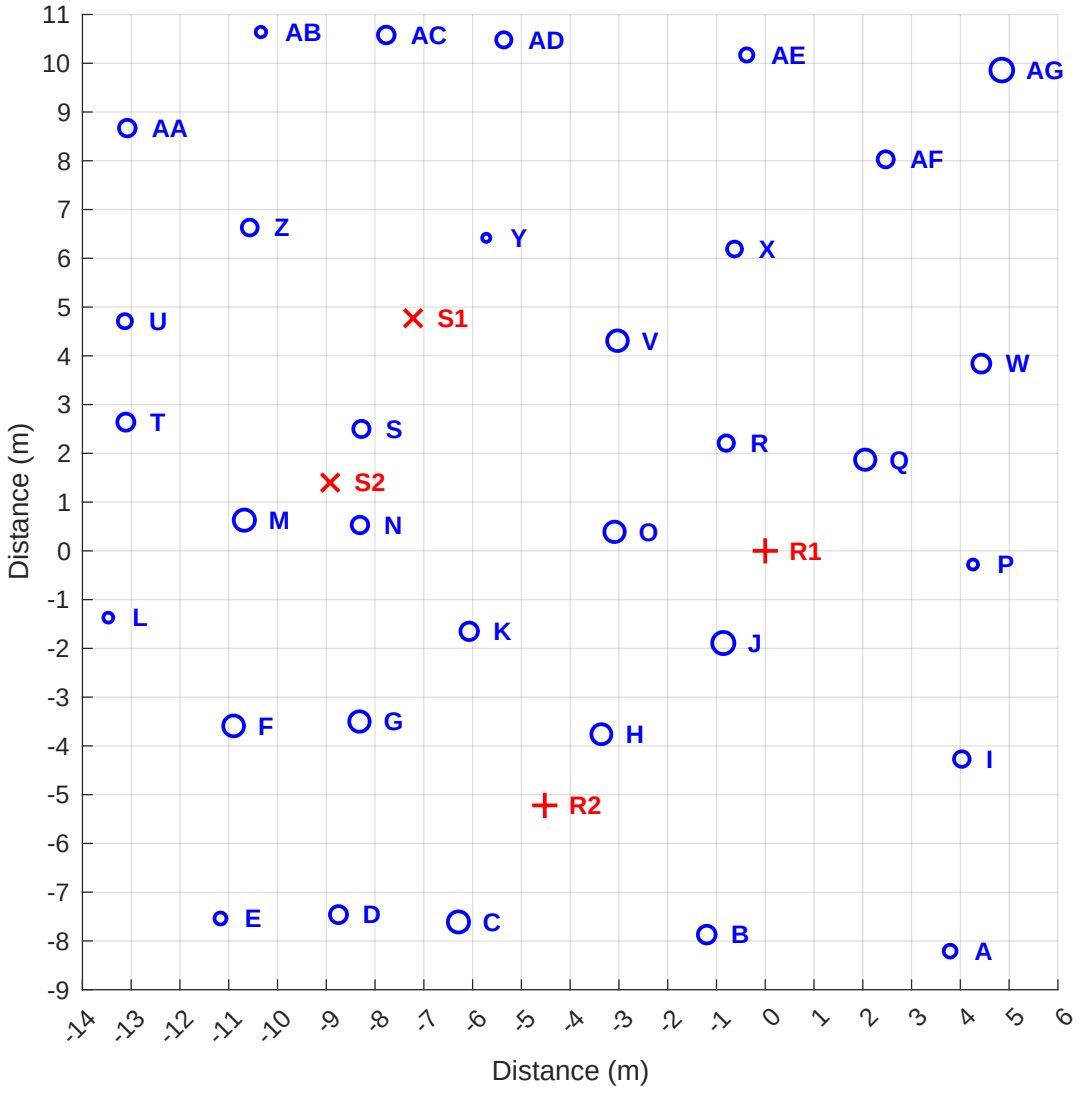

FIGURE 3.10: Forest layout generated in MATLAB.

3.4 Sound attenuation in a forest and an open field

This section presents the sound attenuation measurements in the same forest environment and an open field, using a starter pistol and a sound pressure level. The analysis will provide insight into the characteristics of sound attenuation in a forest environment.

3.4.1 Measure sound attenuation in a forest and an open field

In order to study sound attenuation in a forest environment, another measurement was conducted in the same forest environment and an open field. The open field was found in the Heslington Tillmire Site. In this environment, there are no trees or other reflective surfaces, and the ground is relatively flat with low plantations (Fig. A.20 shows the picture on the site). The source was a starter pistol and was measured with a Class 1 Sound Level Meter PCE-430. The measurement height was 1.5 m and different distances between the source and receiver were examined, which includes 5 m, 10 m, 15 m and 20 m. A tape measure was used to determine the source position, and the receiver was not moved during the measurement (Fig. A.21 shows the picture of measuring the distance in the forest). Two consecutive shots were recorded at each position. The setting for the sound level meter was data logged every 0.1 seconds and each data point was calculated using F (fast) weighting. Octave bands from 8 Hz to 16 kHz and A weighting were measured.

3.4.2 Analyse sound attenuation in a forest and an open field

Fig. 3.11 shows a comparison plot of sound attenuation in a forest and an open field at four distances using A weighting measurement data. Sound pressure levels (SPL) were generated using 5 data points at each impulse and the results were averaged out. It can be observed that the sound attenuation in an open field shows a continuous decrease, which approximately follows the inverse square law. The attenuation in a forest environment shows higher SPLs and does not follow the inverse square law. Comparing the results at 15 m and 20 m, the levels in the open field show a rapid decrease while the levels in the forest show no attenuation. It

indicates that there are reflective surfaces, such as tree trunks, in the forest environment that can provide reverberation.

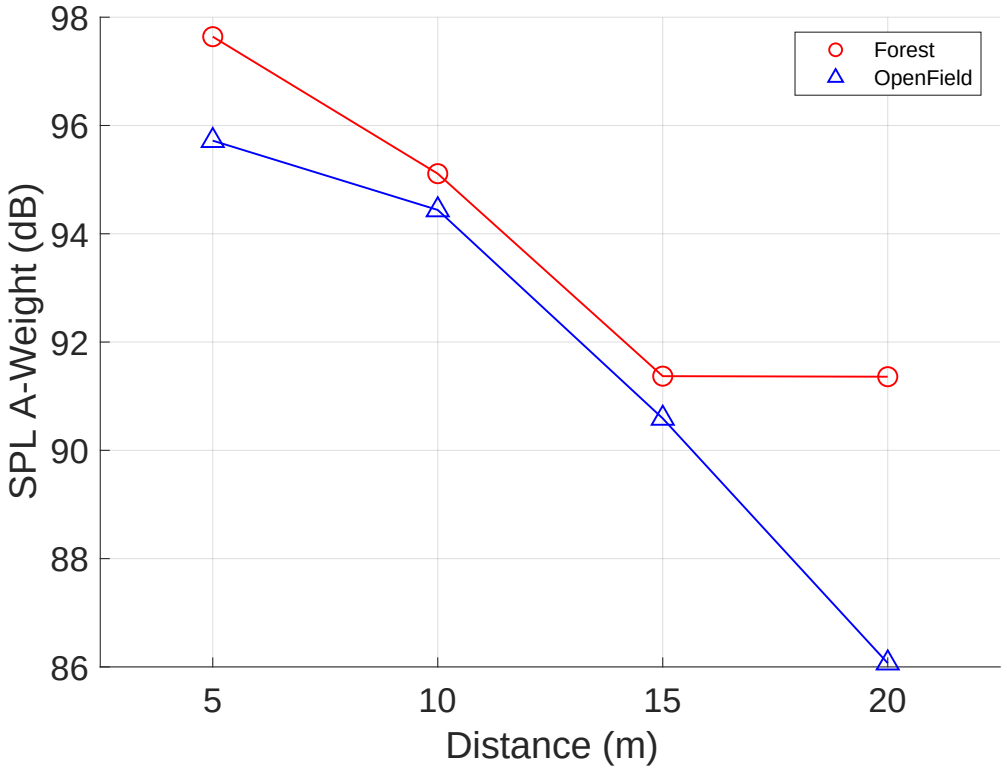

FIGURE 3.11: A comparison plot of sound attenuation in a forest and an open field at different distances, which include 5, 10, 15 and 20 m. The results are generated using A-weighting.

Fig. 3.12 shows a comparison plot of sound attenuation in a forest and an open field in octave bands from 63 Hz to 16 kHz. The measurement data used was a distance of 20 m. The results were generated using 5 data points at each impulse and then averaged out. The SPLs in both open spaces show a similar trend. Below 250 Hz, the levels are relatively low. It should be noted that the SNR of the starter pistol at lower frequencies is worse due to the duration of the impulse being relatively short, hence, the coherence of this frequency range is less pronounced [17]. Comparing the octave bands between 1 kHz to 2 kHz, it can be observed that the SPLs in a forest are at least 5 dB higher than in an open field. The greater levels at the mid-frequency range indicate the reflections in a forest environment, which agrees well with the previous findings [27, 31]. The levels show a roll-off above 4 kHz octave bands, which is due to the open nature of an outdoor environment, these will be detailed in Chapter 4.

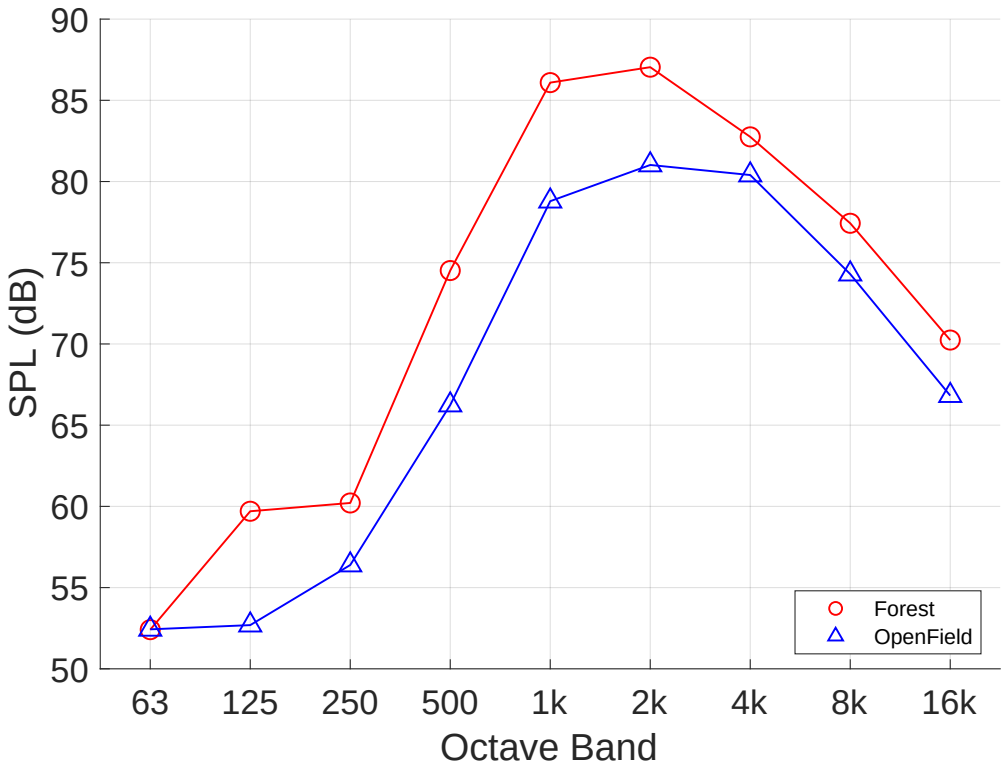

FIGURE 3.12: A comparison plot of sound attenuation in a forest and an open field from octave bands 63 Hz to 16 kHz. The distance between the source and receiver was 20 m.

3.5 Conclusion

This chapter presents the process of forest IR measurement. The recordings can not avoid the outdoor noise and several methods have been used to improve SNR. The forest layout was measured and then converted to coordinates, this process is an approximation as the tree trunks are not perfectly cylindrical or uniform. This layout preserves the condition of the IR measurement height, given that sound propagation mainly affects the horizontal plane in an outdoor environment [21]. Additionally, sound attenuation in a forest environment and an open field was studied. The results show that the sound attenuation in a forest environment does not follow the inverse square law, and the lack of attenuation at a frequency range from 1 and 2 kHz was found. These indicate the reflections in a forest environment, which can be from tree trunks. The forest IR analysis will provide more information on this aspect, which will be presented in Chapter 4.

Chapter 4

Forest IR Analysis

This chapter will present the forest IR analysis. In Section 4.1, the IR analysis at position S1R1 will be presented. This section will detail the methodology of the IR analysis and relate the results to the literature. Section 4.2, 4.3, 4.4 will cover the IR analysis at position S1R2, S2R1 and S2R2, respectively. In Section 4.5, the comparison of these IRs will then be presented by relating the results to their physical properties. In Section 4.6, the similarities of the IRs can reveal the acoustic features of tree trunks in a forest environment.

The IRs recorded with the M30 microphone will be used in the waveform, spectrum, and ISO 3382 acoustic parameters analyses. The IRs recorded with the Soundfield microphone will be used in SIRR analysis and auralisation.

4.1 S1R1 IR analysis

This section will analyse the IR recorded at S1R1. At this position, there is a clear line of sight between the source and receiver and the measured distance between them is 8.65 m, Fig. 3.10 shows this layout.

4.1.1 S1R1 IR waveform analysis

Fig. 4.1 shows the waveform plot of the first 150 ms of the IR recorded at position S1R1. The waveform shows a greatly pronounced direct sound followed by several distinct early reflections. The rate of decay of the IR at position S1R1 sounds relatively short. The sparse response shows similarity with the IR waveform results recorded in the forest in Koli National Park (shown in Fig. 2.6) and the results generated in *Treeverb* and *WGW* forest modelling work (shown in Fig. 2.14) [1, 3, 5]. Previous study indicates that early reflections are the key features in an outdoor space [21]. In a forest environment, the reflections are typically caused by tree trunks. To investigate this feature, the time taken for these early reflections to occur after the direct sound is calculated. The timing of these reflections is also marked as red dot lines in Fig. 4.1. Considering each tree as a reflection node, the path difference between the source-receiver and source-tree-receiver can be calculated with the forest layout data. The speed of sound used in this calculation is 343 m/s. The results are shown in Table. B.5. Relating the timing of the early reflections to the path difference, the potential trees that caused the first-order reflections can be located. The results at positions S1R1 are shown in Table. 4.1.

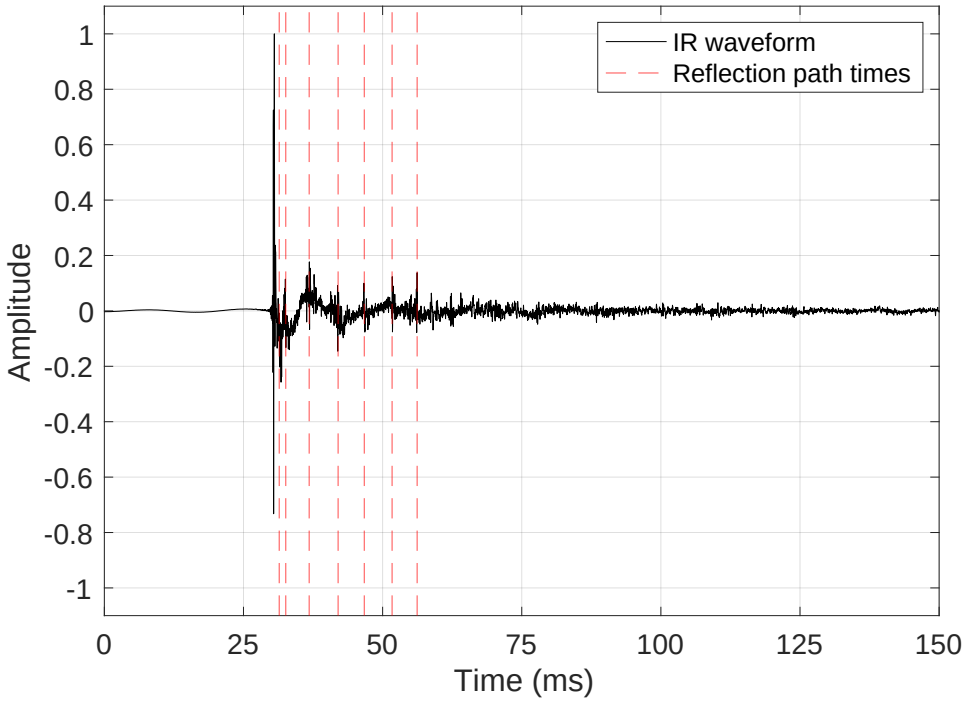

FIGURE 4.1: Waveform plot of impulse response recorded at position S1R1. The red dot lines indicate the timing of the early reflections.

Timing of early reflections	Path difference	Potential reflection at *Tree*
1.42 ms	0.49 m	*O* (0.49 m)
2.52 ms	0.86 m	*R* (0.65 m), *V* (0.86 m)
6.83 ms	2.34 m	*Y* (2.24 m), *S* (2.48 m)
11.89 ms	4.08 m	*Q* (3.88 m), *N* (4.06 m), *K* (4.16 m)
16.65 ms	5.71 m	*H* (5.77 m)
21.73 ms	7.45 m	*M* (7.5 m)
26.19 ms	8.98 m	*G* (8.74 m)

TABLE 4.1: Potential trees caused first-order reflections at position S1R1.

It should be noted that the timing of the early reflections shown in Table. 4.1 represents a range, as there are clusters of reflections around each peak. Additionally, the results were compared with the forest layout (shown in Fig. 3.10), only the trees that have a clear line of sight from both source and receiver were selected. The error range of the results is relatively small, the largest error included in Table. 4.1 was caused by *Tree G*, which was 0.24 m. The results in Table. 4.1 suggests that there are a fair number of trees that could cause early reflections at this position. In Section 4.1.4, SIRR analysis is used to further identify the reflections from trees by making use of the directional information. Although these results are made by considering the reflections from one tree, there are potential second-order reflections that could contribute to the actual propagation [21].

4.1.2 S1R1 IR spectrogram analysis

Fig. 4.2 shows the spectrogram plot of the first 100 ms of the IR recorded at position S1R1. The spectrogram shows a strong direct sound. The energy is greatly pronounced below 1 kHz and between 4 kHz to 5 kHz. There is a strong energy below 500 Hz which lasts for approximately 20 ms after the direct sound. This indicates the lack of attenuation at the low frequencies due to the open nature of a forest environment and reflections from further away trees [49]. Fig. A.22 shows the spectrogram of the IR recorded in the Heslington Church, University of York, which indicates several distinctive reflections from the walls of the first 125 ms. Compared the forest results to the results in the indoor space, it indicates the acoustic characteristic of the forest environment as a sparsely open space.

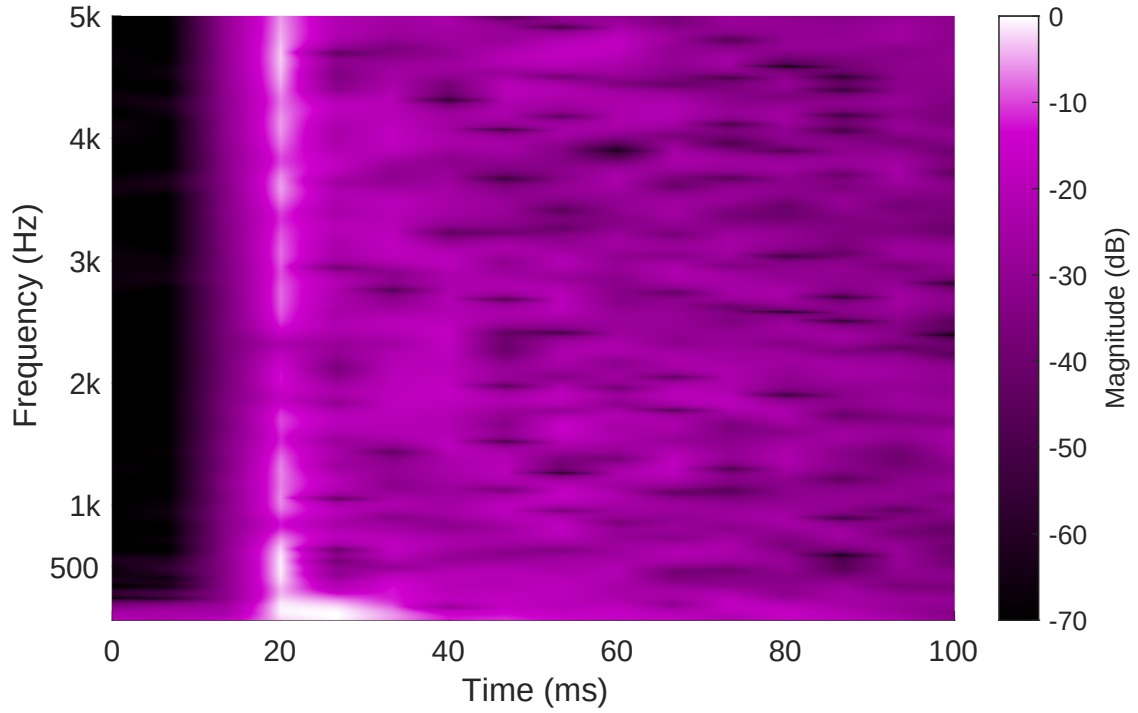

FIGURE 4.2: Spectrogram plot of impulse response recorded at position S1R1.

4.1.3 S1R1 IR ISO 3382 acoustic parameter analysis

Fig. 4.3 shows a comparison plot of Schroeder decay curve of the IR at position S1R1 and the Heslington Church. The weighting is 1 kHz. It can be observed that at the first 80 ms of the forest decay curve, the energy shows a rapid drop down to approximately -20 dB. Similar rapid regression can be also found in the measured bamboo forest [33]. Comparing this result to the Schroeder curve in an indoor space, Heslington Church shows a relatively linear energy loss over time. This implies a significant amount of energy loss in a forest environment due to an open nature [17]. Additionally, the decay curve in the forest shows the energy does not attenuate to -60 dB till the end of the signal, this is due to the noise recorded in the IR.

Although ISO 3382 is the standard for room acoustics, it has been used in the analysis of the Koli National Park forest environment, the ISO 3382 acoustic parameter will be used in this analysis [3]. In order to get an insight into the reverberation time in this forest, the slopes of T20, T30, T40 and EDT are estimated from the decay curve at the interest octave band (1 kHz), which is shown in Fig. 4.4. It can be observed that the extrapolated lines show a relatively less fit line of the decay curve. The EDT shows a better fit line, which estimates the

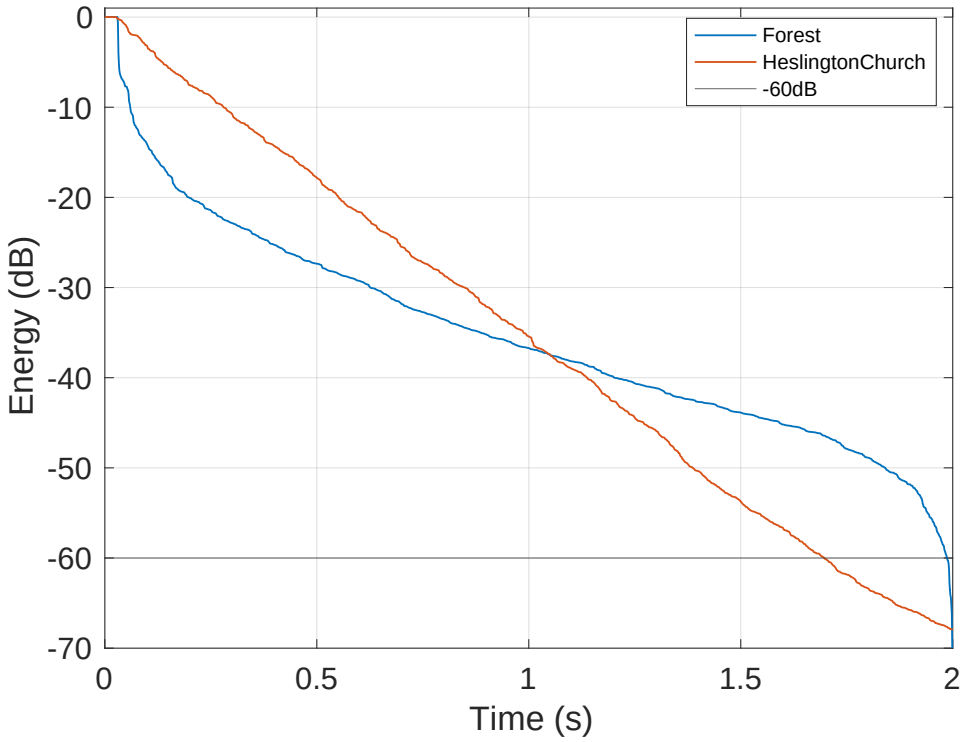

FIGURE 4.3: A comparison plot of Schroeder decay curve of the forest and the Heslington Church. The weighting is 1 kHz.

slope of the decay curve between 0 and -10 dB. Although the EDT values may not be a very useful measurement, given the rapid regression at the start of the curve [50]. Taking the SNR factor into account, the T30 slope has a better fit line compared to the other two reverberation parameters, which will be used as the estimated reverberation time. Fig. 4.5, 4.6, 4.7 show the reverberation time (T30), definition (D50) and early decay time (EDT) comparison plots of four IRs from octave band 125 Hz to 8 kHz, respectively.

In Fig. 4.5, the T30 values at position S1R1 are greatly pronounced at a frequency range of 500 Hz to 2 kHz octave bands, where the values are above 1.5 s, indicating reverberant responses at this range. Outside this frequency range, the reverberation time is below 1.28 s, indicating a relatively dry response. The T30 results align well with the previous findings, suggesting that a forest environment has less impact on sound attenuation at the mid-frequency range [27, 31]. Relating the results to the physical properties of a forest, the ground interference has an impact below 500 Hz [16, 28]. There might be constructive reflections at 500 Hz and destructive reflections and absorption at 250 Hz. Especially at around 500 Hz, the colouration might be significantly pronounced due to the ground impedance [49]. However, wind interference

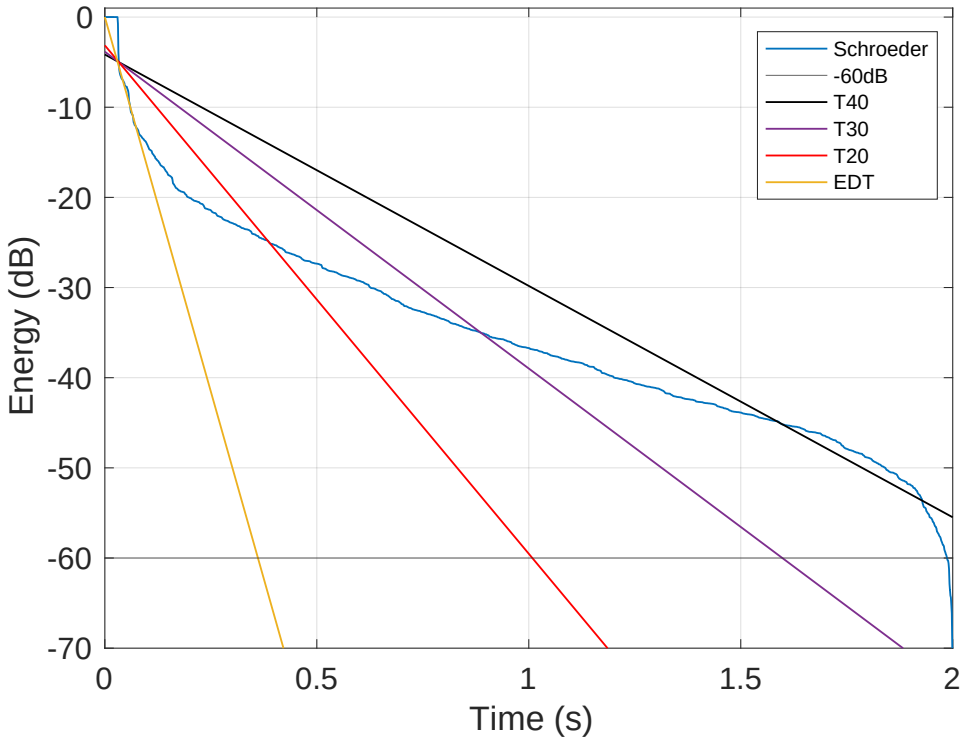

FIGURE 4.4: Schroeder curve of the IR at position S1R1 and the estimation slopes of early decay time (EDT) and reverberation time (T20, T30 and T40). The weighting is 1 kHz.

could potentially exaggerate the result, particularly at the 125 Hz octave band, because the low-frequency noise can be heard in the IR results. The significant attenuation above 4 kHz is due to the open nature of the forest [17]. Additionally, the porosity of the ground can absorb sound at higher frequencies, as well as the bumpy surface of the tree bark can cause diffusion [49].

At the 1 kHz octave band, the reverberation time shows the highest value of 2 s. Table. B.6 shows the recommended reverberation time for an occupied room for different types of musical performances. A result of 2 s indicates that romantic classical performances can be suitable in a forest environment at this frequency range. The reverberation time concentrated at 1 kHz is also indicated in the forest in Koli National Park, with a T30 value of 1.7 s [3]. It is interesting that the T30 in Koli forest (shown in Fig. 2.7a) also shows a similar trend as the results in Fig. 4.5.

Fig. 4.6 shows that D50 values at position S1R1 are all above 90%, indicating the greater energy in the first 50 ms compared to the late energy in sound propagation. The D50 values

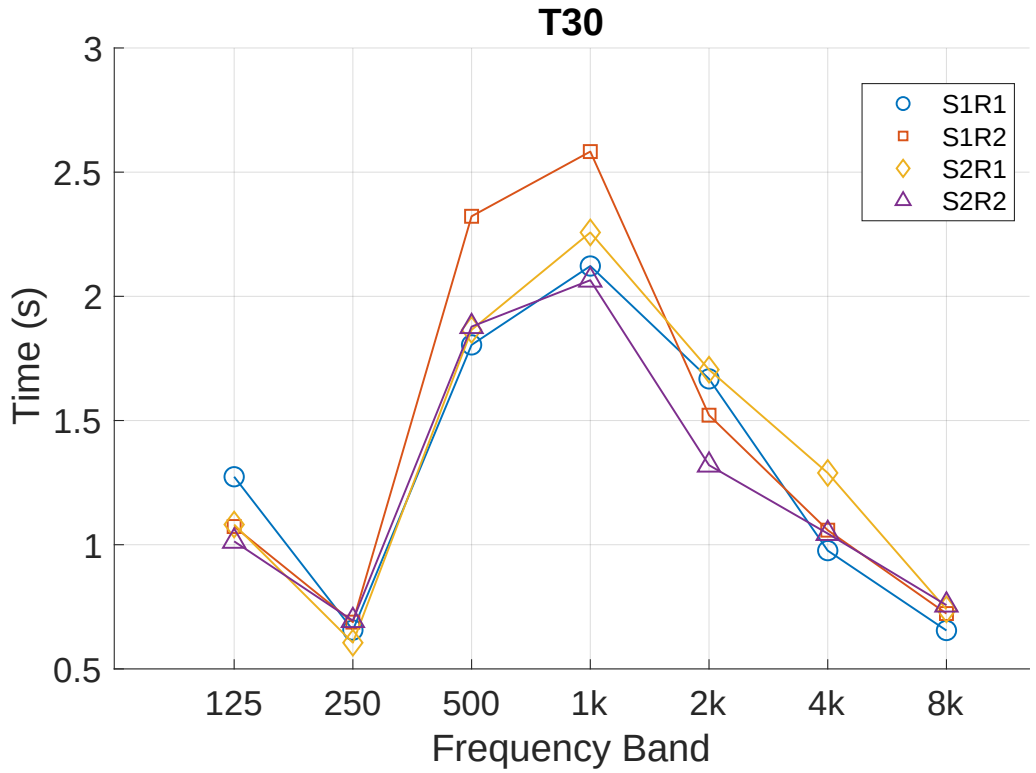

FIGURE 4.5: Reverberation time (T30) of four IRs at octave bands ranging from 125 Hz to 8 kHz.

in Heslington Church are between 25% and 51% at these octave bands [51]. These relate to significant sound attenuation in a forest environment. Similar to the clarity value, the large D50 values indicate good speech intelligibility, which will be detailed in Section. 4.1.4 [3]. The reduction of definition can be found in the IR concentrated at 2 kHz octave band.

The EDT at position S1R1 (shown in Fig. 4.7) indicates that the values are relatively larger above 1 kHz. The highest EDT is about 0.4 s at the 2 kHz octave band. It is interesting to note that the EDT values are much shorter than the T30 values, given the rapid regression at the start of the decay curve.

The acoustic parameter analysis indicates that at position S1R1, the reverberation time is found greatly pronounced at 1 kHz, and the reduction of sound attenuation is found at 2 kHz according to D50 and EDT values. These relate to the tree trunk reflections that mainly affect the frequency range of 1 and 2 kHz, which is associated with the tree trunk apparent diameters [4, 30]. The measured tree trunk diameter ranges from 0.17 m to 0.47 m, and the corresponding frequency range of their wavelengths is between 735.6 Hz and 2072.5 Hz. The

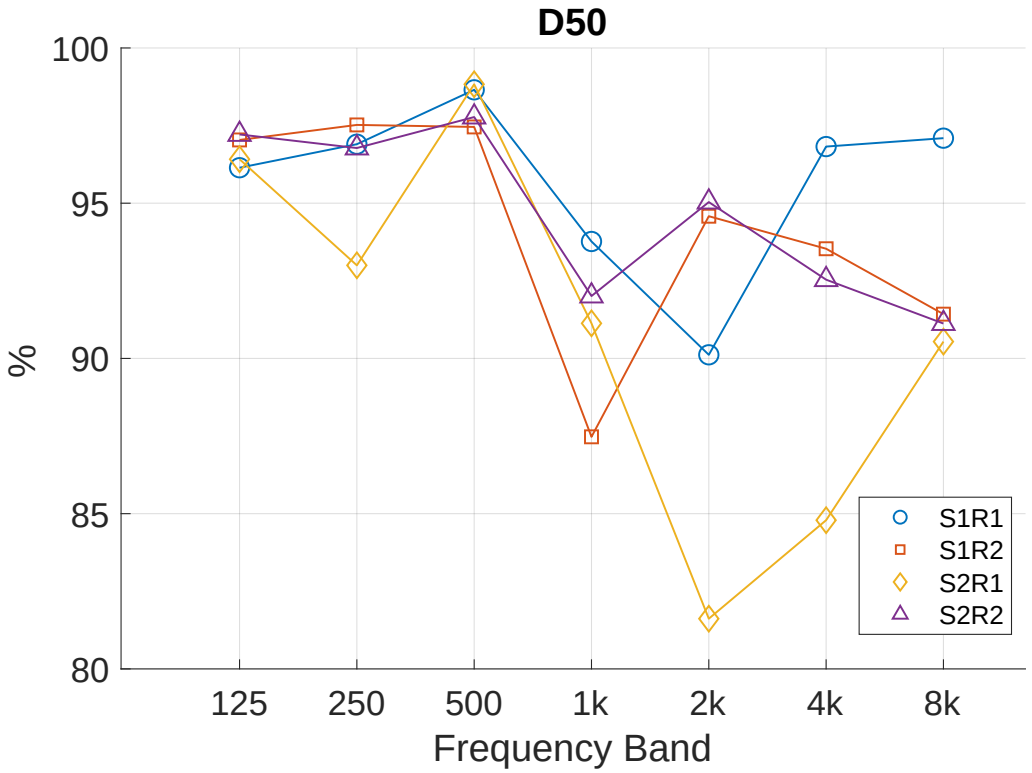

FIGURE 4.6: Defenition (D50) of four IRs at octave bands ranging from 125 Hz to 8 kHz.

finding agrees well with the previous studies indicating that the tree trunks are the key factor in sound propagation above 1 kHz [28, 33, 34].

4.1.4 S1R1 IR SIRR analysis

As discussed in Section 4.1.1, reflections in a forest environment are typically caused by trees. In order to further investigate these features, the directional information needs to be examined by conducting spatial impulse response rendering (SIRR) analysis [21]. Fig. 4.8 shows the SIRR plot up to 5 kHz of IR at position S1R1. Only the horizontal plane was considered in the SIRR analysis, considering the open nature of a forest environment limits the significant directional information in this plane [21]. Each arrow represents the direction of sound in each time-frequency frame. The time frame of each arrow is 1.39 ms. The overlaid spectrogram was generated with the W-channel of the IR.

It can be observed that SIRR plot shows a strong direct sound followed by a set of early reflections coming from different directions. At certain points in time, clusters of arrows can be

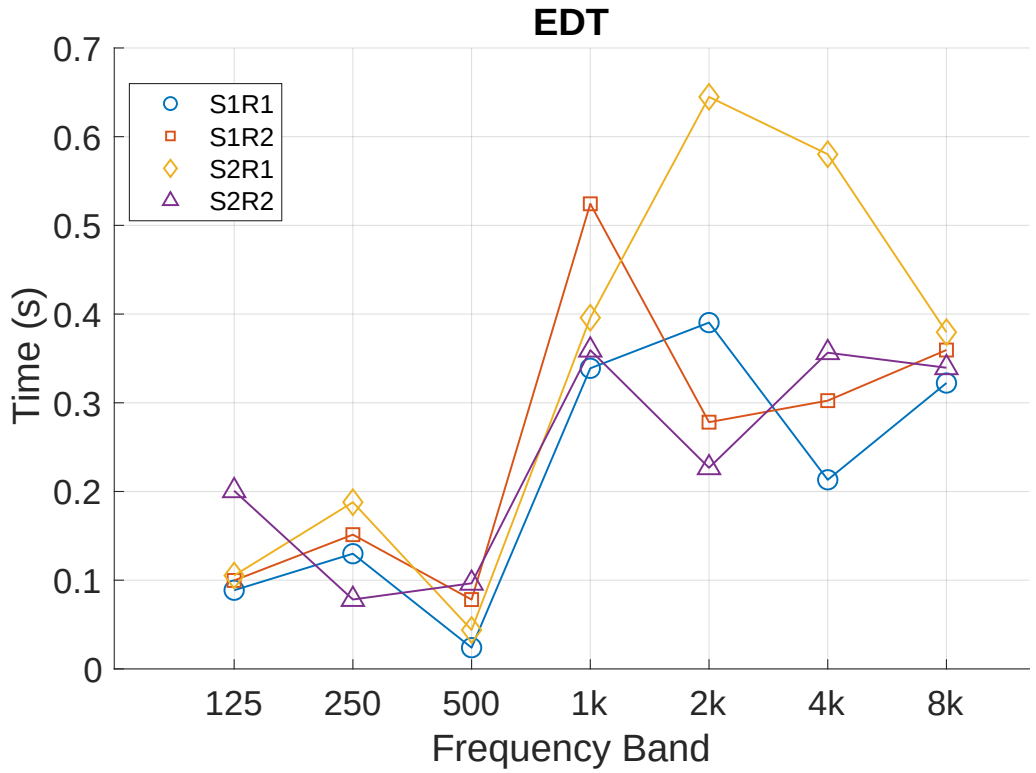

FIGURE 4.7: Early decay time (EDT) of four IRs at octave bands ranging from 125 Hz to 8 kHz.

found lining up and pointing in the same direction along the frequency axis. This plot shares similarities with the SIRR plot in the forest in Koli National Park, which is shown in Fig. 2.4. The distinct reflections are typically from tree trunks [3]. These features can be examined by noting line-up directional vectors and their timing from the SIRR plots and relating these to forest layout and the potential tree truck reflection results (shown in Table. 4.1). It should be noted that the line-up vectors are found mostly at the first approximately 50 ms. The measured path difference between the source-receiver and source-tree-receiver indicates the longest distance is 26.03 m (shown in Table. B.5). The associated timing of the reflections is approximately 76 ms, which should be sufficient for this analysis. Table. 4.2 shows the results of trees cause first-order reflections identified from the SIRR plots at position S1R1. The speed of sound used in this calculation is 343 m/s. The arrow pointing right is defined as 0°, and the arrow pointing downward, left and upward are defined as 90°, 180° and 270°, respectively. Fig. 4.9 shows the diagram of these reflection paths from trees at position S1R1.

The results include the trees that might cause reflections and contribute to the well pronounced

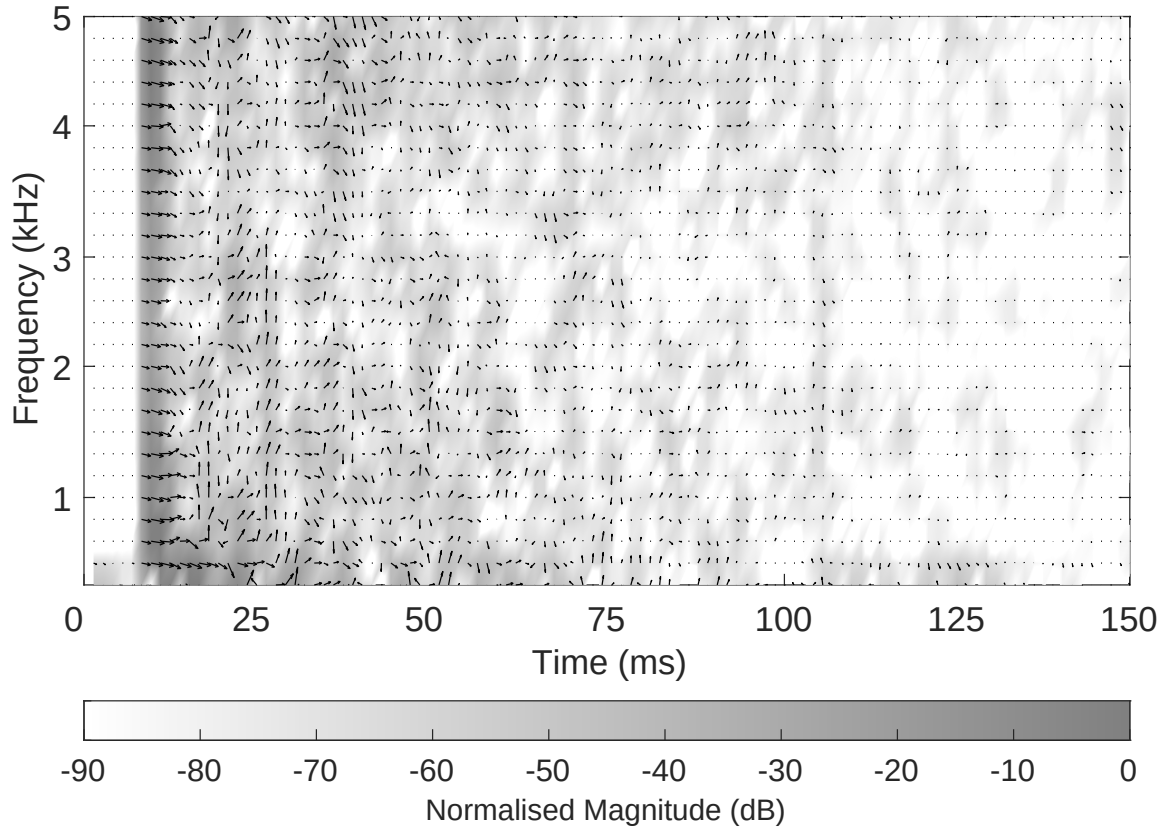

FIGURE 4.8: SIRR analysis plot of IR at position S1R1. The time-frequency distribution of sound intensity vectors **I** in the horizontal plane, overlaid on a spectrogram of the W-channel recording.

Timing of early reflections	Arrow pointing	Frequency range	First-order reflections cause by *Tree*
First 4.2 ms	0°	0-5 kHz	*O*, *R*, *V*
9.7 - 11.1 ms	315°	1-2 kHz	*K*
13.9 - 20.8 ms	270°	0-3 kHz	*H*

TABLE 4.2: Trees caused first-order reflections at position S1R1.

direct sound, as the path difference of the trees is relatively short. It should be noted that not all the distinctive vectors can be related directly to the trees, hence, some relatively strong arrows were not included in the results. As indicated in the modelling work of source localisation in an open space, the calculation of the reflections up to third order can present better results, this suggests the importance of these reflections in the outdoor environments [21]. In some cases, the potential tree reflection fits well in the timing, where the tree location does not agree with the directional vector. This might be due to the presence of second or third-order reflections,

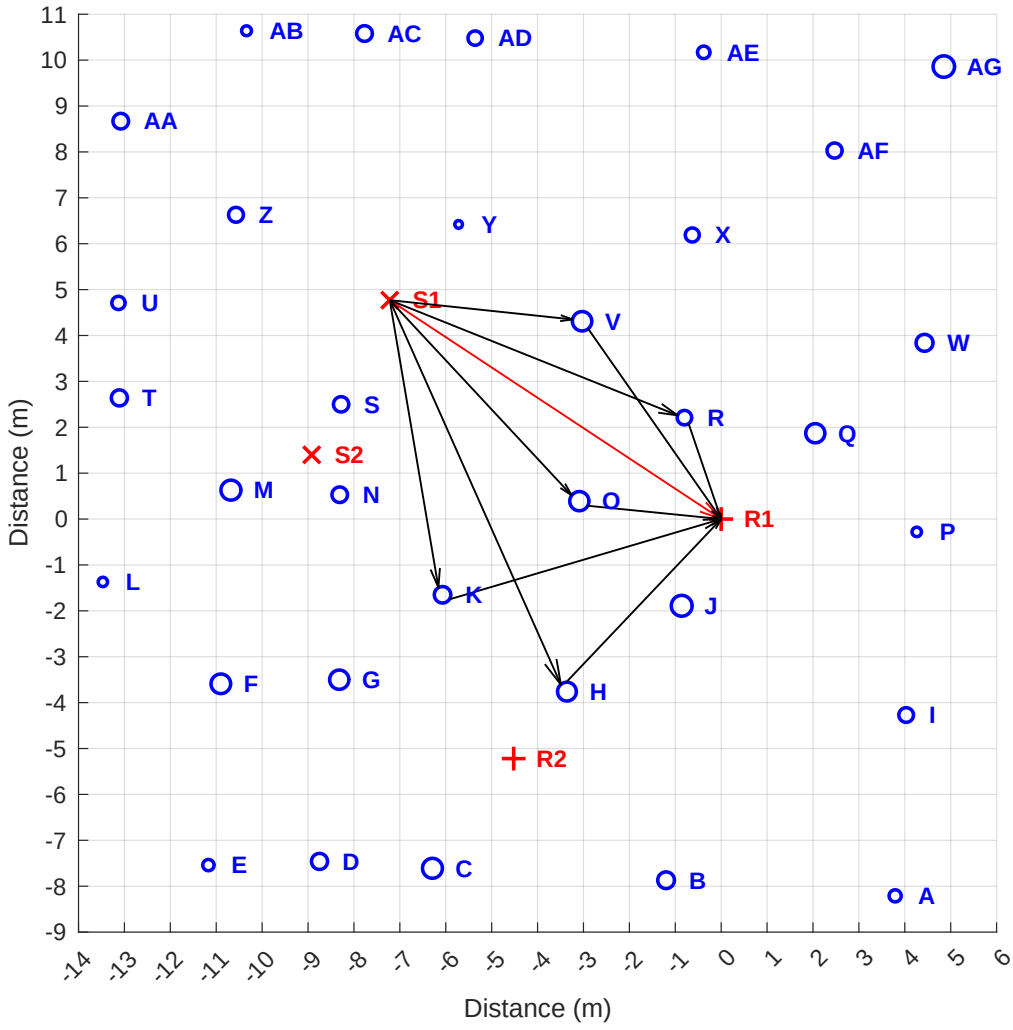

FIGURE 4.9: Diagram of reflection path from trees at position S1R1. The red line indicates the direct sound path from the source to the receiver. The black lines indicate the acoustic paths that form the first-order reflections.

which can potentially alter the direction of the arrow. Generally, SIRR analysis results further identify the reflections from trees at position S1R1.

4.1.5 S1R1 IR auralisation

This section will critically listen to the auralisation results at position S1R1, including drums and singing. The results were convolved with B-format IR recorded with Soundfield microphone, then converted to mid-side stereo. The anechoic audio can be found in Appendix C.1.3; The auralisation results at different IR positions can be found in Appendix C.1.4.

Fig. A.23 shows the spectrogram of a snare drum, which is trimmed from the drum audio. The magnitude shows a noise-like strong energy at frequencies approximately from 200 to 300 Hz. The harmonic frequencies also show relatively clusters of strong energy. The snare drum sounds hard and precise with a penetrating feature.

Fig. 4.10 shows the spectrogram of an auralised snare drum at position S1R1. The result shows the right channel of the mid-side stereo signal. Additionally, both channels of the signals were compared and showed similar results, the following auralised results are all generated using the right channel of the signal. Fig. 4.10 indicates that there is a loss of energy at the fundamental frequency range compared to Fig. A.23, and there is greater energy at the harmonic frequency range. The sound of the auralised snare is brighter and less shrill compared to the anechoic sound. The reverberation can be perceived and the decay time is relatively short. The auralised drum has a significant bass response from the space, which can be related to the lack of low frequency attenuation in a forest environment. The clarity of the drums is generally good. The dynamic changes in the piece can be perceived, indicating a good spatial responsiveness. These relate to the large values in the D50 (shown in Fig. 4.6). It should be noted that the noise recorded in the IR might have an impact on the result, as it can be heard in the auralised results.

Fig. A.24 shows the anechoic singing note at approximately 680 Hz. It can be observed that the magnitude is greatly pronounced at the fundamental frequency and the second-harmonic frequency. The dynamic can be found in the speech, where the energy shows a variation over time at these harmonic frequencies. The sound of the anechoic singing is rich and soft.

Fig. 4.11 shows the strong magnitude at the fundamental frequency, and relatively less pronounced energy at the second-harmonic frequency. The timbre of the auralised singing piece is more warm compared to the anechoic singing. The perceived size of the space is relatively large. The clarity is good and the dynamic changes in the singing can be easily perceived. The openness can be used to describe a forest environment, where there is a fair amount of perceivable reverberation as well as good clarity [52].

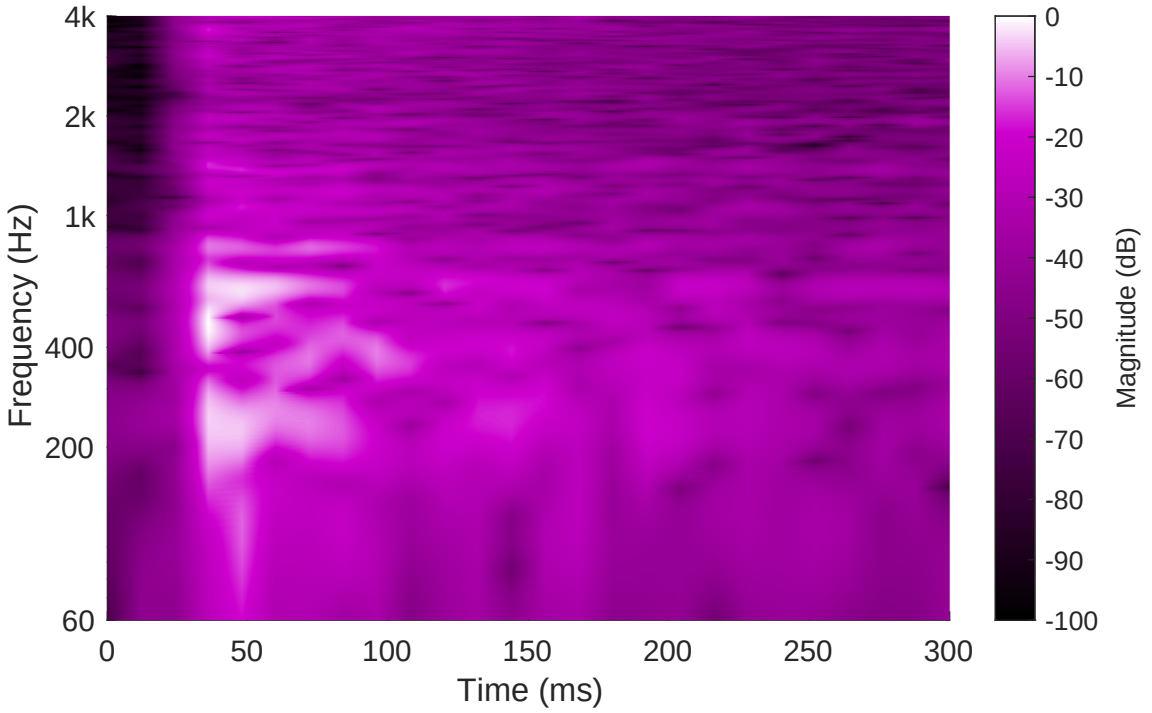

FIGURE 4.10: A spectrogram of an auralised snare drum at position S1R1. The result shows the right channel of the mid-side stereo signals.

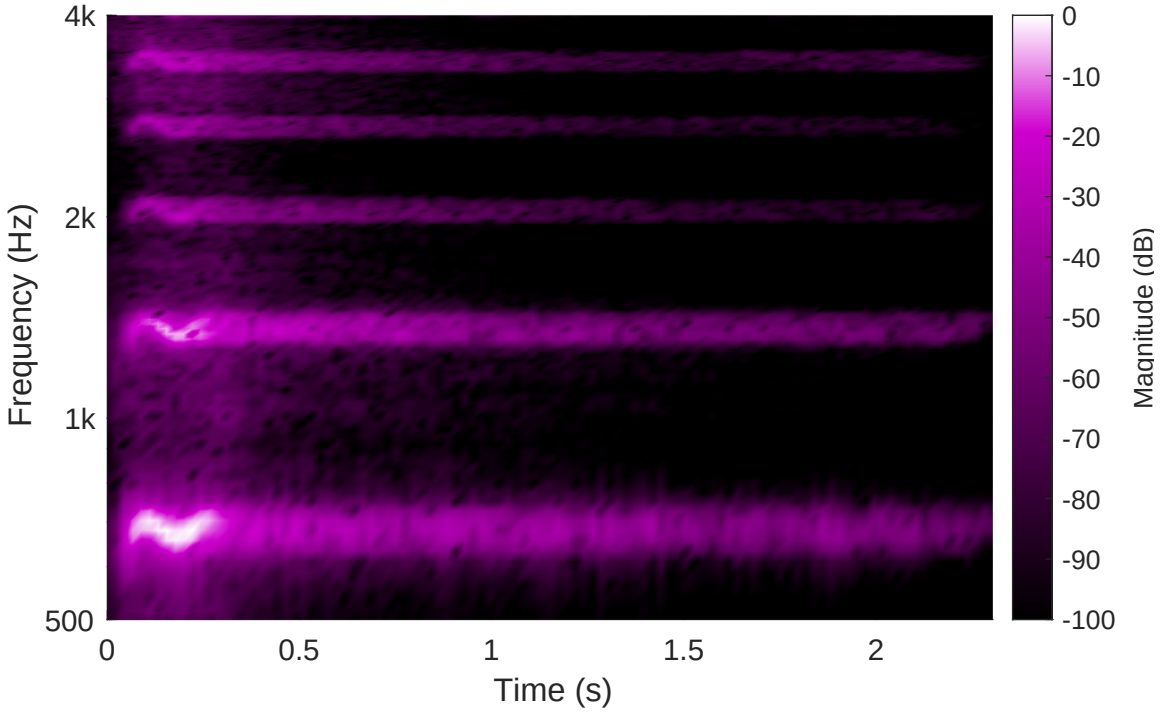

FIGURE 4.11: A spectrogram of an auralised singing note at position S1R1.

4.2 S1R2 IR analysis

This section will analyse the IR recorded at S1R2. At this position, there is a clear line of sight between the source and receiver and the measured distance between them is 10.32 m, Fig. 3.10

shows this layout.

4.2.1 S1R2 IR waveform analysis

The waveform plot of the IR at position S1R2 shows a strong direct sound followed by distinctive early reflections (shown in Fig. 4.12). Similar results can be observed from the waveform of the IR at position S1R1. The characteristics of tree trunk reflections are also investigated, results are shown in Table. 4.3.

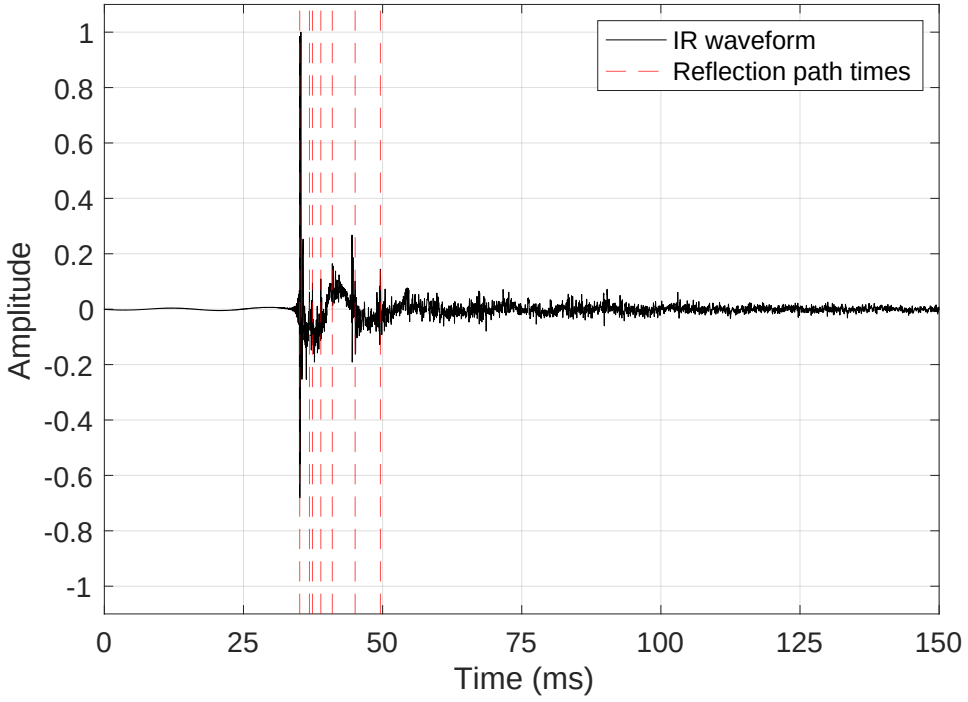

FIGURE 4.12: Waveform plot of impulse response at position S1R2. The red dot lines indicate the timing of the early reflections.

4.2.2 S1R2 IR spectrogram analysis

Fig. 4.13 shows the spectrogram plot of the first 100 ms of the IR recorded at position S1R2. The spectrogram shows a strong direct sound. The energy is greatly pronounced below 500 Hz and between 2 kHz to 3 kHz. A strong energy tail below 500 Hz after the direct sound is also indicated in the results.

Timing of early reflections	Path difference	Potential reflection at *Tree*
0.41 ms	0.14 m	K (0.1 m)
2.17 ms	0.74 m	S (0.73 m)
2.71 ms	0.93 m	H (0.92 m) N (0.92 m)
4.21 ms	1.44 m	O (1.49 m)
6.27 ms	2.15 m	G (2.21 m)
10.38 ms	3.56 m	M (3.53 m) V (3.54 m) Y (3.61 m)
14.92 ms	5.12 m	R (4.92 m) C (5.08 m)

TABLE 4.3: Potential trees caused first-order reflections at position S1R2.

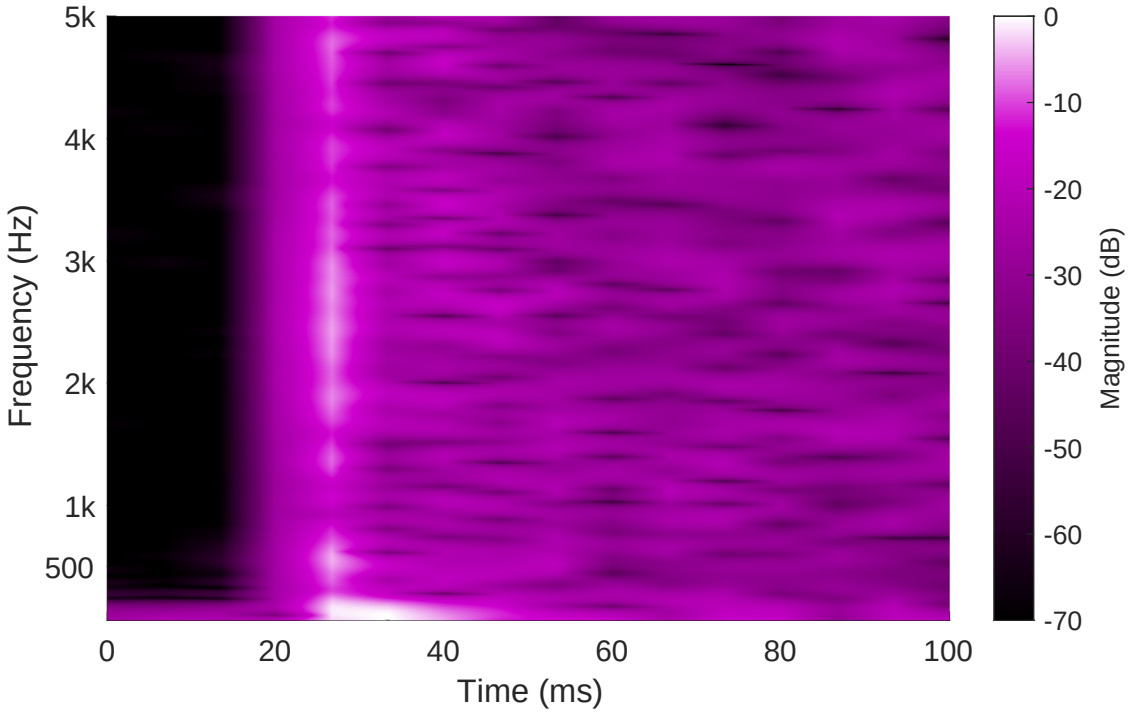

FIGURE 4.13: Spectrogram plot of impulse response recorded at position S1R2.

4.2.3 S1R2 IR ISO 3382 acoustic parameter analysis

Fig. 4.5 shows that the T30 of the IR at position S1R2 shows a similar trend as the results at position S1R1, where the values at octave bands from 500 Hz to 2 kHz are higher than the other octave bands. A greatly pronounced reverberation time (2.5 s) is indicated at octave band 1 kHz, which might be exaggerated due to the distinctive bird song recorded in the sweep. The reduction of D50 values is found at 1 kHz which is around 87%, and a 0.5 s of early decay time (EDT) is also found concentrated at 1 kHz.

4.2.4 S1R2 IR SIRR analysis

Fig. 4.14 shows the results of the SIRR analysis plot of IR at position S1R2. Table. 4.4 shows the results of reflections from trees at this position and Fig. 4.15 shows the diagram of the reflection paths. It should be noted that *Tree C* does not fit in perfectly in the suggested reflection time range, where the tolerance is approximately 1.8 ms (and the associated distance is 0.6 m). Considering the directional vector form by this tree agrees well with well-pronounced arrows in the SIRR plot, and there might be potential second-order reflections caused by this tree, the results are presented in this manner.

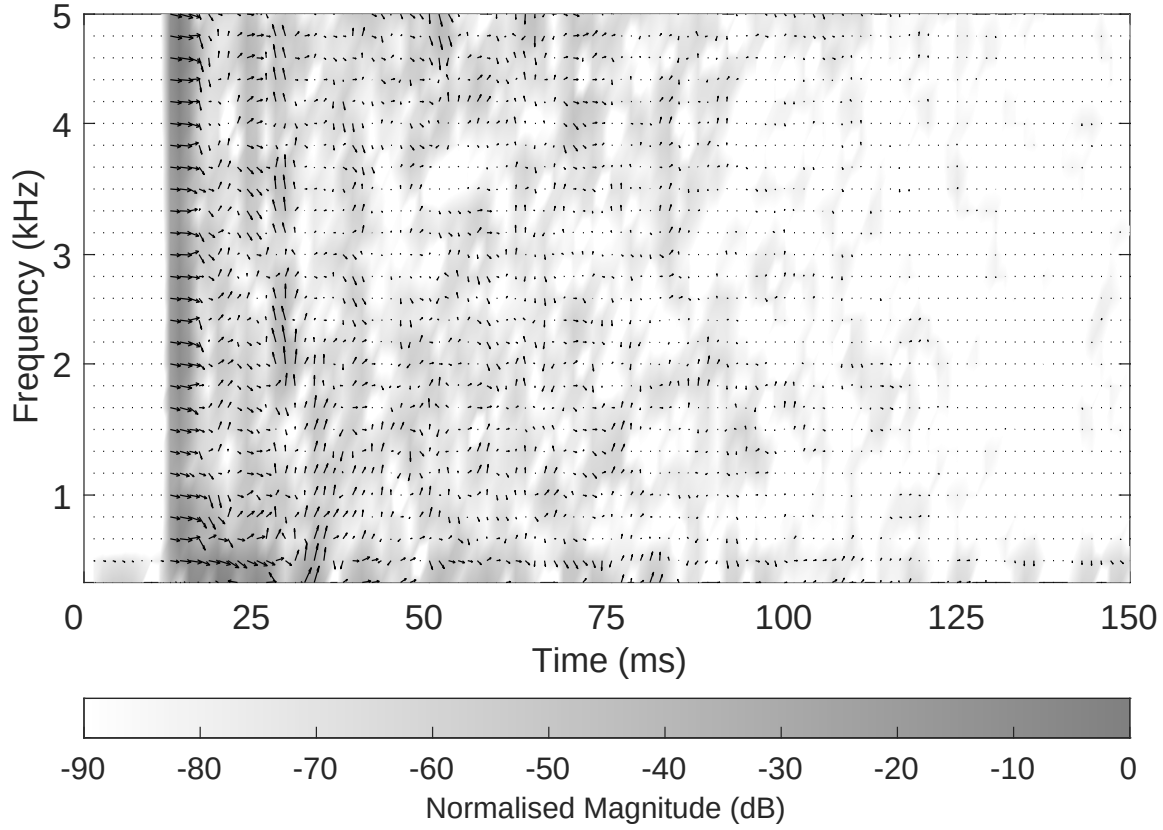

FIGURE 4.14: SIRR analysis plot of IR at position S1R2.

4.2.5 S1R2 auralisation

Fig. A.25 shows the results of the auralised snare drum at position S1R2. The clusters of energy are indicated in the results, which are similar to the anechoic spectrogram (shown in

Timing of early reflections	Arrow pointing	Frequency range	First-order reflections cause by *Tree*
First 4.2 ms	0°	0-5 kHz	*K*, *S*, *H*, *N*, *O*
8.3 - 9.7 ms	315°	1-5 kHz	*M*
11.1 - 13.9 ms	45°	1-4 kHz	*V*, *Y*
16.7 - 18 ms	225°	2-5 kHz	*C*

TABLE 4.4: Trees caused first-order reflections at position S1R2.

Fig. A.23). The sound of the auralised snare is more bright and hard compared to the anechoic snare. Generally, the whole drum piece sounds share similarities to the auralisation results at position S1R1.

The auralised singing results show a better pronounced energy at the second harmonic frequency (shown in Fig. A.26). At position S1R2, the sharpness of attack can be perceived clearer than at position S1R1. This indicates a better listening position than at position S1R2.

4.3 S2R1 IR analysis

This section will analyse the IR recorded at S2R1. At this position, there is an impeded tree, *O*, between the source and receiver. The measured distance between them is 9 m, and the distance between the source and *Tree O* is 5.71 m, Fig. 3.10 shows this layout.

4.3.1 S2R1 IR waveform analysis

Fig. 4.16 shows the waveform plot of IR at position S2R1, and Table. 4.5 shows the results of reflections from trees indicated from the waveform. The distinctive early reflections shown in the waveform share similarities with the results at positions S1R1 and S1R2.

4.3.2 S2R1 IR spectrogram analysis

Fig. 4.17 shows the spectrogram plot of IR at position S2R1. The direct sound shows a less pronounced energy above 1 kHz. This is due to the impeded tree, which causes absorption

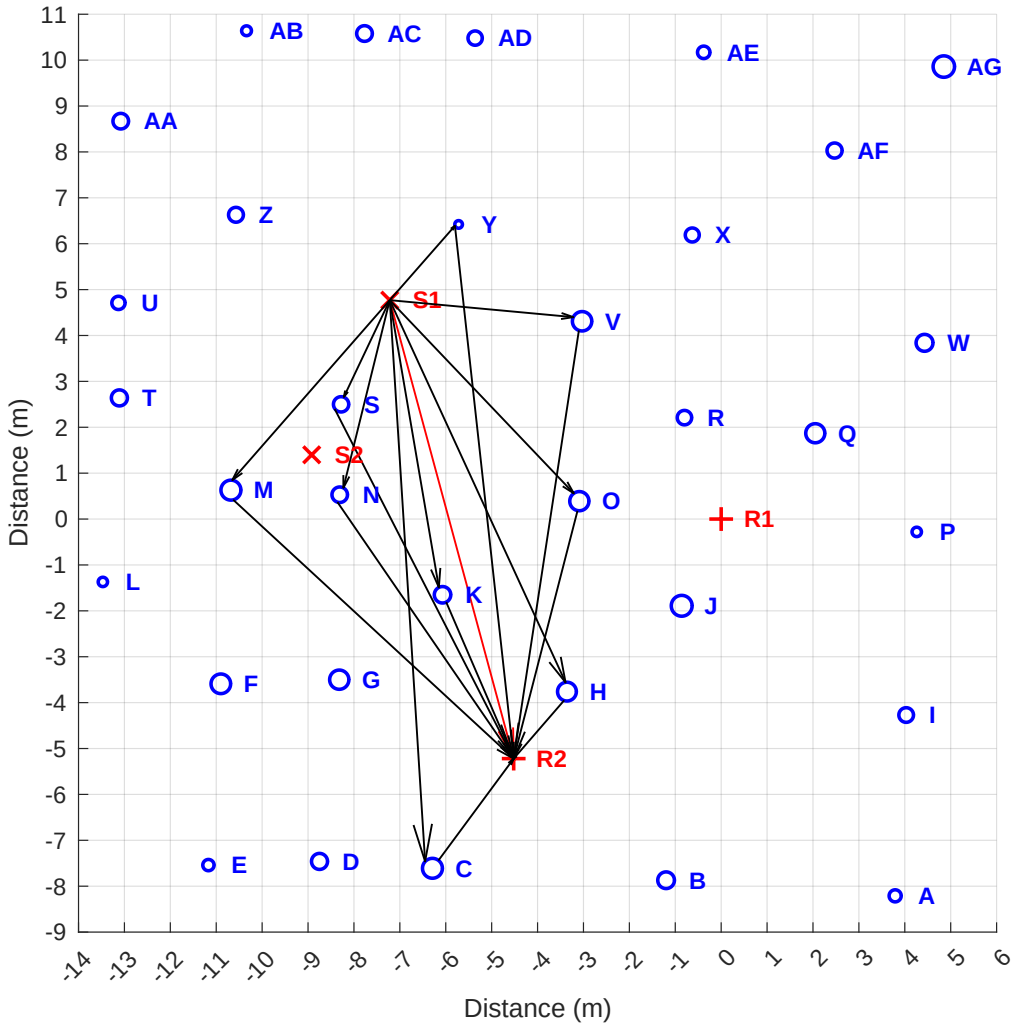

FIGURE 4.15: Diagram of reflection path from trees at position S1R2. The red line indicates the direct sound path from the source to the receiver. The black lines indicate the acoustic paths that form the first-order reflections.

at the high frequencies. Additionally, diffraction might become relatively important in sound propagation when there is no line of sight between the source and receiver [21].

4.3.3 S2R1 IR ISO 3382 acoustic parameter analysis

The reverberation time shows similar values to the results in position S1R1, which is shown in Fig. 4.5. In Fig. 4.6, D50 at position S2R1 indicates a concentrated reduction at the 2 kHz octave band, which is approximately 82%. It's noted that with a clear line of sight from source to receiver, the sound should arrive directly to aid the definition value [53]. Without a clear line of sight, the direct sound from source to receiver is attenuated, which results in an increase

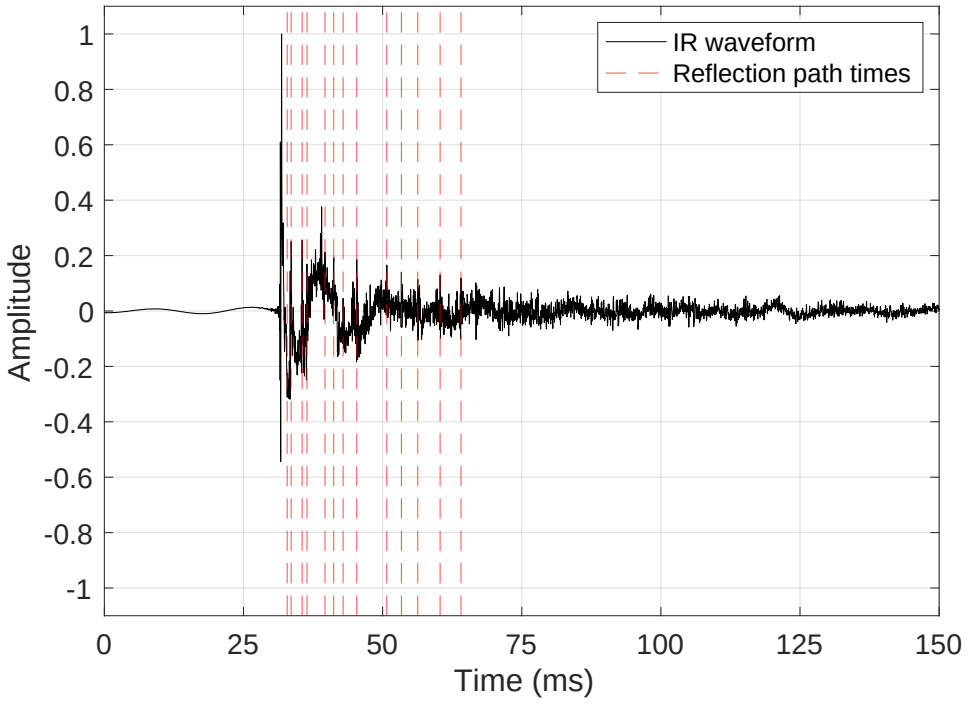

FIGURE 4.16: Waveform plot of impulse response recorded at position S2R1. The red dot lines indicate the timing of the early reflections.

Timing of early reflections	Path difference	Potential reflection at *Tree*
1.41 ms	0.48 m	*N* (0.42 m)
2.13 ms	0.73 m	*S* (0.89 m)
4.10 ms	1.41 m	*K* (1.47 m) *R* (1.52 m)
4.98 ms	1.71 m	*J* (1.79 m)
8.21 ms	2.82 m	*V* (2.82 m)
9.77 ms	3.35 m	*H* (3.65 m)
11.46 ms	3.93 m	*M* (3.72 m)
13.92 ms	4.77 m	*Q* (4.77 m) *G* (5 m)
19.31 ms	6.62 m	*X* (6.81 m)
21.94 ms	7.52 m	*F* (7.85 m)
24.88 ms	8.53 m	*T* (8.75 m)
28.89 ms	9.91 m	*E* (10.29 m) *U* (10.3 m)
32.64 ms	11.20 m	*D* (11.38 m)

TABLE 4.5: Potential trees caused first-order reflections at position S2R1.

in energy decay [9]. This feature can be observed at position S2R1, the reduction can be found in octave bands 250 Hz, 2 kHz and 4 kHz, compared to the D50 at *Source 1* positions. The early decay time is greatly pronounced at octave bands 2 kHz and 4 kHz, which show values of

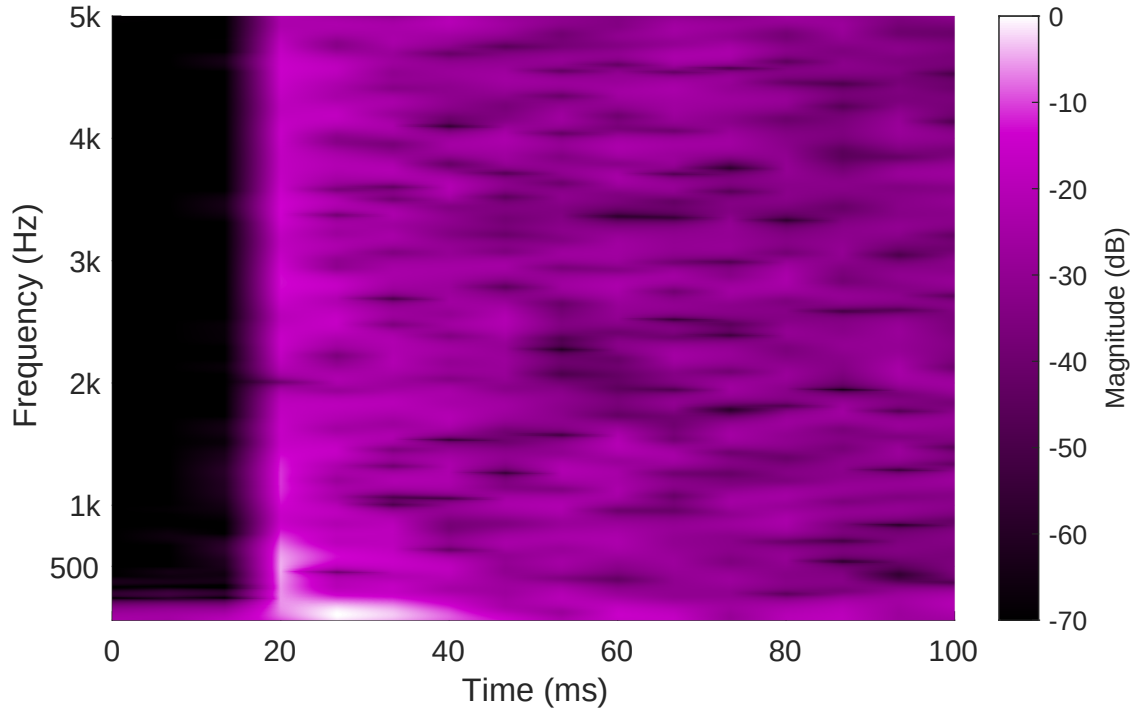

FIGURE 4.17: Spectrogram plot of impulse response recorded at position S2R1.

around 0.6 s.

4.3.4 S2R1 IR SIRR analysis

Fig. 4.18 shows the results of SIRR at position S2R1. Table. 4.6 shows the reflections from trees at this position and Fig. 4.19 shows the diagram of the reflection paths.

Timing of early reflections	Arrow pointing	Frequency range	First-order reflections cause by *Tree*
First 5.6 ms	0°	0-5 kHz	*N*, *S*, *K*, *R*, *J*
22.2 - 23.6 ms	45°	1-4 kHz	*X*

TABLE 4.6: Trees caused first-order reflections at position S2R1.

It should be noted that *Tree X* shown in the results do not fit perfectly in the suggested reflection time range, the tolerance is approximately 2.3 ms (and the associated distance is 0.8 m). Given that there are potential second-order reflections, the results present this tree. Additionally, all paths shown in Fig. 4.19 have a clear line of sight between the two points, as these are based on the layout measurement results and the recreated layout does show clear

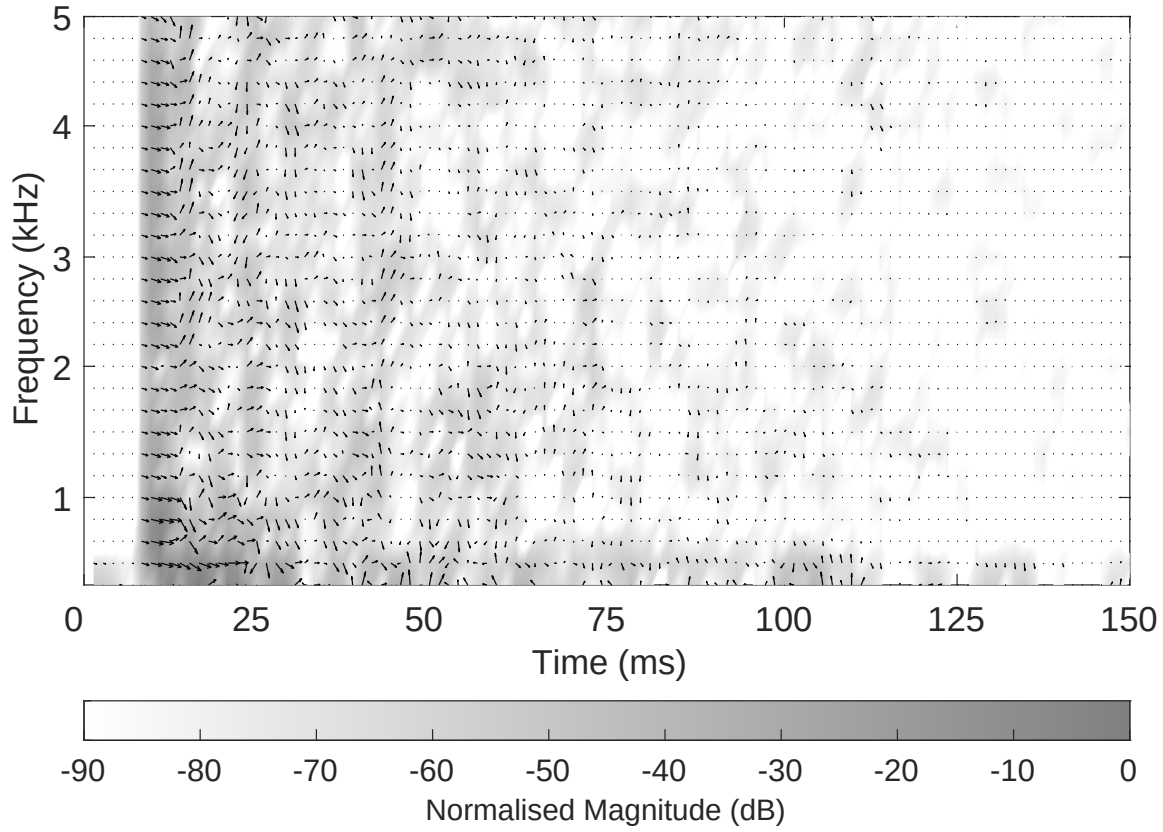

FIGURE 4.18: SIRR analysis plot of IR at position S2R1.

paths. Although it might seem slightly unclear in some cases, such as *Tree O* appears to be in the way of the path from *Tree N* to *Receiver 1*. But for the sake of a clear diagram, the results are presented in this manner.

It's interesting to note that the vectors of two trees that have similar path differences can potentially form the direct sound direction. For instance, the path difference between *Tree J* and *Tree R* is relatively short (0.27 m), and the angles of the two incident waves are approximately symmetrical to the direct sound path. As suggested in Fig. 4.18, between 6.9 ms and 8.33 ms, there are clusters of arrows pointing 315°, which might be formed by the second-order reflections. A possible pathway can be: *Source 2-Tree K-Tree J-Source 1*, and the timing of this path is 7.32 ms, which fits well into the time range. The blue dot line indicates this path in the reflection diagram in Fig. 4.19.

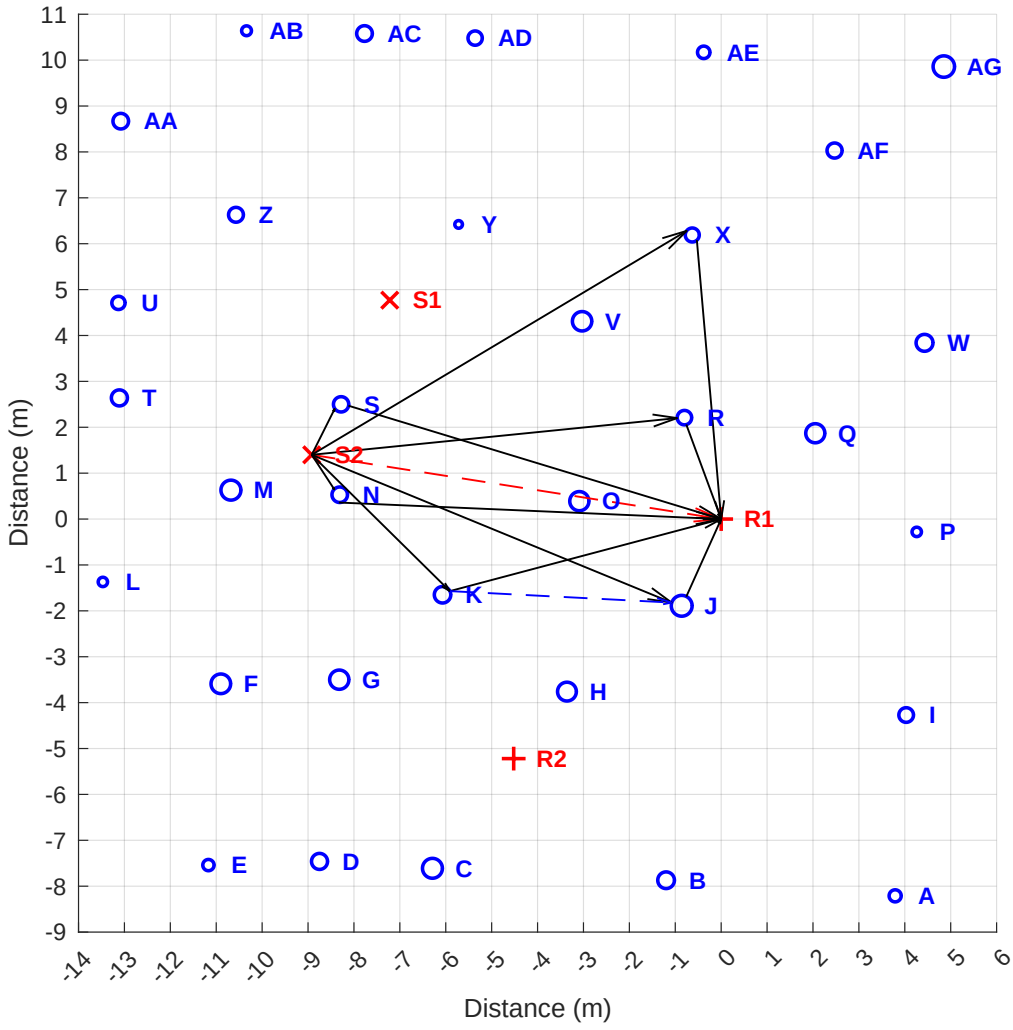

FIGURE 4.19: Diagram of reflection path from trees at position S2R1. The red dot line indicates the direct path from the source to the receiver, which is impeded by *Tree O*. The black lines indicate the acoustic paths that form the first-order reflections. The blue dot line indicates the potential second-order reflection path that is formed by *Tree K* and *Tree J*.

4.3.5 S2R1 IR auralisation

Fig. A.27 shows the spectrogram of the auralised snare drum at position S2R1. It clearly indicates a stronger magnitude with a longer duration. The snare at this position sounds muffled and less precise. The clarity of the whole drum piece is less pronounced compared to the auralisation at *Source 1* position, especially the hi-hat. This relates to the spectrogram of the IR, which indicates the energy loss at high frequencies. The source of presence is less evident at this position, which can be related to the physical property of an impeded tree between the source and receiver.

The spectrogram of the singing note shows less pronounced energy at the second harmonic frequency. The auralised result sounds less clear, and the dynamic changes in the piece are less evident than the results at *Source 1* position. This relates to the D50 shows relatively low values at 2 kHz and 4 kHz octave bands, which is about 85%. It should be noted that the value is still very high, given the space is an outdoor environment.

4.4 S2R2 IR analysis

This section will analyse the IR recorded at S2R2. At this position, there is an impeded tree, *N*, between the source and receiver. The measured distance between them is 7.91 m, and the distance between the source and *Tree N* is 0.9 m, Fig. 3.10 shows this layout.

4.4.1 S2R2 IR waveform analysis

Fig. 4.20 shows the waveform plot of IR at position S2R2, and Table. 4.7 shows the results of reflections from trees indicated from the waveform. The waveform results share similar characteristics as the other IR results.

Timing of early reflections	Path difference	Potential reflection at *Tree*
0.54 ms	0.19 m	*K* (0.17 m)
3.44 ms	1.18 m	*G* (1.23 m)
4.56 ms	1.56 m	*H* (1.56 m)
6.42 ms	2.20 m	*S* (1.90 m) *M* (2.51 m)
11.08 ms	3.80 m	*O* (3.80 m) *F* (4.06 m)
12.58 ms	4.32 m	*C* (4.49 m)
16.54 ms	5.67 m	*J* (5.75 m) *D* (5.77 m)
23.92 ms	8.20 m	*T* (8.09 m) *U* (8.26 m) *E* (8.37 m) *R* (8.55 m)

TABLE 4.7: Potential trees caused first-order reflections at position S2R2.

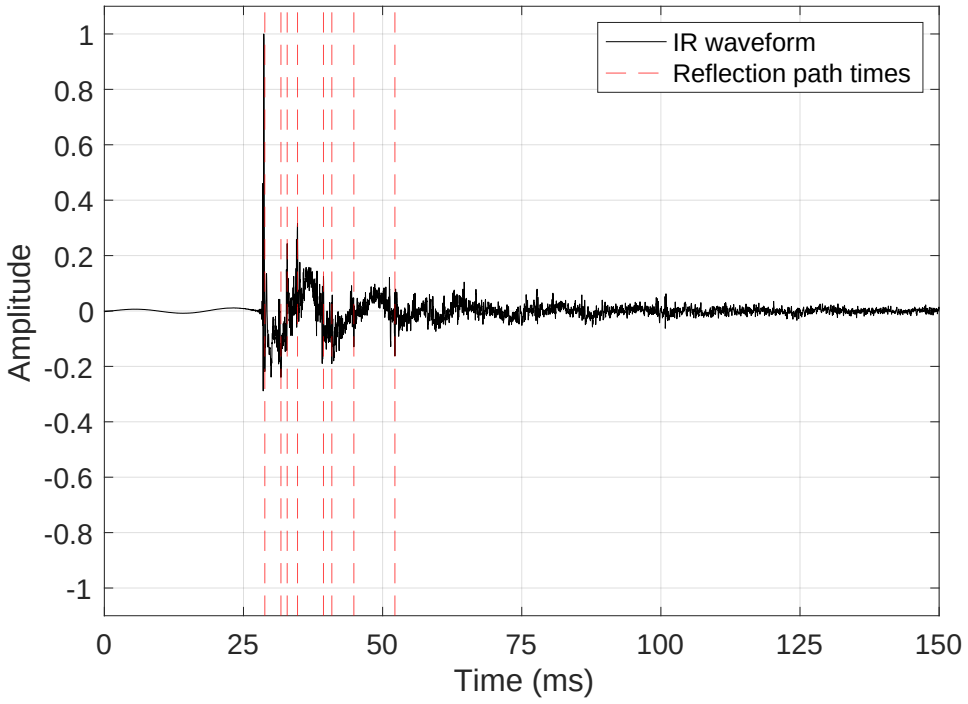

FIGURE 4.20: Waveform plot of impulse response recorded at position S2R2. The red dot lines indicate the timing of the early reflections.

4.4.2 S2R2 IR spectrogram analysis

Fig. 4.21 shows the spectrogram of IR at position S2R2. The result shows less pronounced energy of the direct sound below 500 Hz compared to position S2R1. There are segments of low energy along the direct sound axes up to 2 kHz. This relates to the sound absorption caused by the impeded tree at this position.

4.4.3 S2R2 IR ISO 3382 acoustic parameter analysis

T30 values show similar results to the other IR positions, the highest value of 2 s is found at 1 kHz octave band. The D50 values are very high, which are above 91%. A 0.35 s of the highest EDT value is found at 1 kHz.

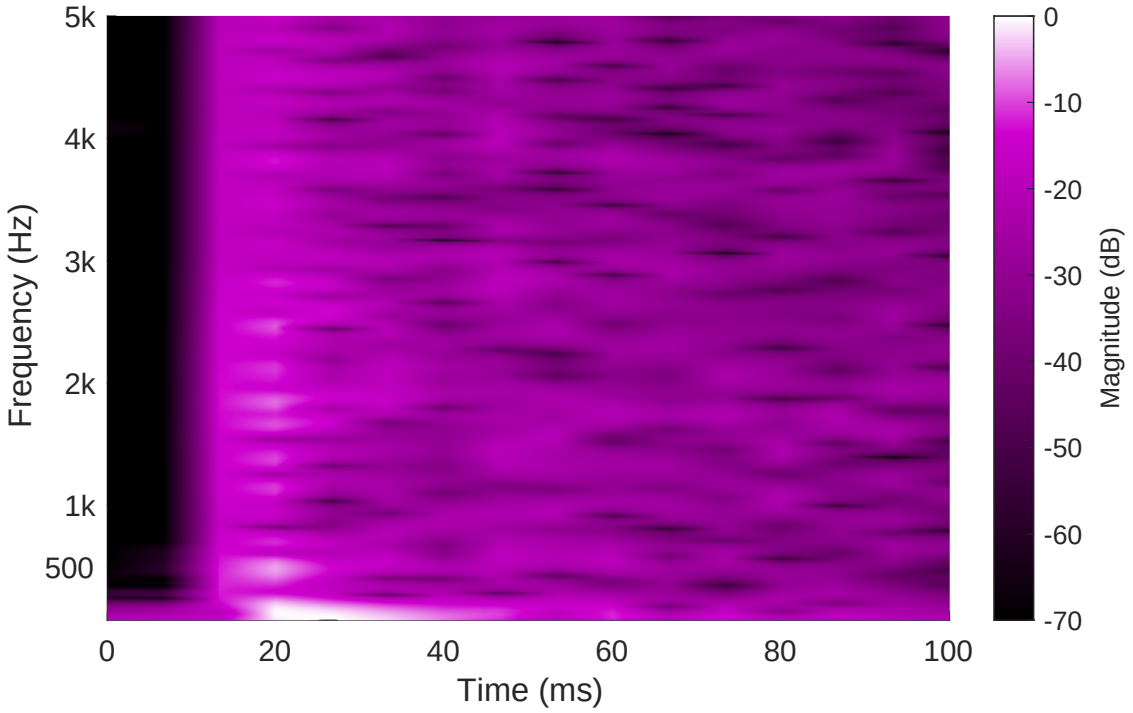

FIGURE 4.21: Spectrogram plot of impulse response recorded at position S2R2.

4.4.4 S2R2 IR SIRR analysis

Fig. 4.22 shows the results of SIRR analysis at position S2R2. Table. 4.8 shows the results of reflections from trees and Fig. 4.23 shows the reflection path at this position.

Timing of early reflections	Arrow pointing	Frequency range	First-order reflections cause by *Tree*
First 11 ms	0°	0-5 kHz	*K*, *G*, *H*, *S*, *M*, *O*, *F*
15.3 - 16.7 ms	270°	2-5 kHz	*D*
18 - 23.6 ms	270°	2-4 kHz	*E*

TABLE 4.8: Trees caused first-order reflections at position S2R2.

In Fig. 4.22, the direct sound indicates a longer duration at this position. This is due to the impeded *Tree N* being closer to the source at S2R2, the direct sound is attenuated and the reflection paths are more apparent, which increases the energy decay [9].

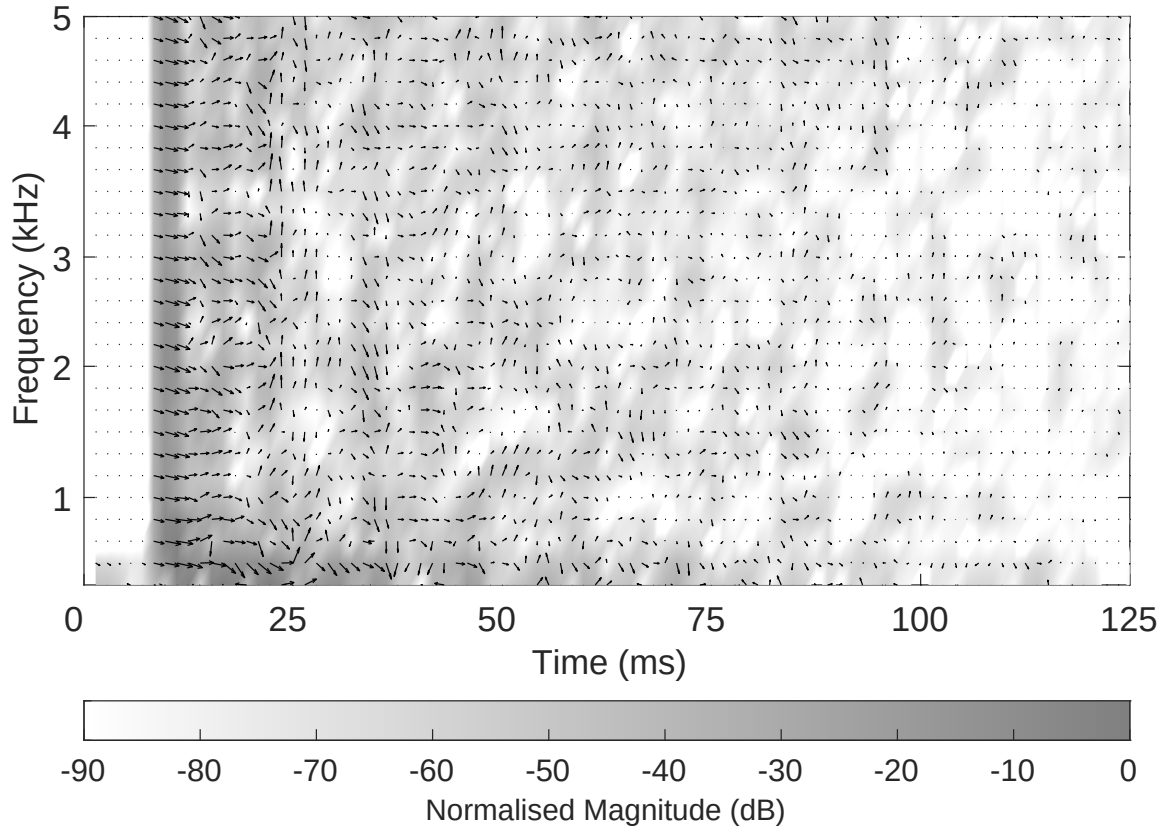

FIGURE 4.22: SIRR analysis plot of IR at position S2R2.

4.4.5 S2R2 IR auralisation

Fig. A.29 shows the spectrogram of the auralised snare drum at position S2R2. The magnitude shows relatively less energy compared to the anechoic result. The whole piece is also muffled but the clarity is evidently better than the result at position S2R1, especially the hi-hat. This relates to the D50 values being relatively higher. The cymbal is less clear compared to the results at *Source 1* positions, where the source of presence is less pronounced. This is related to the physical property that at this position, there is no clear line of sight between the source and the receiver.

Fig. A.30 shows the spectrogram of the auralised singing. It shows a similarity with the result at position S1R1. The clarity of the singing piece is good, but the sharpness of attack is less clear than at position S1R1.

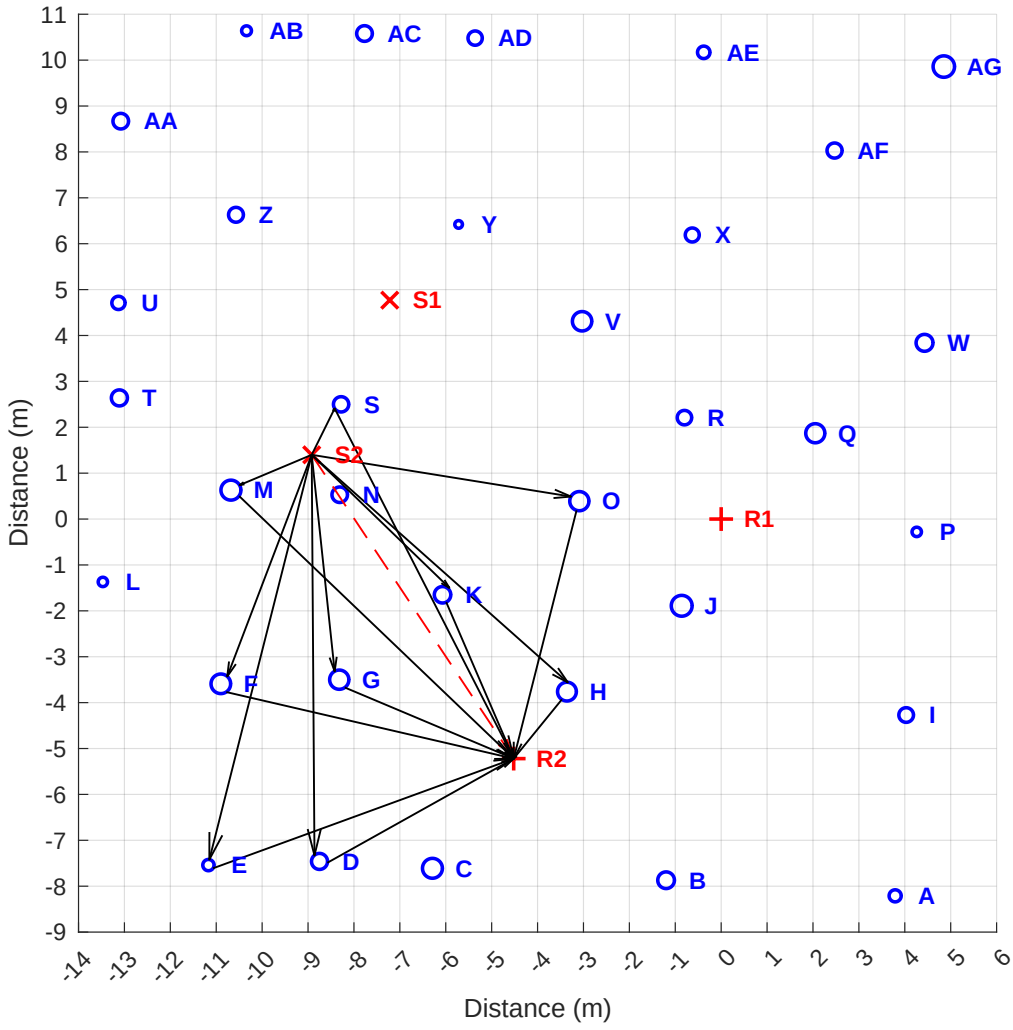

FIGURE 4.23: Diagram of reflection path from trees at position S2R2. The red dot line indicates the direct path from the source to the receiver, which is impeded by *Tree N*. The black lines indicate the acoustic paths that form the first-order reflections.

4.5 Comparison of the forest IRs

Fig. 4.24 shows a comparison plot of the spectrum of four IRs from 80 Hz to 16 kHz in one-third octave bands. This is obtained by filtering the IRs into one-third octave bands and then calculating the dBFS values (decibels relative to full scale) for each band.

It should be noted that there is an increase in magnitude above 8 kHz at position S1R2, this might be due to the bird songs recorded in the sweep and the deconvolution generated extra high-frequency content. All these four IR magnitudes in different octave bands show similar trends. Below 800 Hz, there is a strong energy indicated at 500 Hz and a reduction at 250

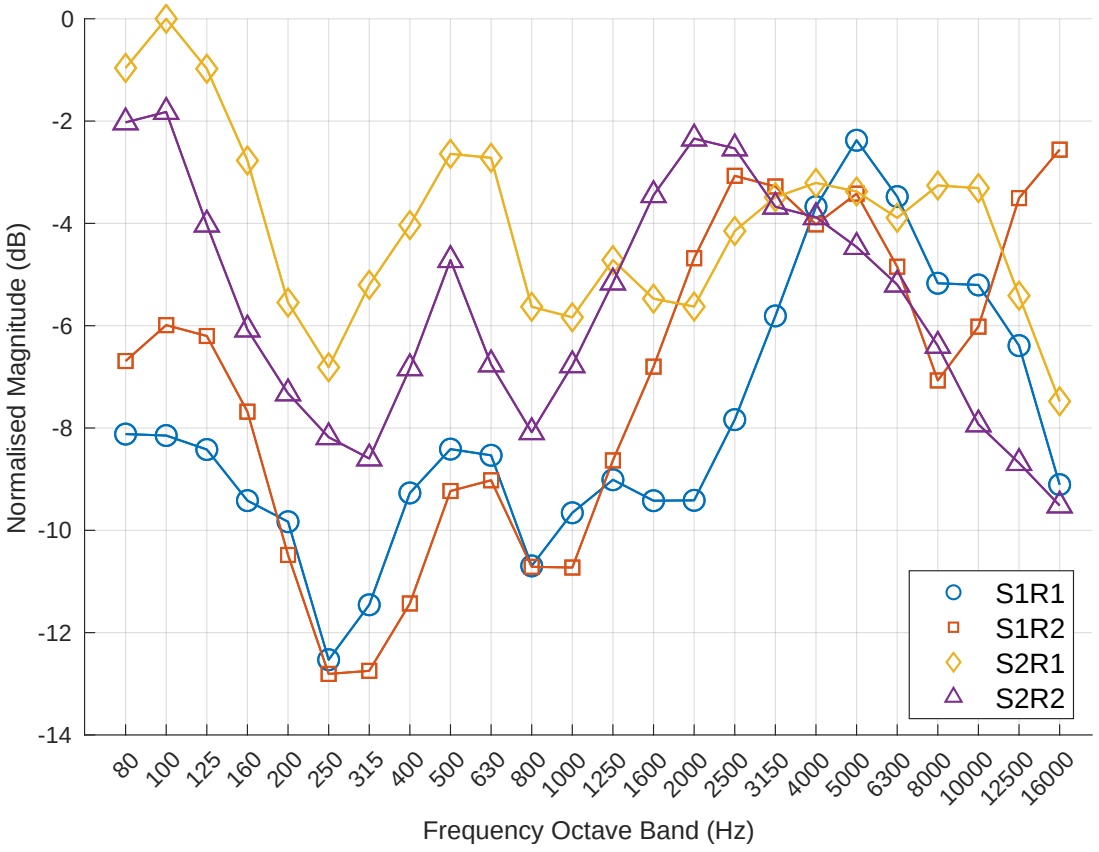

FIGURE 4.24: A comparison plot of the spectrum of four IRs from 80 Hz to 16 kHz in one-third octave bands.

Hz. This is due to the ground reflections. The magnitude is greatly pronounced at frequencies ranging from 2 kHz to 5 kHz due to the tree trunk reflections. Sound attenuates significantly above this range, which can be related to the open nature in a forest environment [17]. The spectrum results agree well with the reverberation time acoustic parameter results, which also reveal the frequency dependent feature in forest acoustics.

In Fig. 4.24, the magnitude is greatly pronounced at *Source 2* positions below 800 Hz. The spectrogram at *Source 2* positions indicates the loss of energy above this frequency. The IRs sound more muddy at these positions compared to the results at *Source 1* positions, and the clarity is less pronounced in auralisation results. These can be related to the physical property at *Source 2* positions, where there is no clear line of sight between the source and receiver. The impeded tree results in significant sound absorption at the high frequencies.

The D50 values are larger at position S2R2 than at position S2R1, and the spectrogram of the IR at position S2R2 shows that there are segments of energy above 1 kHz. The SIRR

analysis results show that the direct sound has a longer duration. It is interesting to note that the clarity and source of presence are generally better in S2R2 auralisation results. These results can be related to the impeded tree closer to the source, and the reflection paths become more apparent in sound propagation.

4.6 Conclusion

This chapter has presented an analysis of the forest IR results, and compared the IRs at different source and receiver positions. The similarities between these four IRs define the acoustic characteristics of a forest environment. They are also the key findings of this analysis, which include:

1. Sound attenuation.
    - The energy decay curve shows a rapid regression, as discussed in Section 4.1.3.
    - The definition (D50) presents overall higher values (above 82%) among frequency bands, as documented in Section 4.1.3.
2. Early reflections from tree trunks are key features.
    - The waveform results indicate a greatly pronounced direct sound and distinctive strong early reflections.
    - The reflections from tree trunks can be identified from the waveform and SIRR analysis.
3. Frequency dependent characteristics.
    - There is a lack of attenuation at a frequency range of 1 kHz to 2 kHz, the reverberation time (T30) results are generally above 1.5 s. The highest T30 value of 2 s is found at 1 kHz in this forest environment, indicating the suitability for romantic classical performances at this range [54]. These relate to the tree trunk reflections are the key features in a forest, which aid sound propagation and provide reverberation mainly

at 1 and 2 kHz. Given the sound attenuation at high frequencies in an outdoor space, tree trunks reflect the frequency of sound with wavelengths in a range around tree trunk diameters [17].

- The reverberation time is generally less than 1.3 s below 500 Hz and above 2 kHz, indicating greater sound attenuation. Below 500 Hz, ground interference has an impact on sound propagation [16, 27, 28, 33].

The forest IR results provide support for the *Treeverb* and *WGW* modelling work, as it verifies the significant tree trunk reflections in forest acoustics. In Chapter 5, the approach of modelling tree trunks as rigid cylinders will be further examined using an acoustic scale model.

Chapter 5

Forest Scale Model IR Measurement

This chapter will detail the design of the scale model and cover the IR measurement process. Section 5.1 will document the choice of the scale and the selected materials for modelling the tree trunks and the forest ground. The construction of mounting the modelled tree trunks on the ground will be presented in Section 5.2. In Section 5.3, the scale model IR measurement process will be presented, along with the tweeter response measurement for the later IR equalisation.

5.1 Design the scale model

To build the acoustic model as large as possible, a scale factor of 1:10 was selected for this project, which made use of the available test space in the anechoic chamber.

The modelled material for the tree trunk was considered using metal tubes because metal has a smooth surface, which can reflect sound at high frequencies, given that the interest frequency range is 10 kHz to 20 kHz. This research is limited in the available data on sound absorption coefficient (SAC) above 8 kHz and the expense of the materials, the aluminium tube was selected for modelling the tree trunk. To avoid the tube resonant sounds, each tube was filled with heavy materials (plaster), which also ensured the modelled tree trunks were as reflective as possible [9]. Due to the limitations in the available sizes of the tubes, 10 different sizes of tubes were selected to minimise the error. The largest diameter error is 6.85% caused by modelled

Tree H, which is generally acceptable. The details of the actual tube diameter for each modelled tree can be found in Table. B.7. Additionally, in this experiment, the height of the tube was 40 cm tall. It is more than two times the height of the source/receiver (15 cm), which should be sufficient for acoustic wave propagation in the vertical plane.

The unvarnished Medium Density Fibreboard (MDF) was used for modelling the grassland surface in the Stonehenge scale model work [9]. Considering the SAC might be similar between the forest ground and the grassland, the same material was selected to model the forest ground. The size of the MDF board was a square of 2.1 m, which is sufficient for modelling the forest ground and allows enough space for layout measurement.

5.2 Construct the scale model

The MDF board was firstly stabilised above the grid-formed surface, which provided an ideal measurement environment. In order to install the modelled tree trunks, the position of each tree needed to be marked directly on the board. The coordinates of the source, receiver and tree positions were converted 10 times smaller than the actual positions. The procedure of the layout measurement is as follows. A scale forest range (2×2 m) was marked on the board, four sides were marked with the distance. The X coordinate of the position was measured on the opposite sides of the board using a ruler, and an acoustic string was positioned at these two positions with the blu tack (Fig. A.31 shows the coordinate marked on one side). The same procedure was conducted for the Y coordinate. The intersection of the two acoustic strings located the position, which was then marked as a point and noted the tree name on the side (Fig. A.32 shows the two acoustic strings located in one position and Fig. A.33 shows the mark of the intersection point). The same process was also applied to marking the source and receiver positions.

The dowel method was used to mount each tree on the board. This was attained by embedding half of the dowel within the plaster and then using glue to stabilise it on the modelled tree trunk (Fig. A.34 shows the bottom of the model tree with a dowel). A hole was drilled at each marked position to dowel the aluminium tube on the board (Fig. A.35 shows the process of

setting up the modelled tree on the board). The final forest scale model setup is shown in Fig. 5.1. Comparing the model setup with the recreated layout and the real forest at position S2R1 shown in Fig. 5.2, the scale model was nicely recreated.

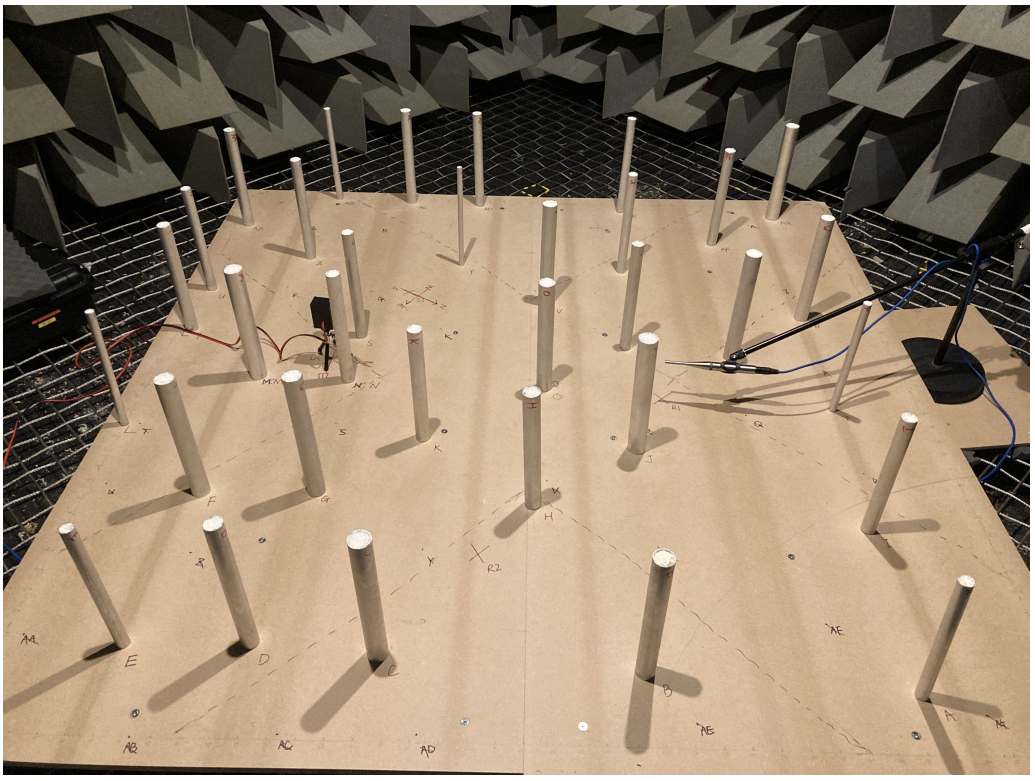

FIGURE 5.1: A picture of the forest scale model setup in the anechoic chamber, formed by 33 aluminium tubes and an MDF board. The source and receiver are at position S2R1.

5.3 Conduct scale model IR measurements

A Peerless OC20SC14-04 tweeter with a diameter of 33.2 mm was used in the scale model measurement. Its frequency response is from 750 Hz to 38 kHz. The same Earthworks M30 omnidirectional measurement microphone was used, possessing the ability to capture ultrasonic measurement range. The source and receiver positions were measured and situated at the height of 0.15 m, which is 10 times lower than the forest measurement height (Fig. A.36, A.37 shows the measurement of the source and receiver height, respectively). A Reference Amplifier A500 preamplifier was used to power the tweeter, and a Fireface UCX was used as the interface (The equipment used for the recordings is shown in Fig. A.38). Considering frequency above 20 kHz

(A) Position S2R1 in the real forest.

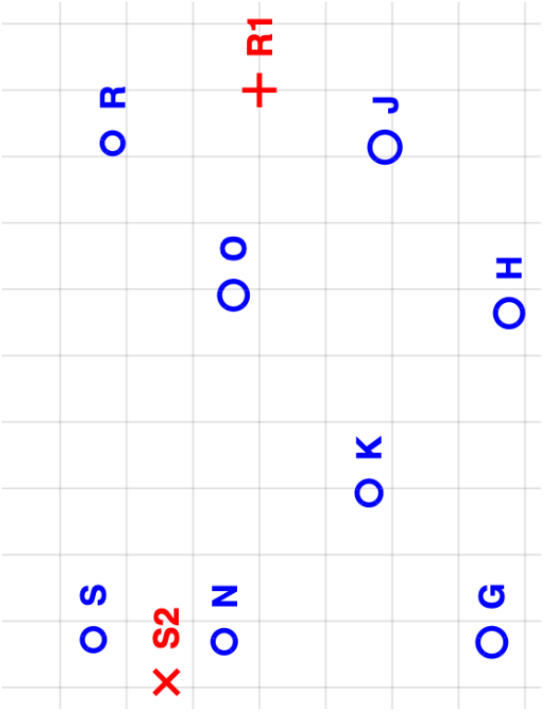

(B) Position S2R1 in the recreated layout.

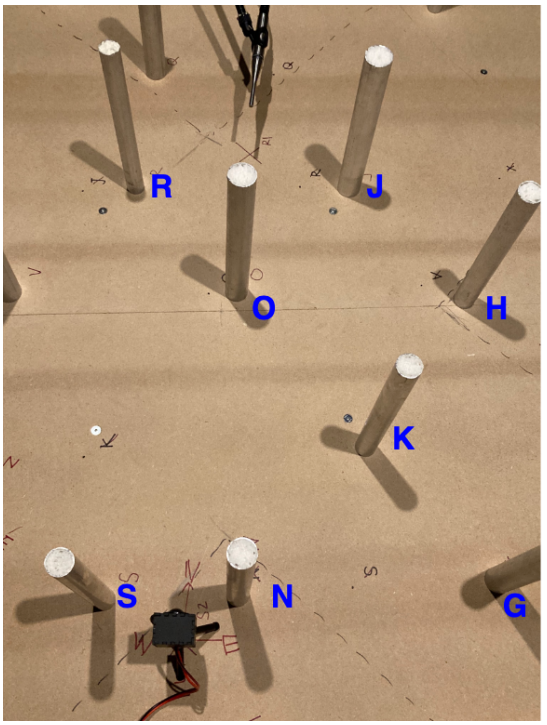

(C) Position S2R1 in the scale model.

FIGURE 5.2: Comparison plots of source and receiver at position S2R1 in three environments, includes real forest, recreated layout and scale model.

can not be heard, the gain of the preamplifier was carefully adjusted to avoid clipping in the recording, and a test sweep was exported to deconvolve before the actual recording.

A 15 s exponential sine sweep with a sampling rate of 96 kHz was used. The frequency range of the sweep for the scale model measurement was from 1 to 30 kHz, which allows for IR analysis at octave bands from 125 Hz to 2 kHz in the real scale. Considering the SNR in the anechoic chamber is relatively high, 2 s of padding was added at the end of the sweep to fully capture the scale model responses. Due to the high frequencies of electrical noise from the recording equipment, the sweep was repeated four times at each source/receiver position to improve the SNR [9]. To approximate the omnidirectional of the source, the method of rotating the source four times was also used for this measurement. Similarly, *N* was noted as the receiver directly pointing at the *Source 1*, which was also marked on the board. The orientations of *East*, *South*, and *West* were noted as the receiver being rotated clockwise 90° subsequently. It should be noted that the four orientations of the source position were found by eye. Fig. A.39 shows the pictures of the four orientations of the tweeter. A total of 64 sweep recordings were taken during the scale model IR measurement process (Fig. A.40 shows the scale model recording in the Reaper project).

Considering the frequency response from the tweeter is not flat, another measurement was conducted to directly record the responses from the tweeter. The results can later be processed to equalise the response from the speaker. The measurement setup is shown in Fig. 5.3. The tweeter and the M30 microphone were placed approximately 30 cm away, two foams were placed between the equipment to absorb the reflections from the board (Fig. A.41 shows the distance measurement between the tweeter and the microphone). The sweep used for the recording was the same as the scale model measurement. To fully get the responses from the tweeter, the microphone was placed in slightly different positions in five recordings, including the microphone directly pointing at the tweeter, and the microphone tilted slightly left and right each time. Fig. A.42, A.43 show the microphone tilted left and right to capture the tweeter responses, respectively. The frequency response of the tweeter is shown in Fig. A.44. The equalised process was conducted with the help of Mr Andrew Chadwick and Mr Tomasz Rudzki. The equalised IR results were then averaged out for each position, which can be found in Appendix C.1.5.

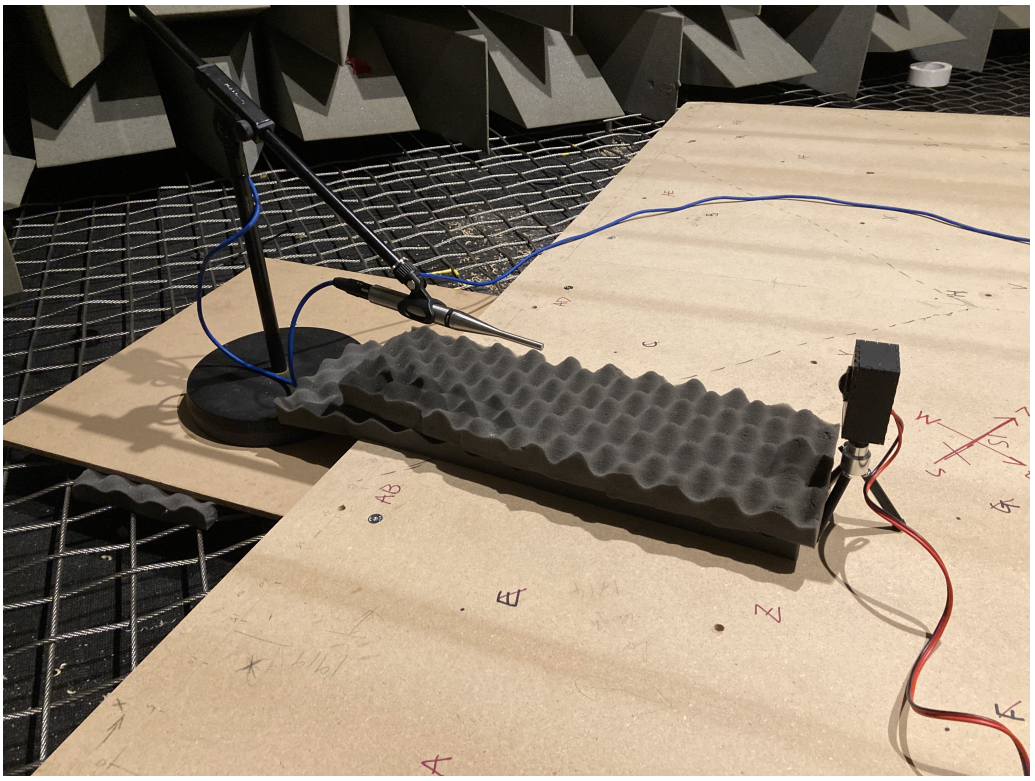

FIGURE 5.3: A picture of the measurement setup for the tweeter responses in the anechoic chamber.

5.4 Conclusion

The choice of a 1:10 scale for this forest scale model was a compromise, taking into account the available test space and the necessity for a stable forest ground in the chamber. Given the limited research in scale models, here are the novel decisions made in this experiment:

1. Choose aluminium tubes to model tree trunks. A method of filling the tube with plaster was applied to avoid sound resonant, which ensured the modelled tree trunk was as reflective as possible.

2. An unvarnished MDF board was selected to model forest ground as an experiment, given that the main focus is on the modelled tree trunks.

3. The choice of the modelled tree trunk's height. A 40 cm of modelled tree trunk height was chosen for this experiment, which is more than two times higher than the height of the IR recording.

The IR measurement repeated the sweep at each rotation to improve the SNR. The speaker's response was also measured, considering the tweeter frequency response is not flat, which can significantly affect the IR results. The design of the model involved a series of compromises and assumptions. There were methods applied in the model, aimed at improving the approximations of the model itself and the recordings. Chapter 6 will present the forest scale model IR analysis, which will also evaluate this model design.

Chapter 6

Forest Scale Model IR Analysis

This chapter will present the scale model IR analysis. Section 6.1 will present the scale model IR analysis at position S1R1. The IR analysis at position S1R2, S2R1 and S2R2 will then be presented in Section 6.2, 6.3 and 6.4, respectively. In Section 6.7 and 6.8, the comparisons of these results with the IRs in *WGW* forest and Stonehenge scale model will overall examine this scale model. Section 6.9 will present the comparisons with real forest IRs, and the effectiveness of this scale model can be then evaluated.

In order to conduct IR analysis in the real scale, the scale model IRs are interpolated to 10 times longer, which can be found in Appendix C.1.6. The results are all generated using the stretched IRs.

6.1 S1R1 scale model IR analysis

This section will analyse the IR recorded at S1R1. At this position, there is a clear line of sight between the source and receiver and the distance between them is 8.65 m in real scale, Fig. 3.10 shows this layout.

6.1.1 S1R1 scale model IR waveform analysis

Fig. 6.1 shows the waveform plot of the IR recorded at position S1R1 in the scale model. The waveform shows a greatly pronounced direct sound, followed by clusters of strong energy early reflections at the first 8 ms. The reflections after this timing show less pronounced energy. Similarly, the reflections from modelled tree trunks are investigated, Table. 6.1 shows the results. The speed of sound used in this calculation is 343 m/s. The results show that the reflections indicated in the waveform align well with the potential reflections indicated in the actual layout, and the error range is minor.

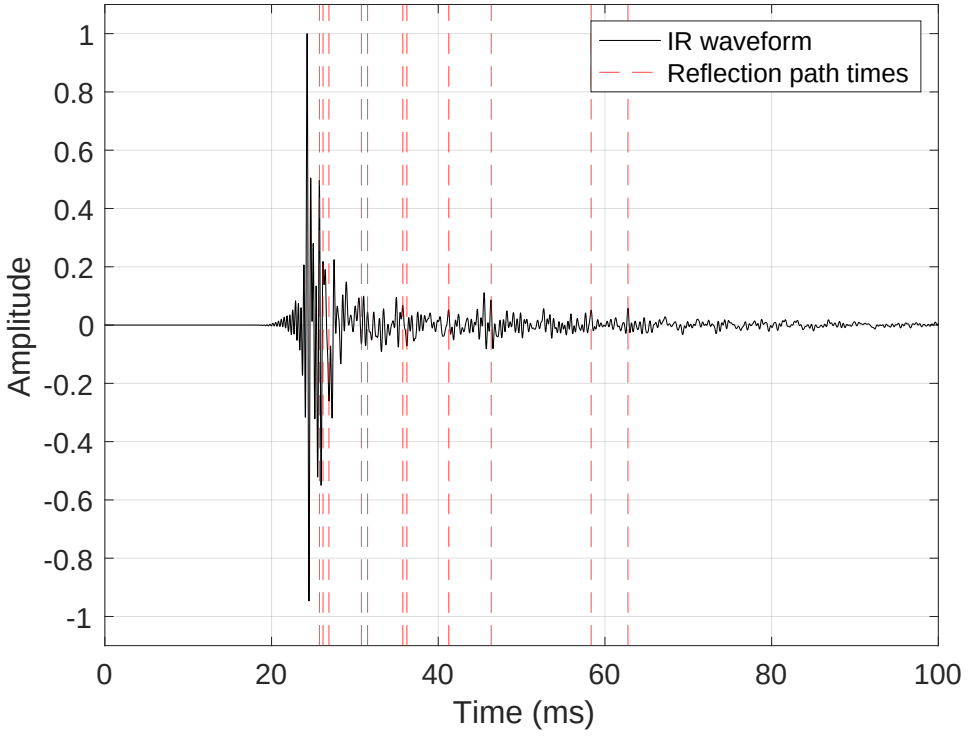

FIGURE 6.1: Waveform plot of impulse response recorded at position S1R1 in the scale model. The red dot lines indicate the timing of the early reflections.

6.1.2 S1R1 scale model IR spectrogram analysis

Fig. 6.2 shows the spectrogram of the IR at position S1R1 in the scale model. The spectrogram shows a strong direct sound energy, and then sound mostly attenuates after this. The direct sound is greatly pronounced approximately above 2 kHz, at a frequency range of 500 Hz to 2

Timing of early reflections	Path difference	Potential reflection at *Tree*
1.48 ms	0.51 m	O (0.49 m)
1.92 ms	0.66 m	R (0.65 m)
2.63 ms	0.90 m	V (0.86 m)
6.52 ms	2.24 m	Y (2.24 m)
7.26 ms	2.49 m	S (2.48 m)
11.49 ms	3.94 m	Q (3.88 m)
11.98 ms	4.11 m	N (4.06 m)
17.00 ms	5.83 m	H (5.77 m)
22.09 ms	7.58 m	M (7.5 m)
34.08 ms	11.69 m	I (11.65 m)
38.50 ms	13.21 m	B (13.31 m)

TABLE 6.1: Potential trees caused first-order reflections at position S1R1 in the scale model.

kHz, the energy is less pronounced. There is a loss of low energy below 500 Hz at the direct sound.

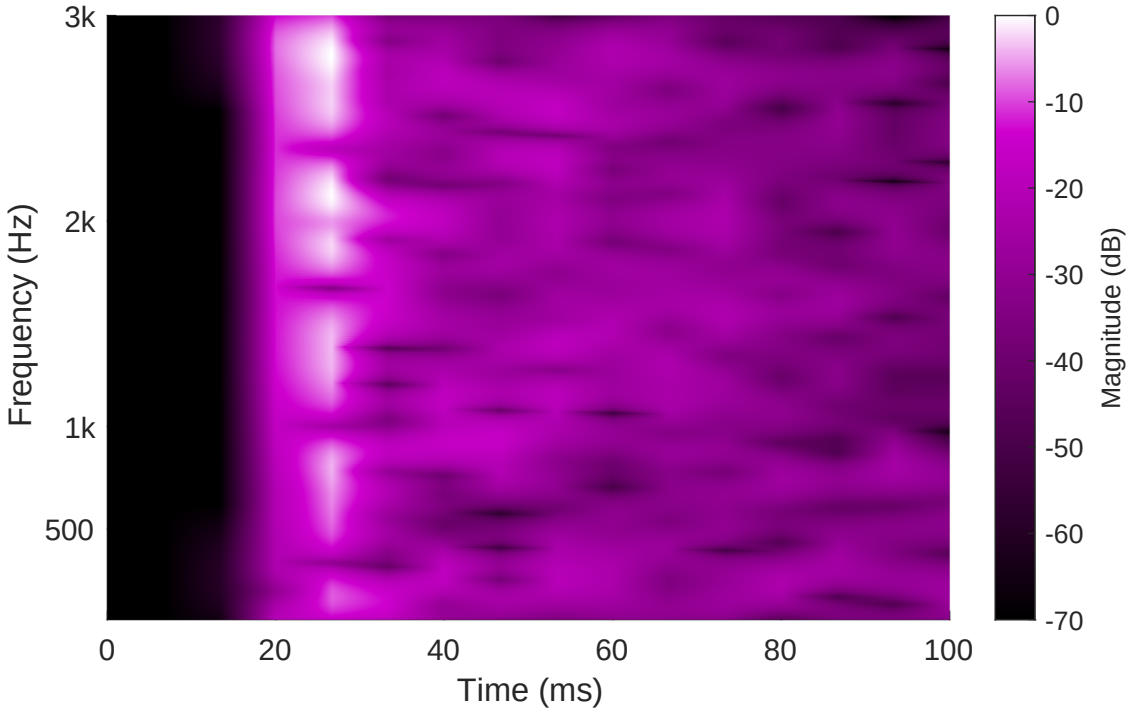

FIGURE 6.2: Spectrogram plot of impulse response recorded at position S1R1 in the scale model.

6.1.3 S1R1 scale model IR ISO 3382 acoustic parameter analysis

In order to get an insight into the reverberation time in the forest scale model, T20, T30, T40 and EDT values are estimated from the decay curve at the 1 kHz octave band, which is shown in Fig. 6.3. The extrapolated EDT and T20 lines show a better fit line at the start of the decay curve, compared with T30 and T40 lines. Additionally, a previous study has also indicated that the EDT is a better parameter compared to the reverberation time (T30) in the scale model [9]. Considering that most early reflections occur at the first 100 ms shown in the waveform results, EDT and T20 will be used in this analysis. Fig. 6.4 shows the early decay time (EDT) comparison plots of four scale model IRs from octave band 250 Hz to 2 kHz.

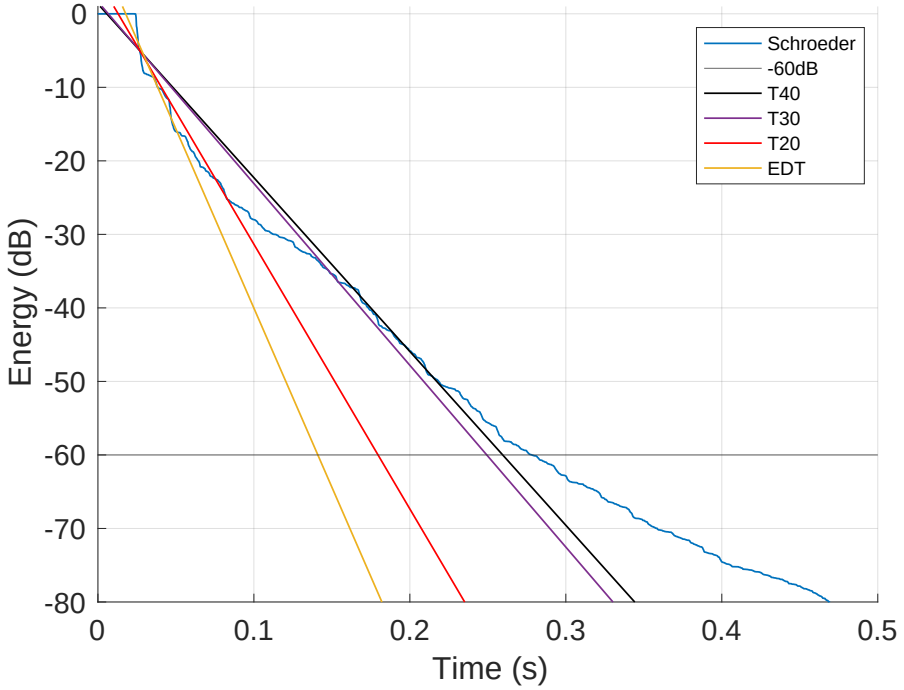

FIGURE 6.3: Schroeder curve of the scale model IR at position S1R1 and the estimation slopes of early decay time (EDT) and reverberation time (T20, T30 and T40). The weighting is 1 kHz.

The largest EDT value at position S1R1 is found at the 250 Hz octave band (shown in Fig. 6.4), which is approximately 0.25 s. Between octave bands 500 Hz to 2 kHz, the values are relatively low, which are approximately 0.05 s. An increase is found at 1 kHz. Generally, the acoustic parameter values at this position indicate a very low reverberation time in the scale model.

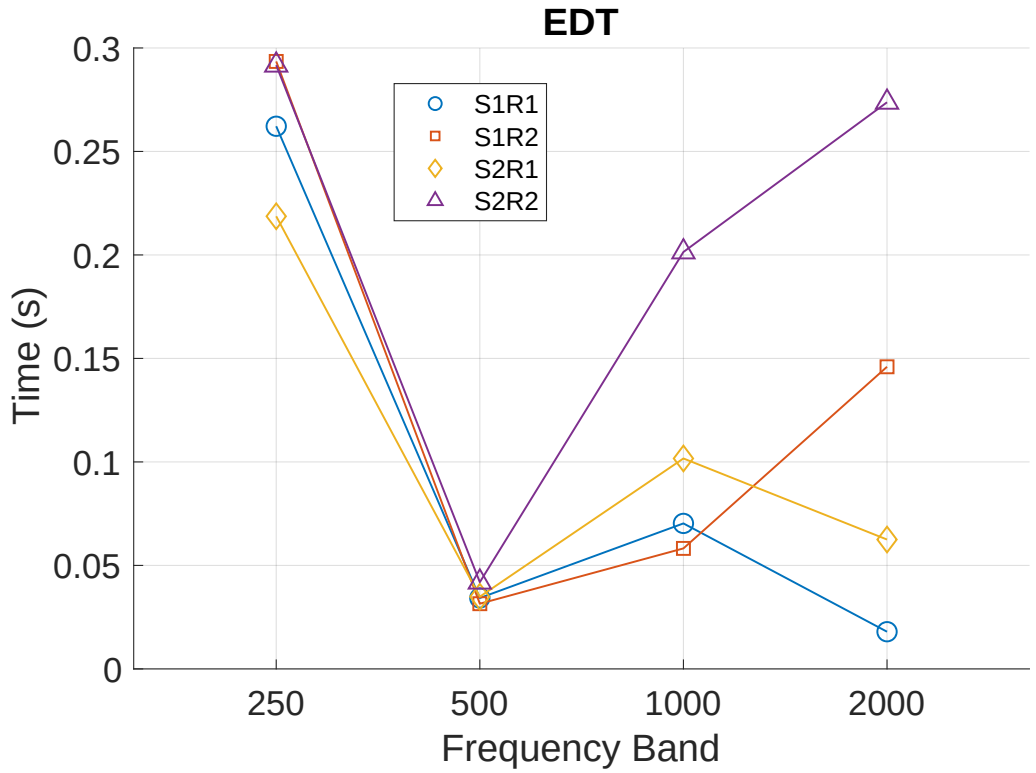

FIGURE 6.4: Early decay time (EDT) of four scale model IRs at octave bands ranging from 250 Hz to 2 kHz.

6.2 S1R2 scale model IR analysis

This section will analyse the IR recorded at S1R2. At this position, there is a clear line of sight between the source and receiver and the measured distance between them is 10.32 m in the real scale, Fig. 3.10 shows this layout.

6.2.1 S1R2 scale model IR waveform analysis

Fig. 6.5 shows the waveform plot of the IR recorded at position S1R2 in the scale model, Table. 6.2 shows the results of the potential reflections from modelled tree trunks. It can be observed that there is a strong early reflection after the direct sound shown in the waveform, which has an amplitude of 0.7. The first order reflection from tree is not suggested at this timing in Table. 6.2. This indicates that the reflection might be second or third order reflections.

Additionally, there are relatively more potential modelled tree trunk reflections found at this position, compared to the position at S1R1.

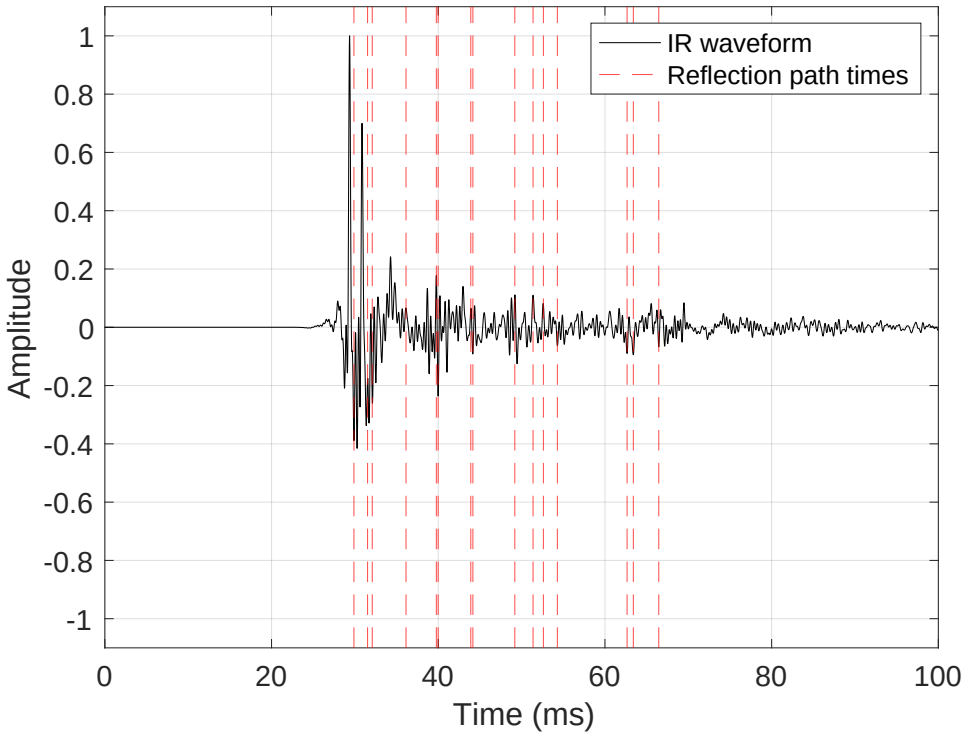

FIGURE 6.5: Waveform plot of impulse response recorded at position S1R2 in the scale model. The red dot lines indicate the timing of the early reflections.

Timing of early reflections	Path difference	Potential reflection at *Tree*
0.51 ms	0.18 m	K (0.10 m)
2.15 ms	0.74 m	S (0.73 m)
2.71 ms	0.93 m	H (0.92 m) N (0.92 m)
6.76 ms	2.32 m	G (2.21 m)
10.40 ms	3.57 m	M (3.53 m) V (3.54 m)
10.61 ms	3.64 m	Y (3.61 m)
14.53 ms	4.98 m	R (4.92 m)
14.78 ms	5.07 m	C (5.08 m)
19.81 ms	6.80 m	Z (6.80 m)
22.00 ms	7.55 m	T (7.57 m)
23.24 ms	7.97 m	B (7.93 m)
24.92 ms	8.55 m	X (8.51 m)
33.28 ms	11.42 m	AD (11.41 m)
34.03 ms	11.67 m	AC (11.66 m)
37.08 ms	12.72 m	I (12.68 m)

TABLE 6.2: Potential trees caused first-order reflections at position S1R2 in the scale model.

6.2.2 S1R2 scale model IR spectrogram analysis

Fig. 6.6 shows the spectrogram of the IR at position S1R2 in the scale model. The spectrogram shows a pronounced direct sound at frequencies from 500 Hz to 1 kHz. The magnitude shows distinctively less pronounced energy above 2 kHz compared with the results at position S1R1. The loss of low frequency is also shown in this result.

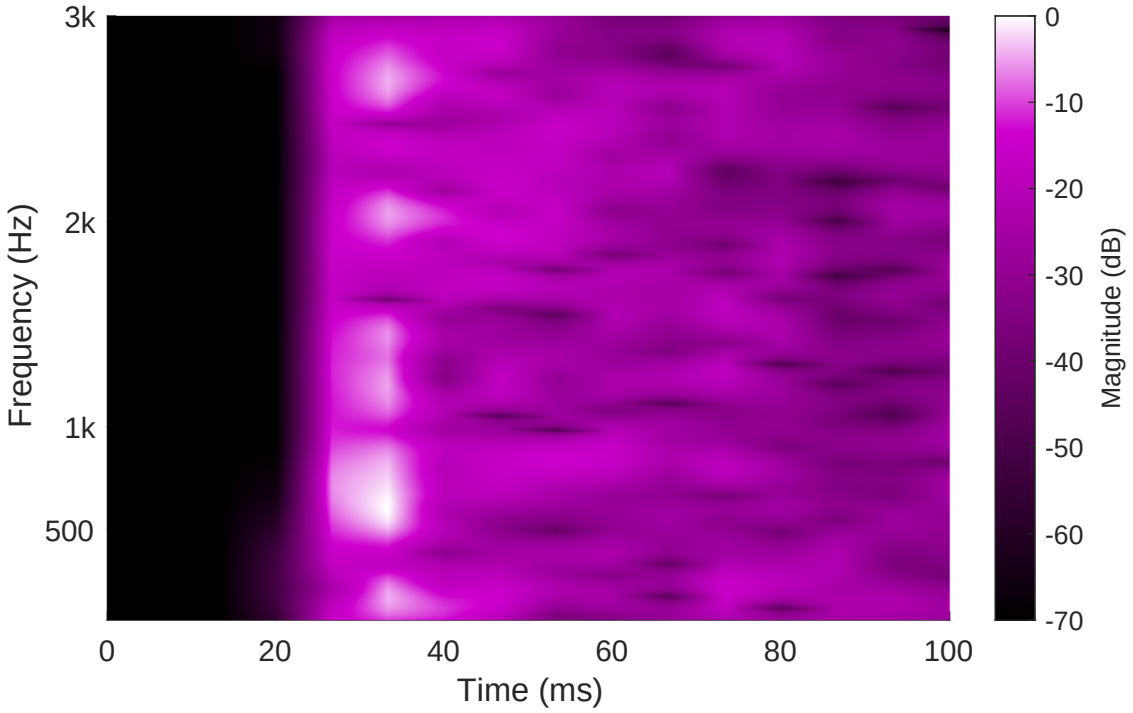

FIGURE 6.6: Spectrogram plot of impulse response recorded at position S1R2 in the scale model.

6.2.3 S1R2 scale model IR ISO acoustic parameter analysis

The largest value of EDT at position S1R2 can be found at 250 Hz (shown in Fig. 6.4), which is around 0.25 s. The lowest value is shown at 500 Hz, then there is an increase at 1 and 2 kHz. An EDT value of 0.15 s is found at 2 kHz.

6.3 S2R1 scale model IR analysis

This section will analyse the IR recorded at S2R1. At this position, there is an impeded tree, *O*, between the source and receiver. The distance between them is 9 m in the real scale, and the distance between the source and *Tree O* is 5.71 m, Fig. 3.10 shows this layout.

6.3.1 S2R1 scale model IR waveform analysis

Fig. 6.7 shows the waveform plot of the IR recorded at position S2R1 in the scale model, Table. 6.3 shows the results of the potential reflections from modelled tree trunks. The waveform shows there is a relatively strong reflection at approximately 38 ms, which has an amplitude of 0.2. This might be caused by second or third order reflections as it's not suggested in Table. 6.3.

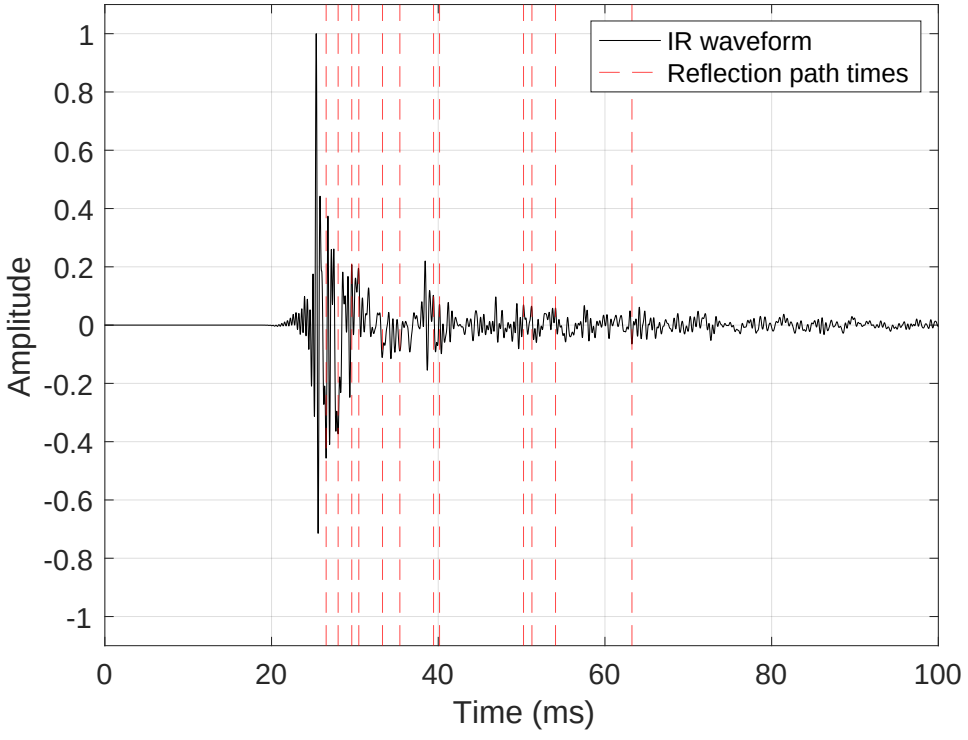

FIGURE 6.7: Waveform plot of impulse response recorded at position S2R1 in the scale model. The red dot lines indicate the timing of the early reflections.

Timing of early reflections	Path difference	Potential reflection at *Tree*
1.20 ms	0.41 m	*N* (0.42 m)
2.64 ms	0.90 m	*S* (0.89 m)
4.27 ms	1.46 m	*K* (1.47 m) *R* (1.52 m)
5.11 ms	1.75 m	*J* (1.79 m)
7.96 ms	2.73 m	*V* (2.82 m)
10.04 ms	3.44 m	*H* (3.65 m)
14.08 ms	4.83 m	*Q* (4.77 m)
14.80 ms	5.08 m	*G* (5 m)
24.88 ms	8.53 m	*P* (8.54 m)
25.89 ms	8.88 m	*T* (8.75 m)
28.72 ms	9.85 m	*L* (9.90 m)
37.89 ms	12.99 m	*Z* (13.06 m)

TABLE 6.3: Potential trees caused first-order reflections at position S2R1 in the scale model.

6.3.2 S2R1 scale model IR spectrogram analysis

Fig. 6.8 shows the spectrogram of the IR at position S2R1 in the scale model. The results show that sections of energy are greatly pronounced above 500 Hz, which is similar to the results at position S1R1. There is an impeded *Tree O* between the source and receiver, although the loss at high frequency is not shown in the results. There is a relatively low energy tail at the frequencies below 200 Hz after the direct sound.

6.3.3 S2R1 scale model IR ISO 3382 acoustic parameter analysis

The EDT values at position S2R1 show a similar trend to the results at position S1R1. An increase is found at 1 kHz between 500 Hz and 2 kHz (shown in Fig. 6.4), which has a value of 0.1 s.

6.4 S2R2 scale model IR analysis

This section will analyse the IR recorded at S2R2. At this position, there is an impeded tree, *N*, between the source and receiver. The distance between them is 7.91 m in the real scale, and

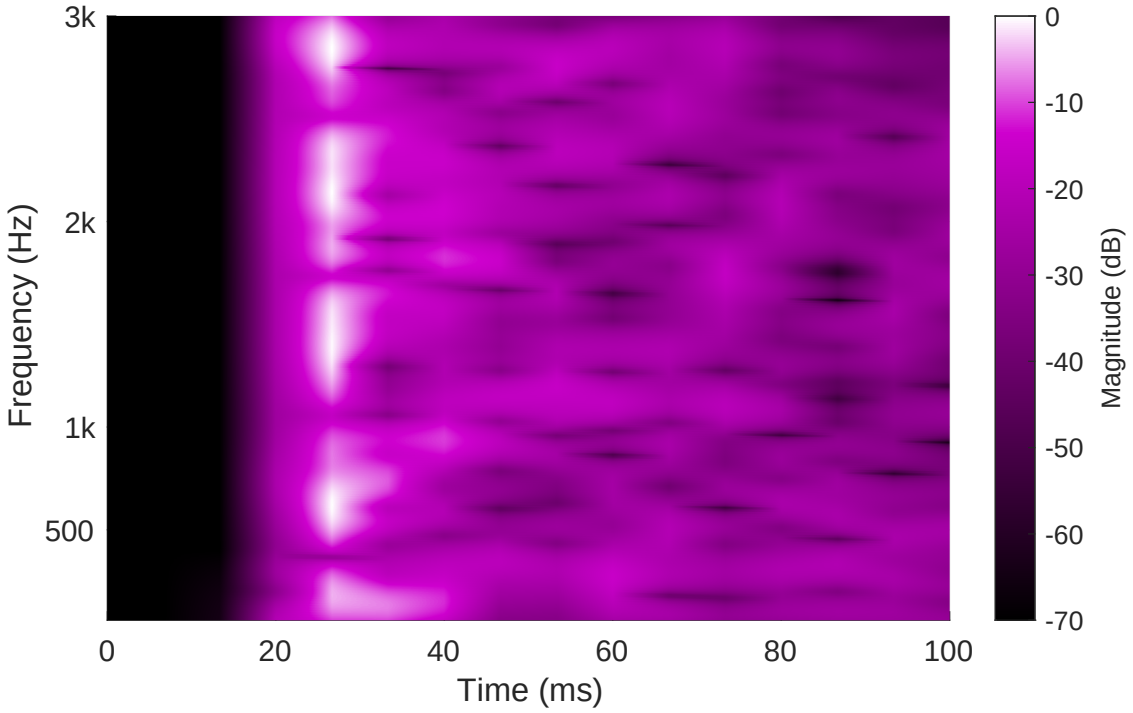

FIGURE 6.8: Spectrogram plot of impulse response recorded at position S2R1 in the scale model.

the distance between the source and *Tree N* is 0.9 m, Fig. 3.10 shows this layout.

6.4.1 S2R2 scale model IR waveform analysis

Fig. 6.9 shows the waveform plot of the IR recorded at position S2R2 in the scale model, Table. 6.4 shows the results of the potential reflections from modelled tree trunks. The waveform shows greatly pronounced early reflection energy compared with the other three waveform results. This relates to the impeded *Tree N* closer to the source, which results in the direct sound being mainly attenuated, and the reflection paths being more apparent.

6.4.2 S2R2 scale model IR spectrogram analysis

Fig. 6.10 shows the spectrogram of the IR at position S2R2 in the scale model. The spectrogram shows a greatly pronounced energy at the direct sound below 1 kHz. There is a lack of energy above 1 kHz, given there is an impeded tree close to the source. The energy tail after the direct sound is shown below 1 kHz.

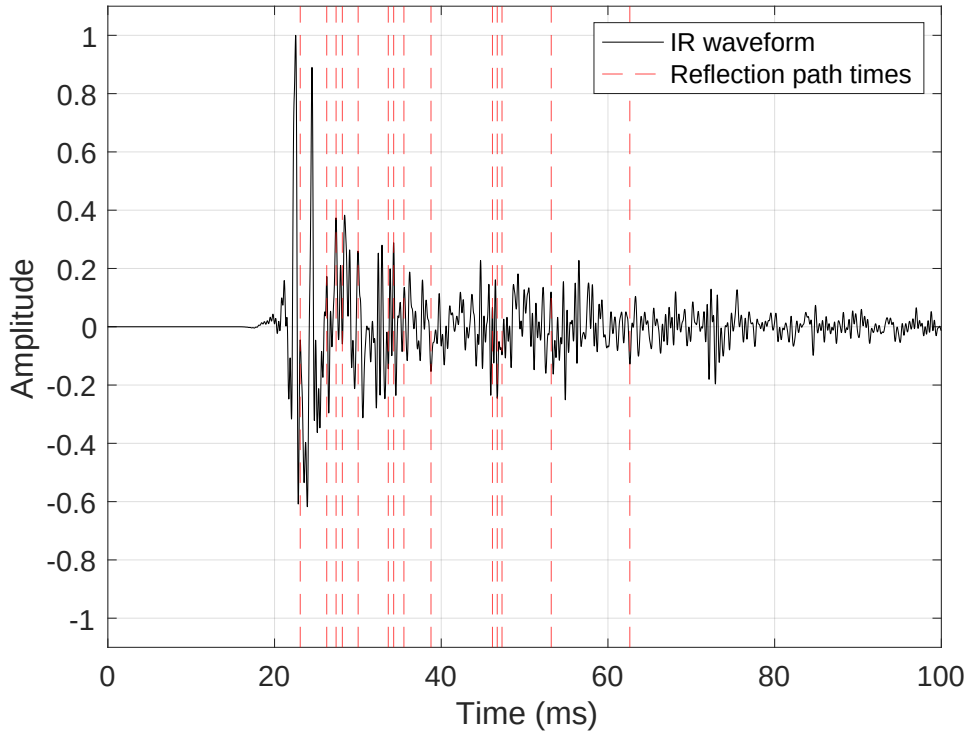

FIGURE 6.9: Waveform plot of impulse response recorded at position S2R2 in the scale model. The red dot lines indicate the timing of the early reflections.

Timing of early reflections	Path difference	Potential reflection at *Tree*
3.72 ms	1.28 m	*G* (1.23 m)
4.84 ms	1.66 m	*H* (1.56 m)
5.59 ms	1.92 m	*S* (1.90 m)
7.49 ms	2.57 m	*M* (2.51 m)
11.10 ms	3.81 m	*O* (3.80 m)
11.75 ms	4.03 m	*F* (4.06 m)
12.98 ms	4.45 m	*C* (4.49 m)
16.23 ms	5.57 m	*D* (5.77 m) *J* (5.75 m)
23.60 ms	8.10 m	*T* (8.09 m)
24.18 ms	8.29 m	*V* (8.26 m) *E* (8.37 m)
24.75 ms	8.49 m	*R* (8.55 m)
30.66 ms	10.52 m	*U* (10.54 m)
40.08 ms	13.75 m	*X* (13.7 m)

TABLE 6.4: Potential trees caused first-order reflections at position S2R2 in the scale model.

6.4.3 S2R2 scale model IR ISO 3382 acoustic parameter analysis

The EDT values at position S2R2 have a similar trend to the results at position S1R2 (shown in Fig. 6.4). At 500 Hz, the EDT has the lowest value (0.05 s). Then there is a rapid increase

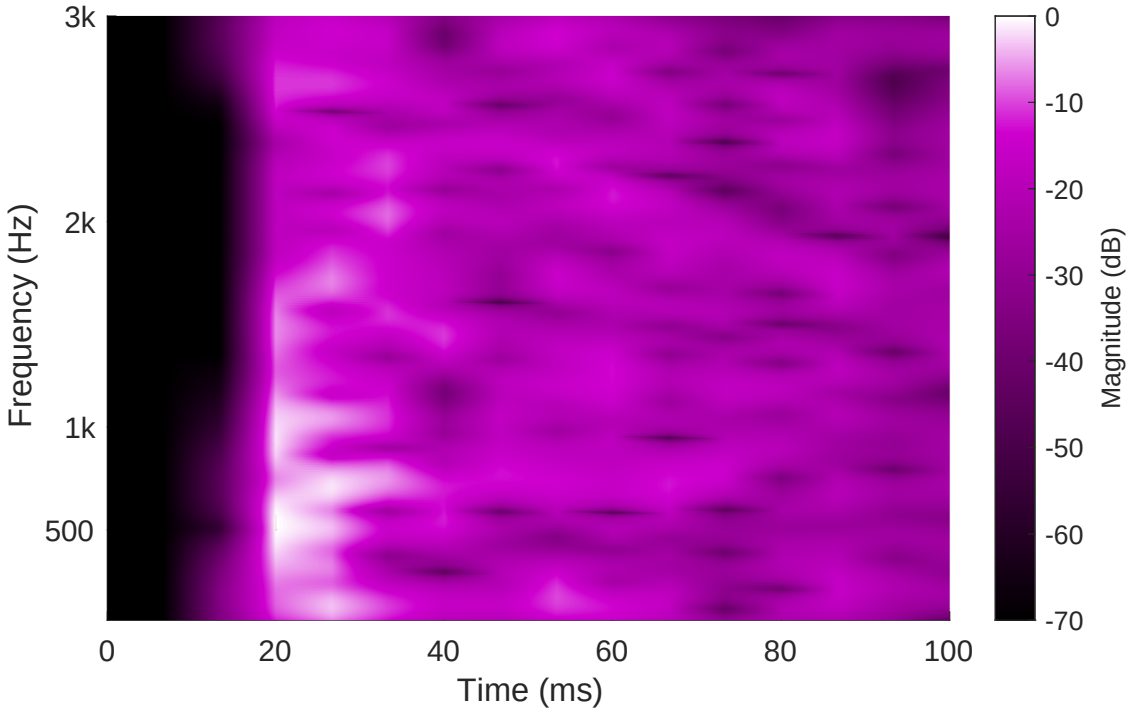

FIGURE 6.10: Spectrogram plot of impulse response recorded at position S2R2 in the scale model.

between 500 Hz and 2 kHz, where the EDT shows a value of 0.2 s at 1 kHz, and at 2 kHz, EDT shows 0.28 s. At this position, the EDT indicates the largest values compared to the other three IR results.

6.5 Scale model IR spectrum analysis

Fig. 4.24 shows a comparison plot of the spectrum of four scale model IRs from 125 Hz to 2.5 kHz in one-third octave bands. The spectrum of these four IRs shows a similar trend, where there is a reduction at around 250 Hz and an increase clearly indicates after this range. The largest magnitude of each IR can be found at a frequency range from 500 Hz to 2.5 kHz, which indicates relatively strong energy at this range in the scale model.

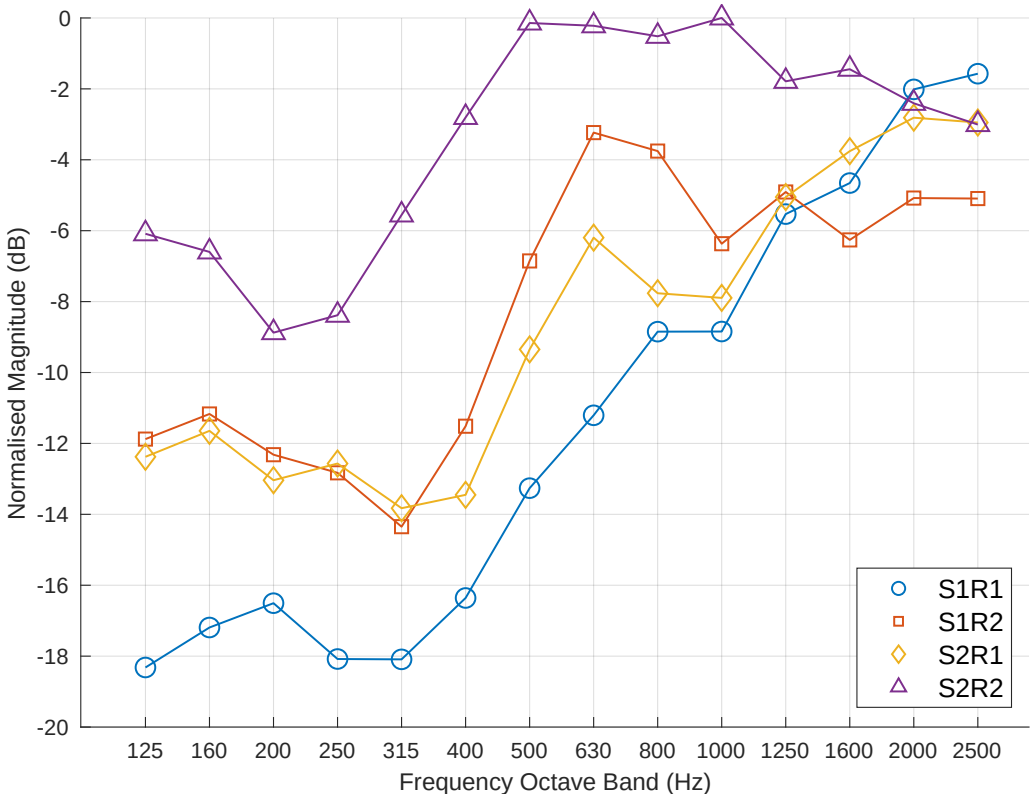

FIGURE 6.11: A comparison plot of the spectrum of four scale model IRs from 125 Hz to 2.5 kHz in one-third octave bands.

6.6 Summary of the scale model IRs

Generally, the scale model waveform results indicate a fair amount of reflections from modelled tree trunks. The spectrogram result indicates a strong direct sound then most energy attenuates after this. The EDT indicates a very dry response in the scale model forest. The spectrum results indicate a relatively strong energy in the frequency range between 500 Hz and 2.5 kHz.

Additionally, the auralisation results generated with the stretched scale model IRs sound muffled, given the IRs were only recorded up to 3 kHz in the real scale. The perceived size of the space is relatively small, and the reverberation can not be perceived, given the recording space is an anechoic chamber. The auralisation results can be found in Appendix C.1.7.

6.7 Comparisons with *WGW* forest IRs

As discussed in Chapter 2, *WGW* reverberator simulated a forest formed by 25 trees within a 30×30 m region [1]. The layout is shown in Fig. A.3. The density of the scale model forest is higher, given that this forest in real scale has 33 trees within a 20×20 m region. It should be noted that the simulation only considers the reflections from tree trunks, while the scale model captures the wave effects, such as ground interference. Fig. 6.12 shows a comparison plot of the reverberation time (T20) of the scale model IRs and *WGW* IR at octave bands ranging from 250 Hz to 2 kHz. The *WGW* IR is taken from OpenAir, and the results are generated in MATLAB [51].

The reverberation time (T20) shows a similar trend for four scale model IRs, where there is a decrease from 250 Hz to 2 kHz. At 1 and 2 kHz, the reverberation time ranges from 0.2 to 0.25 s. The *WGW* results indicate a value of 0.4 s from 500 Hz to 2 kHz, and the lowest value (0.2 s) is found at 250 Hz. The results between these two forests do not show a similar trend in octave bands. Given that the numbers of trees are similar in these two environments, and the reverberation time in the scale model does fall in the range of the *WGW* results, this finding suggests the scale model IR results are reasonable.

6.8 Comparisons with scale model Stonehenge IRs

The Stonehenge scale model is approximately 2.5 m wide, which is a similar size to the scale model forest [9]. The Stonehenge model forms of circle of stones (the layout is shown in Fig. 2.15), and the modelled stones are relatively reflective. There are gaps in between the stones, which makes it comparable with the scale model forest.

Fig. 6.13 shows a comparison plot of the definition (D50) of scale model IRs at octave bands ranging from 250 Hz to 2 kHz. D50 values indicate a very high energy loss at octave bands from 500 Hz to 2 kHz, which are above 98%. Apart from IR at position S2R2, the results show a reduction after 500 Hz, a value of 92% is found at 2 kHz. The lowest D50 value of each IR can be found at the octave band 250 Hz, and a value of 90% is found at position S2R2. D50 in the

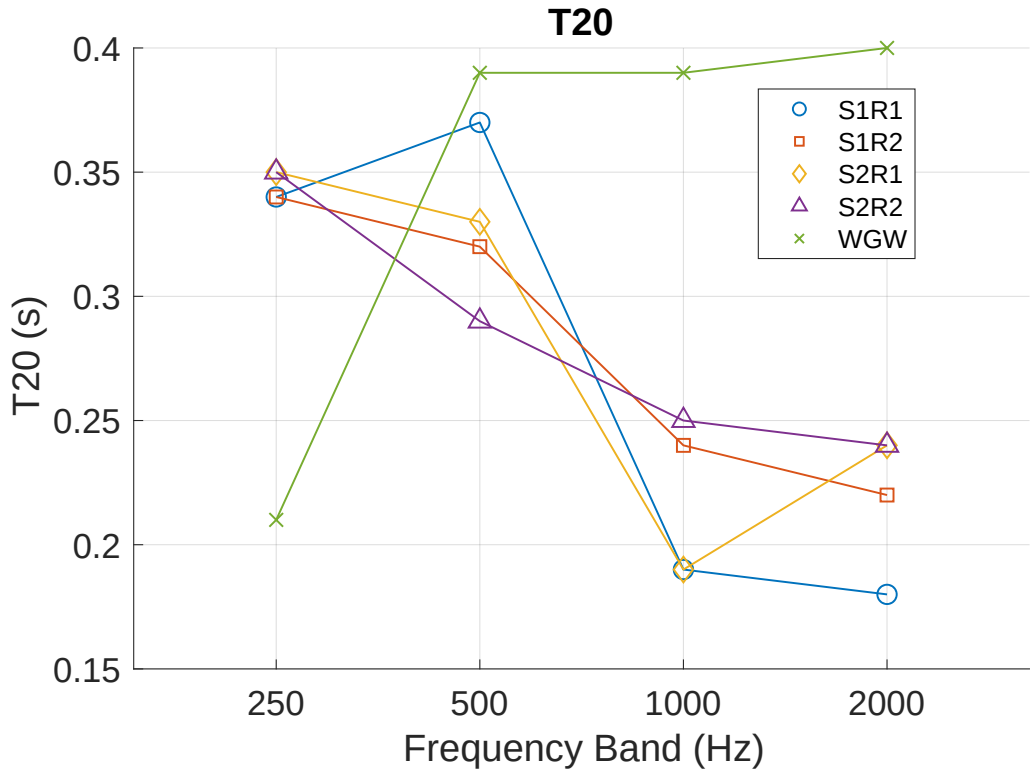

FIGURE 6.12: A comparison plot of the reverberation time (T20) of scale model IRs and *WGW* IR at octave bands ranging from 250 Hz to 2 kHz.

Stonehenge model ranges from 45% to 97%, where the lowest value is given by the source fully hidden behind a tall modelled stone [9]. These results share similarities in the great energy loss in the model given the recording space is an anechoic chamber, and a reduction in D50 when there is an obstruction. Additionally, the mean mid-frequency EDT values (average of 500, 1000, and 2000 Hz octave bands) in the Stonehenge model range from 0.49 to 0.75 s. The range of EDT in the scale model forest at these octave bands is from 0.02 to 0.27 s, the difference is approximately 0.5 s higher in the Stonehenge model. Given the density, size, and reflective surface of the modelled stones are relatively higher in the Stonehenge model, the comparisons of the EDT also suggest the forest scale model IR results are reasonable.

6.9 Comparisons with the real forest IRs

The comparisons with *WGW* forest and the Stonehenge scale model have indicated the forrest scale model IR results are reasonable. This section will compare the results with the real forest

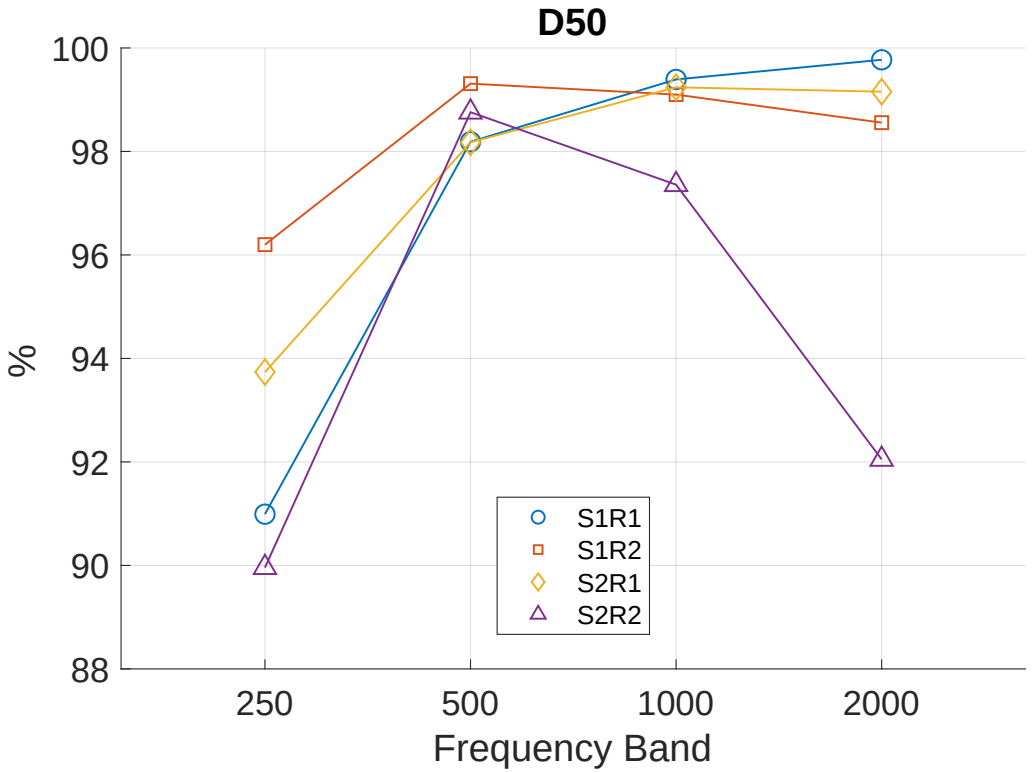

FIGURE 6.13: A comparison plot of the definition (D50) of scale model IRs at octave bands ranging from 250 Hz to 2 kHz.

IR results, which will provide insight into the effectiveness of the scale model.

6.9.1 Waveform comparisons

The waveform plots of the real forest IR at positions S1R1, S1R2, S2R1 and S2R2 are shown in Fig. 4.1, 4.12, 4.20 and 4.20, respectively. The scale model IR waveforms are shown in Fig. 6.1, 6.5, 6.7 and 6.9. The waveform results in both environments show similar features, where there are strong early reflections. Some weak amplitude of the distinct reflections is shown at approximately 80 ms after the direct sound in the real forest results, while in the scale model results, it's found at around 60 ms. This indicates that modelling 33 trees might not be enough for modelling a forest environment. Given that the reflections in the scale model waveform results can be nicely related to tree trunk reflections, this model is still sufficient. It's interesting that the SIRR analysis results indicate there is a longer direct sound with greater energy at position S2R2 (shown in Fig. 4.22), and the waveform at this position in the scale model also

shows relatively greater reflection energy. This indicates that the scale model can simulate the physical property of an impeded tree being close to the source.

Some strong energy reflections in the scale model waveform results do not fall in the timing of the first order reflections. Given the physical properties of the scale model and the forest are similar, this finding indicates that higher order reflections also play an important role in sound propagation in forest environments.

6.9.2 Spectrogram comparisons

The spectrogram plots of the real forest IR at positions S1R1, S1R2, S2R1 and S2R2 are shown in Fig. 4.2, 4.13, 4.17 and 4.21, respectively. The scale model IR spectrograms are shown in Fig. 6.2, 6.6, 6.8 and 6.10. The spectrograms in the forest IRs indicate the lack of low frequency (800 Hz) attenuation, given there are reflections from further trees and it's an outdoor environment [17]. This feature is not indicated in *Source 1* scale model IR results, at *Source 2* positions, there is a relatively low energy tail below 200 Hz. This might be due to the number of modelled trees remaining limited. The scale model spectrogram at position S1R1 shows greatly pronounced energy from 1 kHz to 3 kHz at the direct sound, compared to the results in the real forest. This might be due to the sound absorption coefficients (SACs) of the aluminium tube being relatively low at the scale frequencies. At *Source 2* position of the real forest IRs, the sound absorption at high frequencies by the impeded tree trunk is indicated in the results. The scale model IR at position S2R2 aligns with this feature while the S2R1 result does not. This might be due to the impeded modelled tree trunk being close to the source at position S2R2. The impeded tree trunk at position S2R1 tends to reflect sound rather than absorb sound, given the aluminium tubes might be relatively reflective and result in higher order reflections.

6.9.3 ISO 3382 acoustic parameter comparisons

Fig. 6.14 shows a comparison plot of Schroeder decay curve of the scale model forest and the real forest. Both IR positions are at S1R1. The weighting is 1 kHz. It can be observed that the regression of the decay curve in the scale model IR is very rapid, given that it only considers

reflections from 33 trees and the recording space is anechoic. Additionally, the drop off at the first 10 dB of these two decay curves can still be found similar.

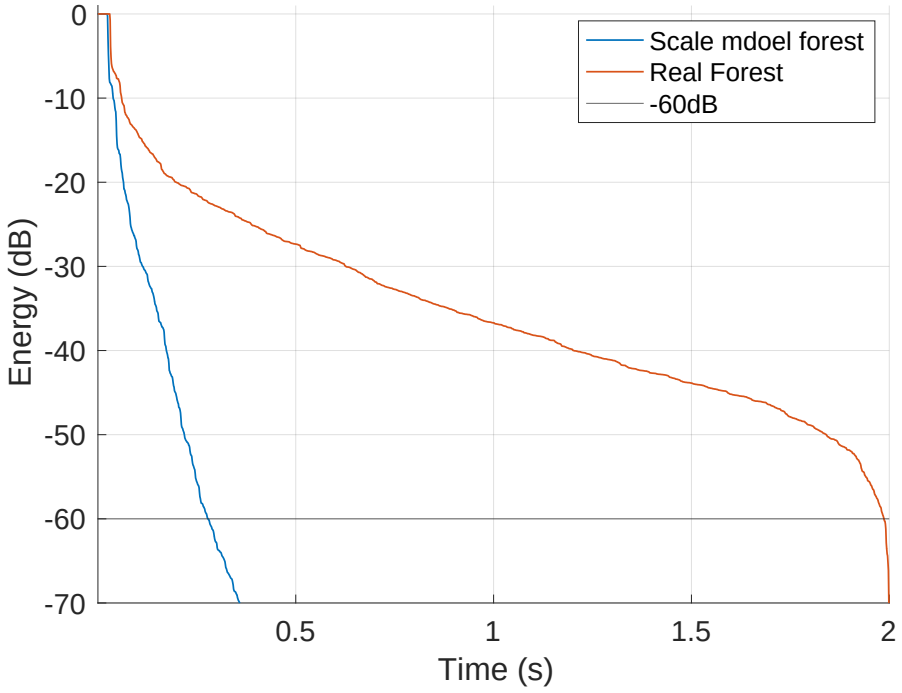

FIGURE 6.14: A comparison plot of Schroeder decay curve of the scale model forest and the real forest. Both IR positions are at S1R1. The weighting is 1 kHz.

The EDT values of the real forest IRs are shown in Fig. 4.7, and the scale model IR results are shown in Fig. 6.4. The EDT in the scale model shows 0.1 s higher at octave bands 250 Hz, compared to the results in the forest IRs, while the results at 500 Hz are relatively similar. These indicate that the scale model results are comparable to the real forest results below 500 Hz. At octave bands 1 and 2 kHz, the results in the scale model are generally lower, ranging from 0.02 to 0.27 s, while the range of the real forest is between 0.22 and 0.64 s. As discussed in Section 6.9.2, the SACs of the aluminium tubes are relatively low at this frequency range in real scale, so the EDT values should be higher. The reason for this might be the loss of energy through the air does not scale linearly with frequency [9]. Although a similar trend is shown in the real forest and scale model IRs: a reduction is found at 500 Hz, and an increase is shown at 1 or 2 kHz. It is interesting to note that, in the real forest IRs, an increase is found at 1 kHz in *Receiver 2* positions, and in *Receiver 1* positions, the increase is found at 2 kHz. While in the scale model IR results, the increase is found in reverse for these two receiver positions. This

suggests that the early decay time has a receiver position dependent characteristic, although the reason for the reverse in the results is uncertain.

The T20 results in the scale model IRs (shown in Fig. 6.12) indicate discrepancies with the reverberation time (T30) in the forest IRs (shown in Fig. 4.5). The values are generally low, and there is no similar trend shown in the results. The D50 results of the forest and the model are shown in Fig. 4.6 and 6.13, respectively. D50 values are generally large in both environments, which are mostly above 90%. Although the D50 values in the scale model also struggle to find a similar trend with the forest results.

Given the energy decay curves of both environments show a similar regression at the first 10 dB and the EDT results show similar trends in both environments, these findings indicate that EDT is a more comparable acoustic parameter in the forest acoustic scale model. However, the EDT values at 1 and 2 kHz are less comparable with the results in the real forest, given the air absorption correction was not applied to the results.

6.9.4 Spectrum comparisons

The spectrum results of the real forest are shown in Fig. 4.24, and the scale model results are shown in Fig. 6.11. There are similarities found in both spectrum results, where from the octave band 125 Hz and 2.5 kHz, there is a reduction at around 250 Hz, and then the magnitude shows an increase after this range. The spectrum in the forest shows a small decrease at around 800 Hz, which is between 2 to 4 dB, and the results in the scale model show a similar reduction at positions S1R2 and S2R1. In the case where the source and receiver are obstructed by the tree, the frequencies are greatly pronounced below 800 Hz in the real forest. The IR at position S2R2 in the scale model agrees with this result, while the results at position S2R1 do not. This might be due to the surface of the impeded modelled tree producing more reflections at position S2R1. Compared the magnitude between the octave band 250 Hz and 2.5 kHz, the increase in the scale model is generally higher than in the real forest. For instance, the difference between these two octave bands at position S1R1 in the real forest is approximately 4 dB, and in the scale model is 16 dB.

6.9.5 The effectiveness of the scale model design

The recording space of the scale model is an anechoic chamber, which models the sound attenuation in an outdoor environment [9]. The energy decay curve shows a more rapid regression than the outdoor environment, as it only captures acoustic propagation within the forest scale model range. Additionally, the spectrum results in the scale model generally show similar trends to the results in the real forest, where there is an increase from 250 Hz to 2.5 kHz. This result shares similarities with the sound attenuation results in the open spaces (shown in Fig. 3.12), which indicates that an anechoic chamber is sufficient to model an outdoor space. Although the limited number of modelled tree trunks might constrain the simulation of low frequency attenuation.

The spectrogram results of the scale model IR at positions S1R1 and S2R1 show the greatly pronounced direct sound energy above 1 kHz. This indicates the SACs of the aluminium tubes might be relatively low for modelling tree trunks. Given the ground mostly affects sound propagation below 500 Hz, the EDT values at octave bands 250 Hz and 500 Hz show generally good agreement with the forest IR results, this indicates the unvarnished MDF board is a valid material for modelling forest ground at the scale of 10.

The scale of 1:10 makes use of the available space in the chamber. As discussed in Section 6.9.1, modelling 33 trees is sufficient for modelling a forest. The choice of this scale is fairly sensible.

6.10 Conclusion

This chapter presents the scale model IR analysis, along with comparisons with the real world forest IR results. The scale model waveform results show distinctive early reflections, which can be related to the tree trunk reflections. The waveform results at position S2R2 indicate that the scale model can simulate the physical property of an impeded tree being close to the source. The spectrum results share similarities in both environments, where the energy is greatly pronounced above 800 Hz. In general, scale model waveform and spectrum results align

well with the real forest results. The EDT results in the scale model share similar trends as the real forest results, although at the 1 and 2 kHz octave bands, the results are less comparable. As discussed in Section 6.9, the discrepancies in the EDT and the spectrogram results can be explained and further improved.

The scale model results provide a proof of concept as the results bear sufficient simulation to the real world acoustics, even with the number of assumptions that have been made. The limitations and avenues for possible improvements will be further discussed in Chapter 7. Here are the key findings of this scale model:

1. The method of modelling an outdoor space in the anechoic chamber is sufficient.
2. The aluminium tubes for modelling tree trunks at a scale of 10 are overly reflective at high frequencies. The unvarnished MDF board is valid for modelling forest ground.
3. Given the limited test space in the anechoic chamber, the modelled 33 tree trunks can simulate sufficient reflections to model a forest environment.
4. The higher order reflections from tree trunks have an important role in forest sound propagation.
5. Given that the method of modelling the tree trunks as rigid cylinders is based on the assumption made in the *Treeverb* and *WGW* modelling work, this assumption is somewhat valid.

Chapter 7

Conclusion

This report had investigated the acoustic characteristics of tree trunks in a forest environment. IR measurements were conducted in a forest with prominent tree trunks, and the layout of the forest was documented. By relating the IR results to the forest layout, the acoustic properties of the forests were analysed. IR measurements were also conducted in an acoustic scale model of this forest. The model was formed of a set of rigid cylinders and a flat ground surface to evaluate the assumptions made in previous modelling work. A comparison of the IR results from both environments demonstrated the validity of this approach. The use of an acoustic scale model has been shown to be suitable for modelling a forest environment.

7.1 Summary

This section provides a summary of this work, and an evaluation of the extent to which the research questions have been answered.

1. What are the acoustic properties of tree trunks in a forest environment?

The literature review presented in Chapter 2, and the IR measurements and analysis in Chapter 3 and 4 have shown that tree trunk reflections are the main acoustic features in a forest environment, which provides reverberation mainly at 1 and 2 kHz. Here are the key findings:

1. Frequency dependent characteristics. The acoustic parameter T30 results show reverberant responses from 500 Hz to 2 kHz, which are above 1.5 s. Outside this range, attenuation increases, where the T30 values are below 1.3 s. The highest reverberation time of 2 s was found at 1 kHz.

2. Tree trunk reflections are the key features in a forest environment, which mainly affect the frequency of sound with wavelengths in a range around tree trunk diameters, typically at 1 and 2 kHz. The forest scale model suggests that higher order reflections also play an important role in sound propagation.

2. Is an acoustic scale model a good approach to studying forest acoustics?

There is previous work using acoustic scale modelling techniques for outdoor spaces, however, there is no up to date example of doing this for a forest. Therefore, this work has been experimental. But results have shown the approach to be valid, with the following caveats:

1. The size of the anechoic chamber limits the number of modelled tree trunks. Consequently, it limits the scale of the model, where the scale of 1:10 was chosen out of necessity.

2. The choice of the modelled materials of tree trunks and the ground, given the limited research in sound absorption coefficients (SACs) of tree trunks and forest floor above 8 kHz.

3. The choice of the modelled tree trunk height, given the limited research in the forest scale model and the limited expense of the project.

4. There are limitations in the recording equipment:

   (a) This experiment is limited to the measured octave bands (from 250 Hz to 2 kHz in the acoustic parameter analysis), given the capability of the tweeter is up to 30 kHz.

   (b) The measurements were conducted with the source rotated, but the directivity of the tweeter has not yet been tested, and the approximation of the omnidirection remains uncertain.

(c) The SIRR analysis is not conducted in this model because the size of the available four channel microphone is relatively large, and not suitable for the scale model measurement. This limits the directional factor analysis to identify the reflections from modelled tree trunks further.

3. Are the assumptions made in the Treeverb *and* WGW *valid?*

As discussed in Section 2.3, the *Treeverb* and *WGW* modelling work assume that the tree trunks are an important feature of the forest environments and they can be modelled as rigid cylinders. Forest IR analysis verifies the role of tree trunks in forest acoustics. Scale model results show similarities to the real world forest IRs, indicating that these assumptions are somewhat valid. There is work to be done to further evaluate this modelling work:

1. The comparisons between a rigid cylinder and a tree trunk.
2. The effect of branches and foliage.

7.2 Contributions to the field

The main contribution to the field made by the work presented in this thesis is the comparison and analysis of IRs recorded in the real-world forest and in the scale model, as no previous studies of this kind are available. The findings presented here may be useful in the development of acoustic modelling algorithms, such as the *WGW*.

Novel decisions in the design and construction of a forest scale model (aluminium tube filled with plaster, unvarnished MDF, the height of the tube) represent a minor but useful contribution to the field, and further work is required to assess the validity of these design decisions.

7.3 Project management

There was a planned schedule in a GANTT chart before this project work (shown in Fig. 7.1a), and another GANTT chart was used to document each week's actual work (shown in Fig. 7.1b). The planned schedule of both measurement work in the forest and the scale model allowed for an extra week for re-measurement. As both measurements went well in practice, the measurements only took one week each and were on schedule. Fig. 7.1b shows the sound attenuation measurement in a forest and an open field was an extra measurement for this project, which was decided during the project work. The plan was allocated for scale model experiments from Week 2 to Week 5, and the actual work mostly noted the forest IR analysis. During this month, there were meetings and discussions with the supervisor and technician. This process allowed for the model design. The thesis writing was started at the beginning of the project work (Week 2), and the main body (Chapter 2 to Chapter 6) was finished on Week 8. This allowed time for modifications to the thesis. In general, a comparison of these GANTT charts shows that the project work was completed essentially as planned.

This project involved weekly supervision meetings with the first supervisor, which included the discussion of the literature review, practical work and evaluation of the results. There were checkpoints with the thesis writing and feedback sessions provided by the supervisor. There were weekly update reports sent to the second supervisor and supervision meetings at each phase. This project included the practical work of the scale model, which required constant communication with the technician. The feedback provided by the supervisors and technician was significantly helpful for the project development.

During the construction of the scale model, there was a mistake made in the first layout measurement. The layout was measured with the tree positions flipped, as the negative on the Y axis was ignored. It should have been conducted by marking a few tree positions at each corner and checking the layout, before measuring other tree positions. The outcome was a re-measuring session, which took another three hours. The progress was not delayed because of this mistake, but it was a lesson to learn to be more meticulous.

The thesis writing in forest IR analysis was delayed, as it included a rewrite process on Week 7 (shown in Fig. 7.1b). The first draft was finished on Week 5, and feedback provided by the supervisor in the same week suggested a reconstruction for this chapter, which was an unexpected challenge. The actual work needed to prioritise the scale model measurement and generate the model IR results. These work were conducted on Week 5 and Week 6. After an evaluation of the work for the final month in the supervision meeting on Week 6, the plan was rescheduled and it allowed time for the reconstruction of the chapter.

In general, the evidence of good time management, regular sessions of discussion and the capability of risk management indicate effective and realistic project management.

7.4 Future Work

The short term future work can make use of the *WGW* reverberator to simulate the same forest in both environments. Compare the results with real forest results, which can directly evaluate the *WGW* model. For instance, the spectrum results can examine the simulation of the frequency dependent features of a forest. The spectrogram results can be used to evaluate how well the model simulated the different physical properties of the source and receiver positions. The reverberation time and waveforms can be used to investigate the sufficiency of modelling 33 tree reflections. Critically listening to the auralisation can evaluate the success of the simulation perceptually. The effectiveness of the modelling methods, which model scattering caused by tree trunks, can be further investigated. It would be worth comparing the *WGW* results with the scale model results, as both environments model sound propagation among 33 trees. The discrepancies in the results can identify the limitations of either model.

The long term future work can focus on the limitations found in the scale model. One approach to be taken might be to conduct scale model IR measurements with different modelling methods. For instance, it would be worth experimenting with using aluminium tubes to model tree trunks and covering the tubes with foam to model tree bark absorption. Compare the spectrogram results between foam covered and uncovered with the real forest results, which can evaluate the simulation of tree bark absorption. Another modelling method that can be

investigated is placing reflective barriers, such as unvarnished MDF boards with bobbles, at each side of the model to simulate reflections from further trees. This approach aims to improve the simulation of the limited number of trees. Additionally, there are a few corrections that might be worth making to further improve the results. Applying air absorption correction is potentially useful to improve EDT results at higher octave bands (above 1 kHz). Test the directivity of the tweeter, which allows for a better simulation of the omnidirectional source.

Another approach to be taken might be to conduct the IR measurement on a single tree and a rigid cylinder in an anechoic chamber, which aims to evaluate the assumption made in *Treeverb* and *WGW*. The real tree trunk should be as cylindrical as possible, and a perfect cylinder can potentially use unvarnished MDF material. The IR measurement is conducted by rotating the source position with different angles, around the tree and the cylinder. The comparisons of both measurement results can provide insight into the effectiveness of this modelling method.

7.5 Personal reflection

The project work was hugely relevant to the module in virtual acoustics and spatial audio, as most of the project work was about IR measurements and their analysis. Although this project considered an outdoor environment, which was different from room acoustics. Analysing the forest IR results became the biggest challenge during the project work. There were efforts in literature reviews in this field and discussions with Frank to understand the results. The structure of this chapter writing was also challenging, as it was rather difficult to clearly present the results and also point out the key findings. There was a reconstruction of this chapter that I did during the project work. The process was hard and I was frustrated, but I enjoy the project I have taken on. Given the results from this work can provide valuable findings, it is worth being written in a better manner. (I sound like a nerd, but there we are.)

The things that I have learned are way too many (e.g., writing reports and MATLAB), but I do want to mention the symposium talk. I have learned to communicate in front of academics and peers in a clear and concise manner. My peers could understand my project pretty well

after my speech, it was very pleasing. It was good to receive positive feedback from Andy, he said that I looked like I was in my own world.

It was a fun and weird project that I did. The fun part is that Andrew has driven us to the forest three times, along with Frank's challenging music. The weird part is that the scale model constructed in the chamber was an installation art, which was absolutely beautiful. I should say I am more than happy to see how well this project went, as we didn't expect the scale model would be valid after just one experiment, along with other valuable findings. Obviously, I am willing to further investigate forest acoustics at a higher academic level.

Plan Schedule	S10	V1	V2	V3	V4	V5	V6	V7	V8	V9	V10	V11
w/c	19/06	26/6	03/07	10/7	17/07	24/7	31/07	7/8	14/08	21/8	28/08	4/9
Real forest IRs measurement												
Real Forest IR analysis												
Scale model experiments												
Scale model construction												
Scale model IRs measurement												
Both IRs results analysis and comparison												
Thesis write up												
Final write up												
Final final write up												

(A) A GANTT chart of the planned schedule.

Actual Work	S10	V1	V2	V3	V4	V5	V6	V7	V8	V9	V10	V11
w/c	19/06	26/6	03/07	10/7	17/07	24/7	31/07	7/8	14/08	21/8	28/08	4/9
Real forest IR measurement												
Draw forest layout & Deconvolve IR results												
Write Matlab - average IRs, ISO and SIRR data. Write thesis - forest measurement.												
Write Matlab - waveform, auralisation script. Literature review - IR analysis.												
Write Matlab - spectra, decay curve. Measure attenutaion in forest and open field. Write thesis - forest IR analysis.												
Build scale model & Measure scale model IR. Finish write thesis - forest IR analysis (first draft).												
Write Matlab - scale IR results. Write thesis on scale model measurement.												
Write thesis - Measurement & Analysis sound attenuaion. Rewrite/Reconstrcut forest IR analysis.												
Write thesis - Analyse scale model IRs. Consise Background theory.												
Write Matlab comment. Write thesis - conclusion & introduction & abstract												
Write thesis - conclusion & introduction. Modify all chapters. File up hand-in files and write Appendix.												
Final write up.												

(B) A GANTT chart of the actual work over the allocated time.

FIGURE 7.1: Two GANTT charts presented the planned schedule and the actual work.

Appendix A

Figures

A.1 Figures of background theory

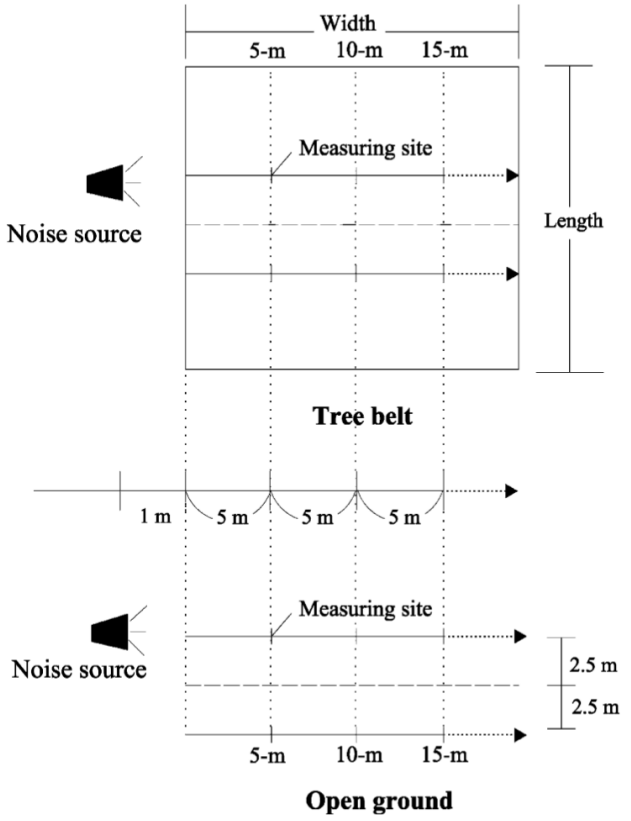

(A) The design of measurement sites.

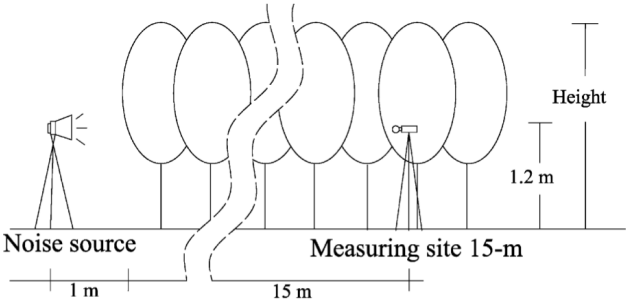

(B) The profile of measurement sites.

FIGURE A.1: The sites of the sound attenuation measurement in Fang et al.'s study. From [2].

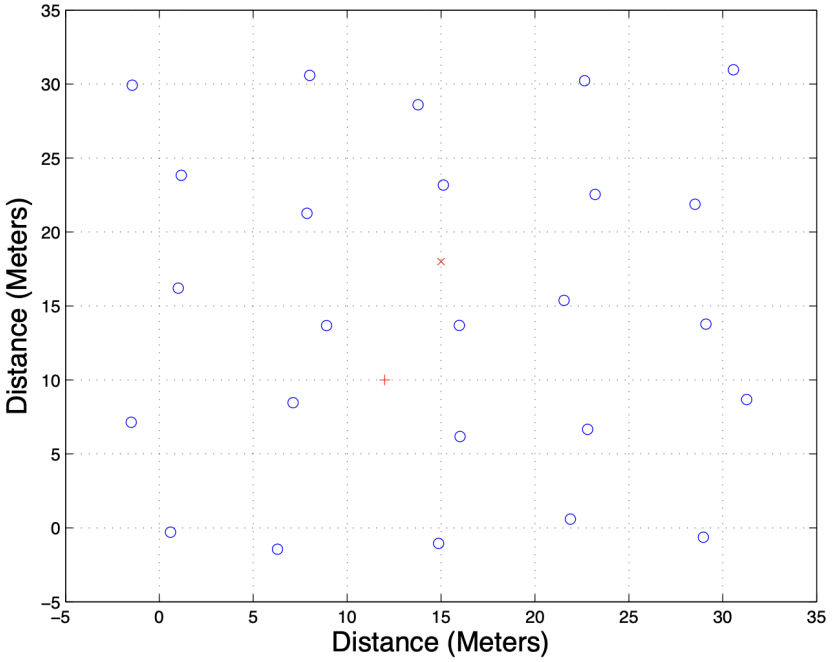

FIGURE A.2: Forest layout formed of 25 trees used in *Treeverb* simulation. Each tree's radii is 0.5m. From [5].

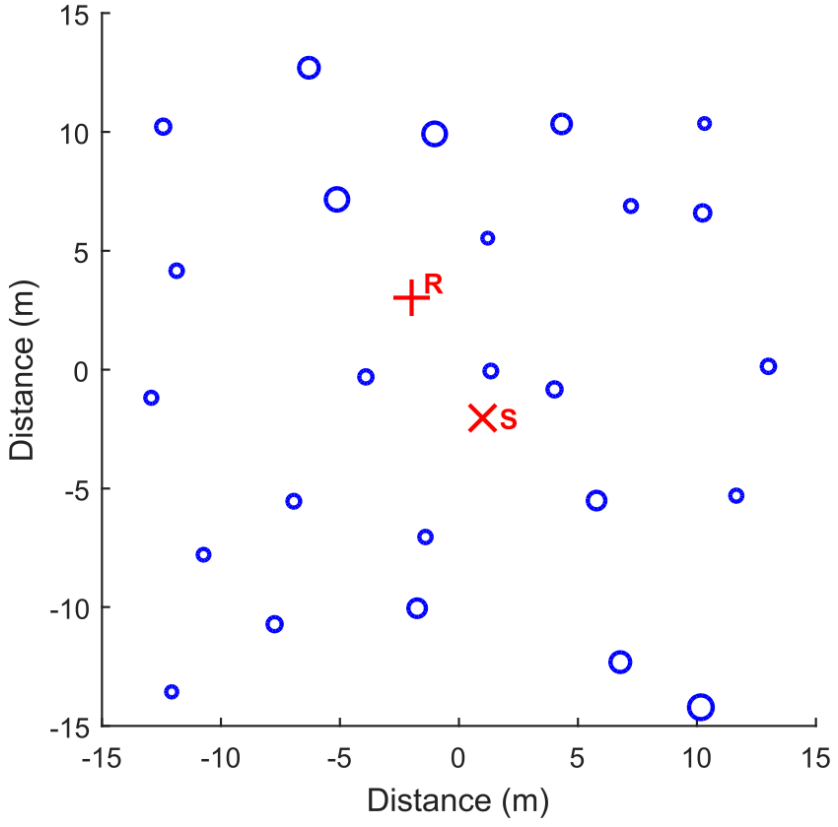

FIGURE A.3: The forest layout used in *WGW* reverberator. The configuration formed of 25 trees with radii between 0.2 to 0.5 m. The region is 30×30 m. From [1].

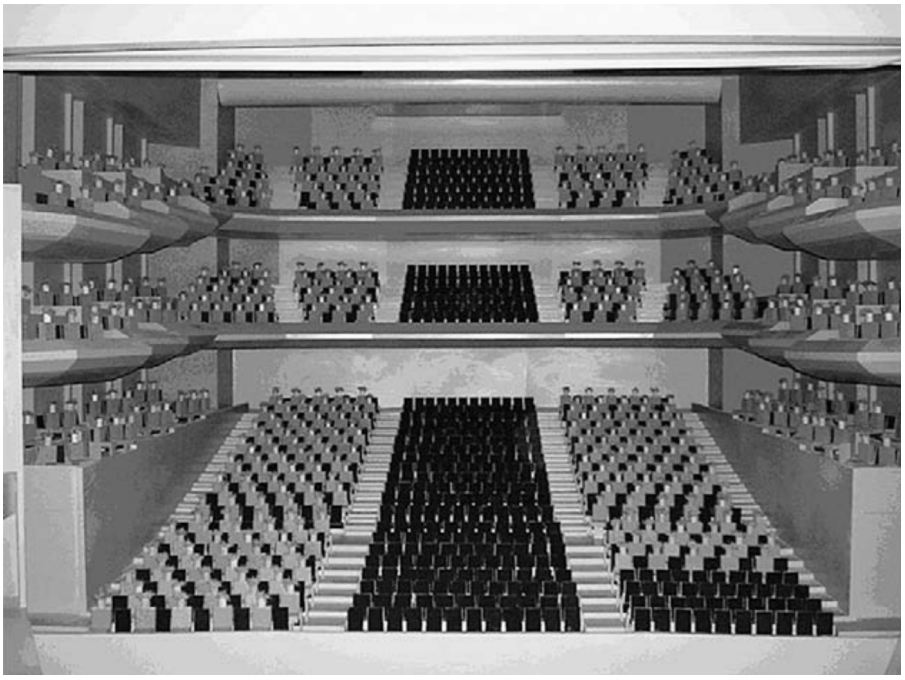

FIGURE A.4: A scale model of the GAH hall in the reverberation chamber in Jeon et al.'s study. From [8].

FIGURE A.5: The microphone (left) and loudspeakers array (right) used in Stonehenge scale model. From [9].

A.2 Figures of forest IR measurement

(A) A picture of measurement team hiding behind the trees. Left to right: Andrew Chadwick, Richie Cully, Frank Stevens.

(B) A picture of measurement team hiding behind the trees. Left to right: Andrew Chadwick, Sinuo Feng, Frank Stevens.

FIGURE A.6: Picture of forest IR measurement team.

FIGURE A.7: A flag that drew the measurement range situated at NE (Northeast) directivity.

FIGURE A.8: A Geenelec 8130A loudspeaker was used as the source at the height of 1.5 m for the forest IR measurement. The speaker was powered by an inverter generator placed on the ground and covered in a plastic bag.

(A) An Earthworks M30 measurement microphone placed at the height of 1.5 m.

(B) A Soundfield ST450 MkII microphone placed at the height of 1.5 m.

FIGURE A.9: Two microphones used for the forest IR measurements.

(A) A Soundfield ST450 MkII recorder (bottom) and a Zoom F8 multitrack field recorder (top) were powered by two Sony battery packs separately.

(B) The recorders connections. Four breakout leads were used to reduce the gain from the Soundfield recorder to the Zoom recorder.

FIGURE A.10: Two recorders used for the forest IR measurements.

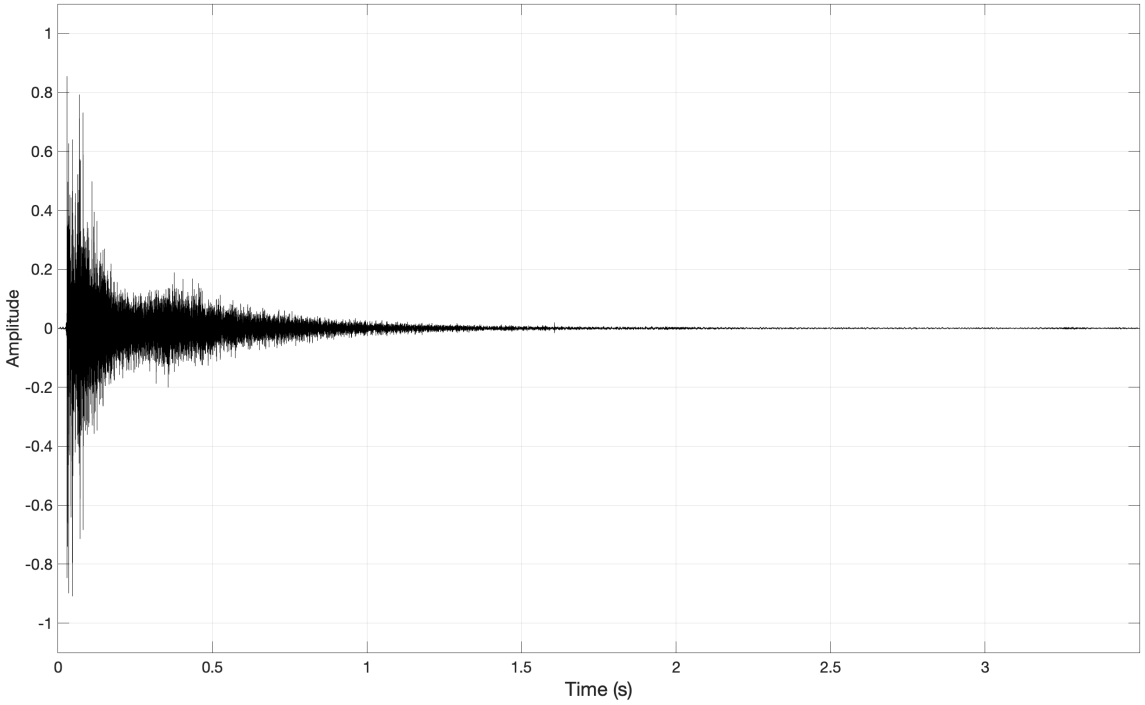

FIGURE A.11: Recorded starter pistol waveform at the forest recording site.

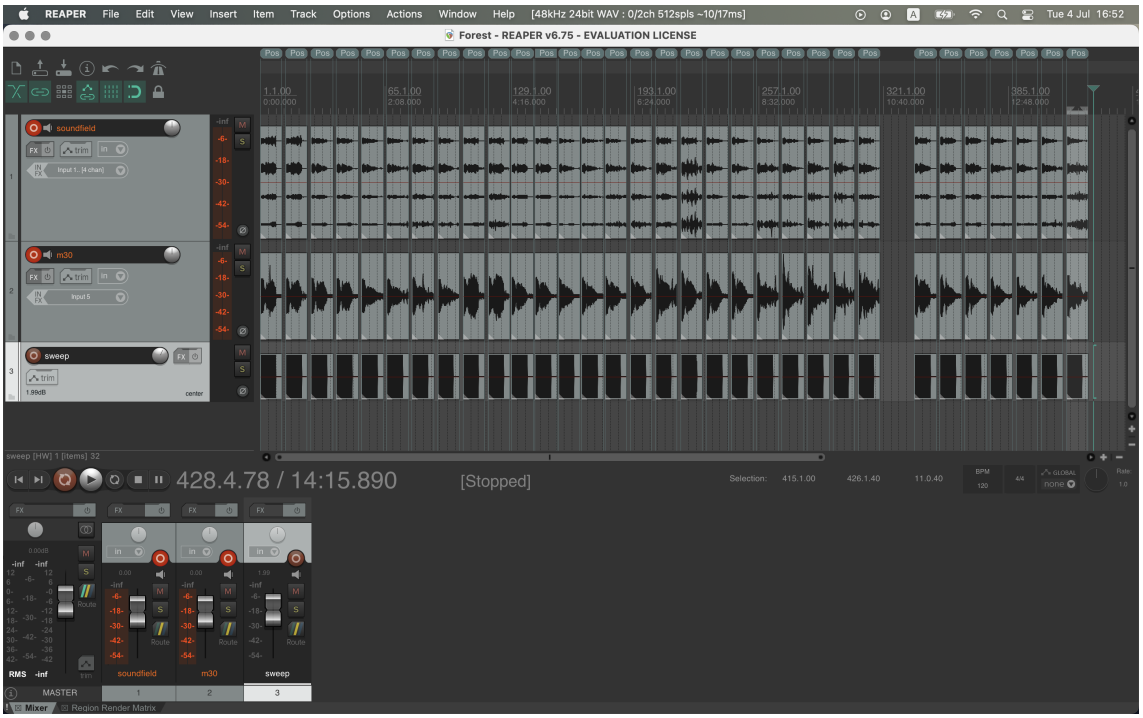

FIGURE A.12: A screenshot of Reaper used as DAW for the forest IR measurement.

(A) Loudspeaker facing *North*. Microphone at *Recevier 1*.

(B) Louspeaker facing *East*. Microphone at *Recevier 1*.

(C) Louspeaker facing *South*. Microphone at *Recevier 2*.

(D) Louspeaker facing *West*. Microphone at *Recevier 2*.

FIGURE A.13: Four orientations of the loudspeaker for the forest IR measurements.

FIGURE A.14: The measurement of the tree has no clear sight to the standing point was noted with a soft measure tape.

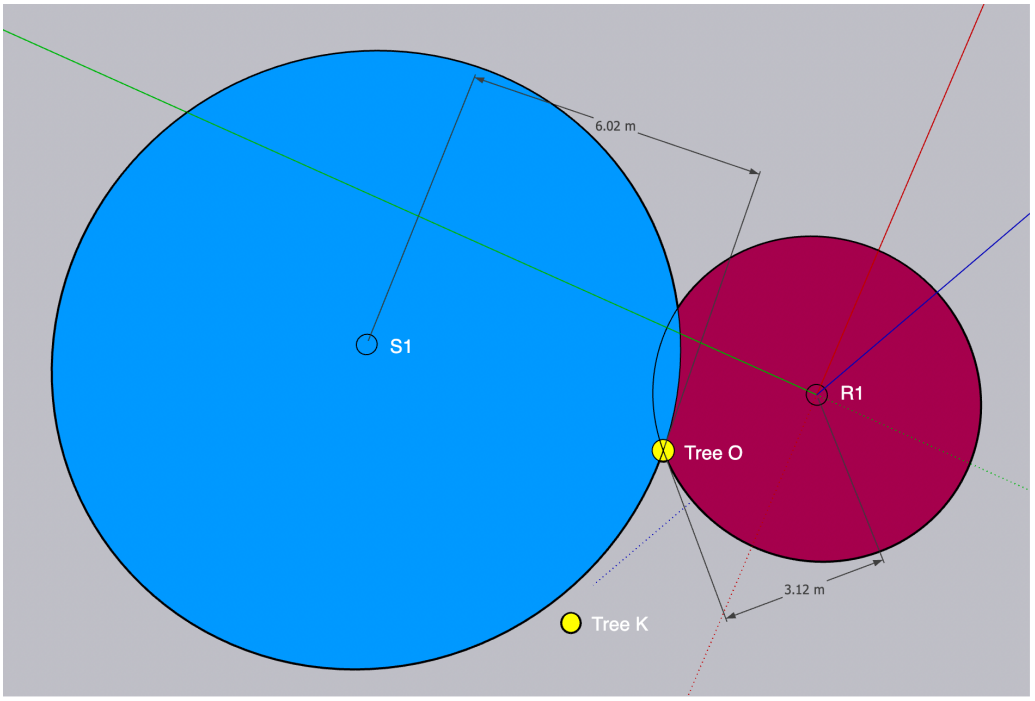

FIGURE A.15: The process of defining *Tree O*. *Source 1* and *Receiver 1* were used as standpoints to define *Tree O* position with their associated distance.

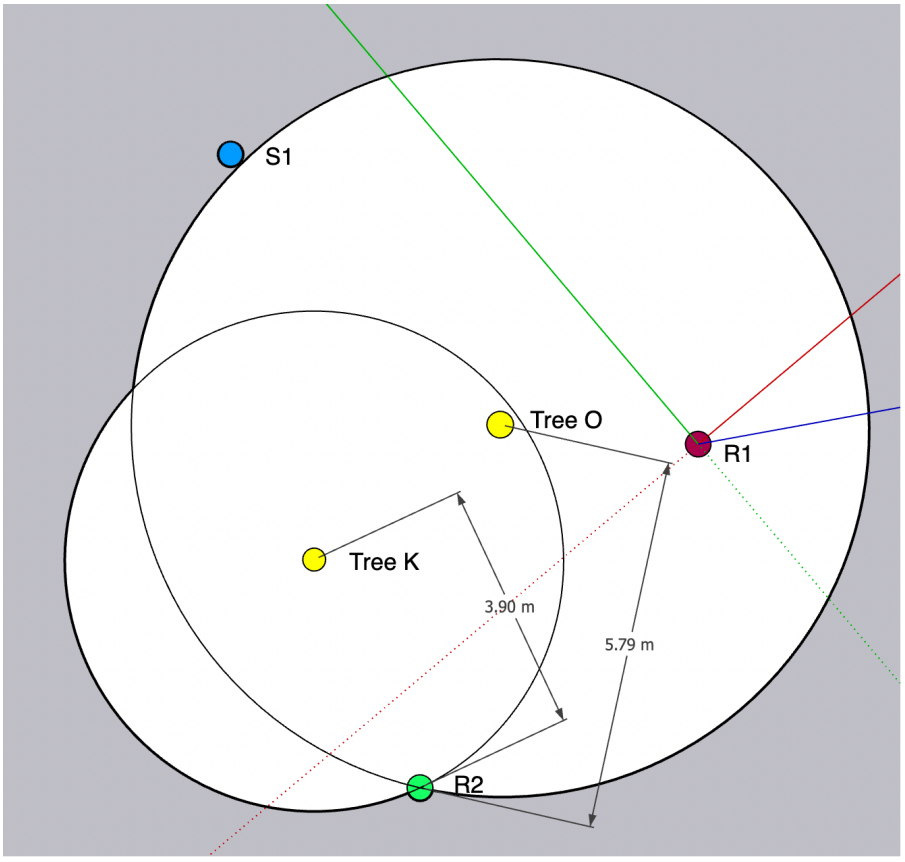

FIGURE A.16: The process of defining *Receiver 2*. *Tree K* and *Tree O* were used as standpoints to define *Receiver 2* position with their associated distance.

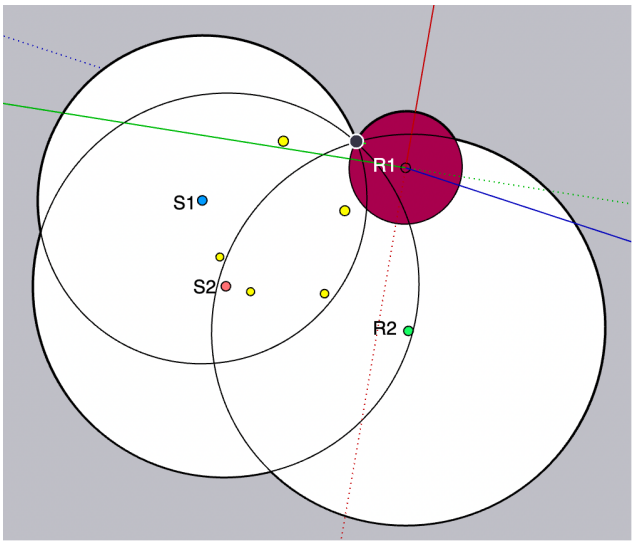

(A) Four standpoints (sources and receivers) were used to determine the position of *Tree R*. The intersection point indicates the centre position of *Tree R*.

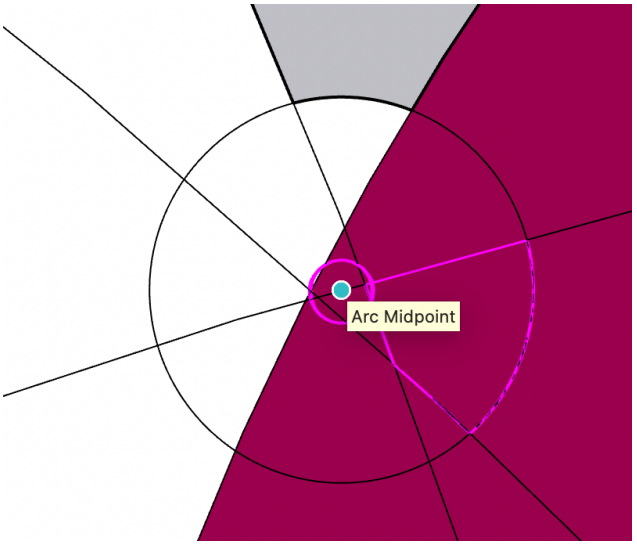

(B) A zoom-in view of *Tree R* intersection point. The tree position was estimated by finding the arc midpoint within this measured range.

FIGURE A.17: Define *Tree R* position using four measurement data.

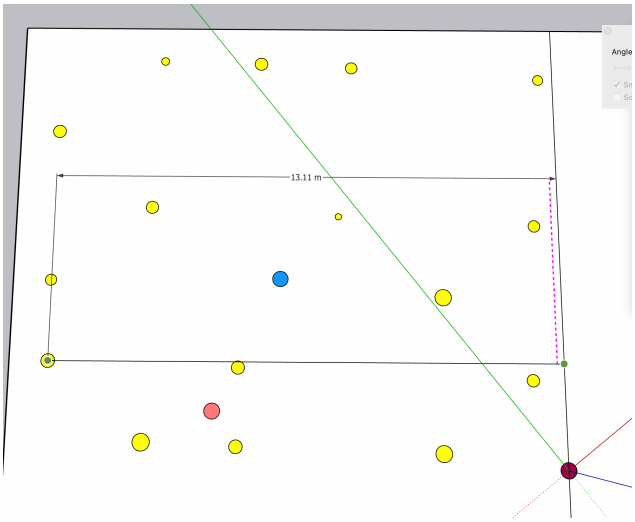

(A) Measure the x coordinate of *Tree X*.

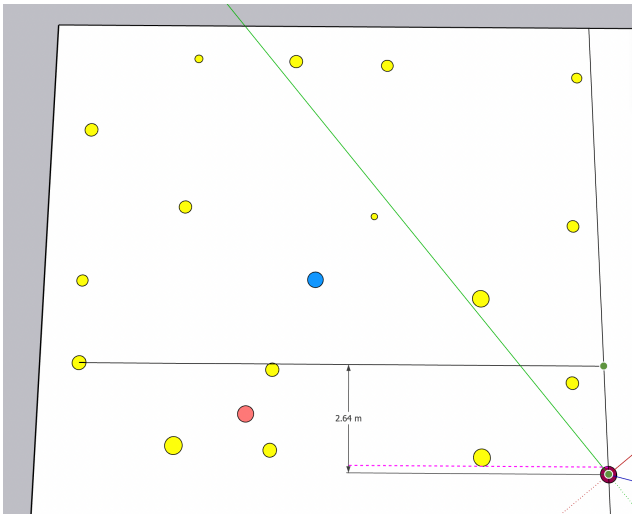

(B) Measure the y coordinate of *Tree X*.

FIGURE A.18: Measure coordinates of *Tree X*.

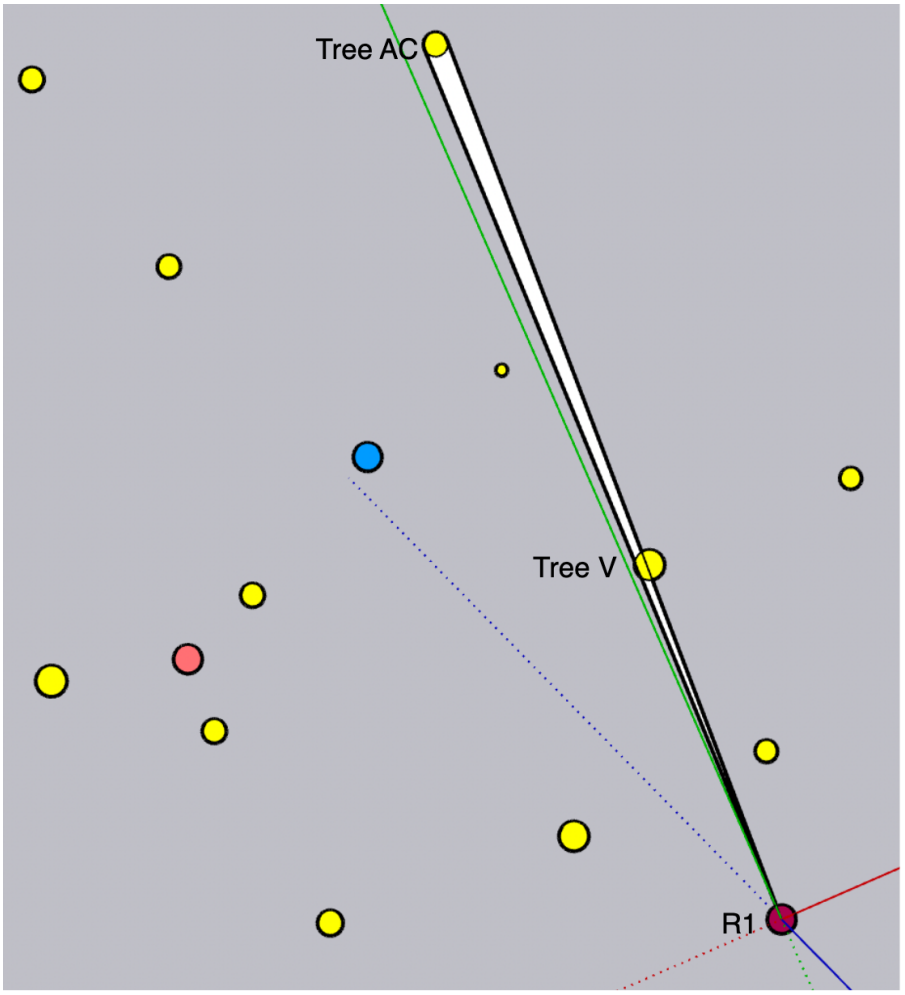

FIGURE A.19: The converted layout shows that *Tree AC* is impeded by *Tree V* from *Receiver 1*.

FIGURE A.20: Measure sound attenuation in an open field in Heslington Tillmire Site. The source used was a stater pistol and the receiver was a sound level meter. The measurement height was 1.5 m.

FIGURE A.21: Measure sound attenuation in the same forest environment as the IR measurement. The receiver position was not moved during the measurement, and the source position was found using a tape measure.

A.3 Figures of forest IR analysis

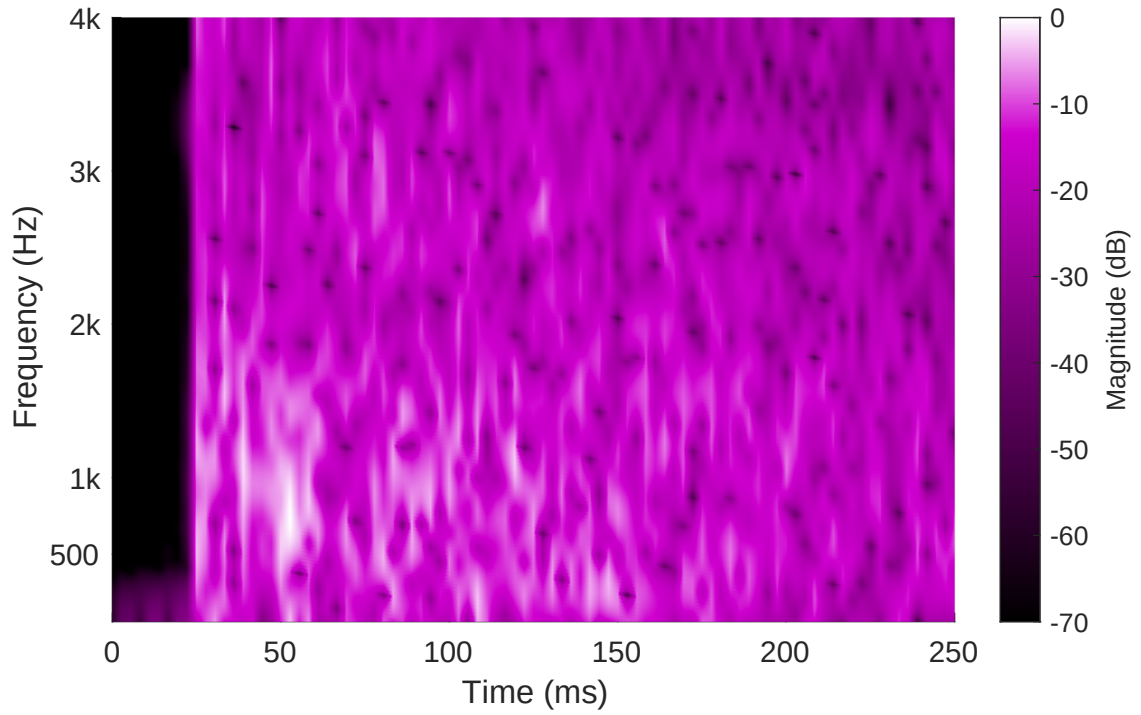

FIGURE A.22: Spectrogram plot of the W-channel response of an IR recorded in Heslington Church, University of York. The IR is taken from [51].

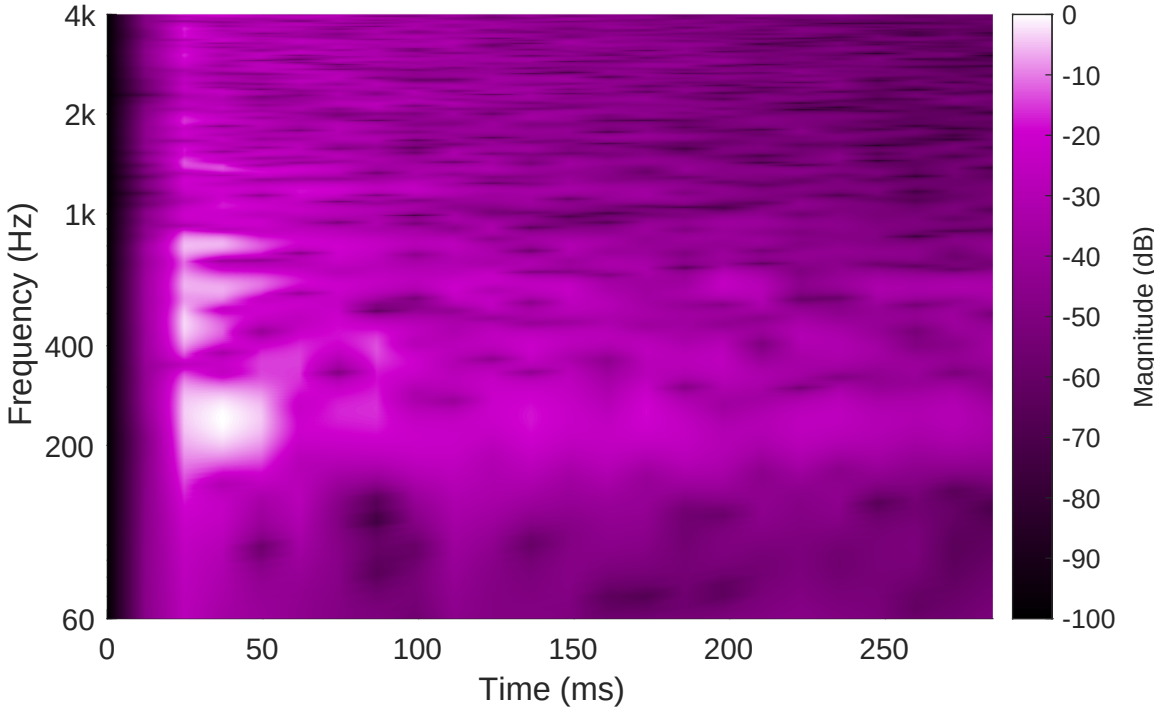

FIGURE A.23: A spectrogram of a snare drum.

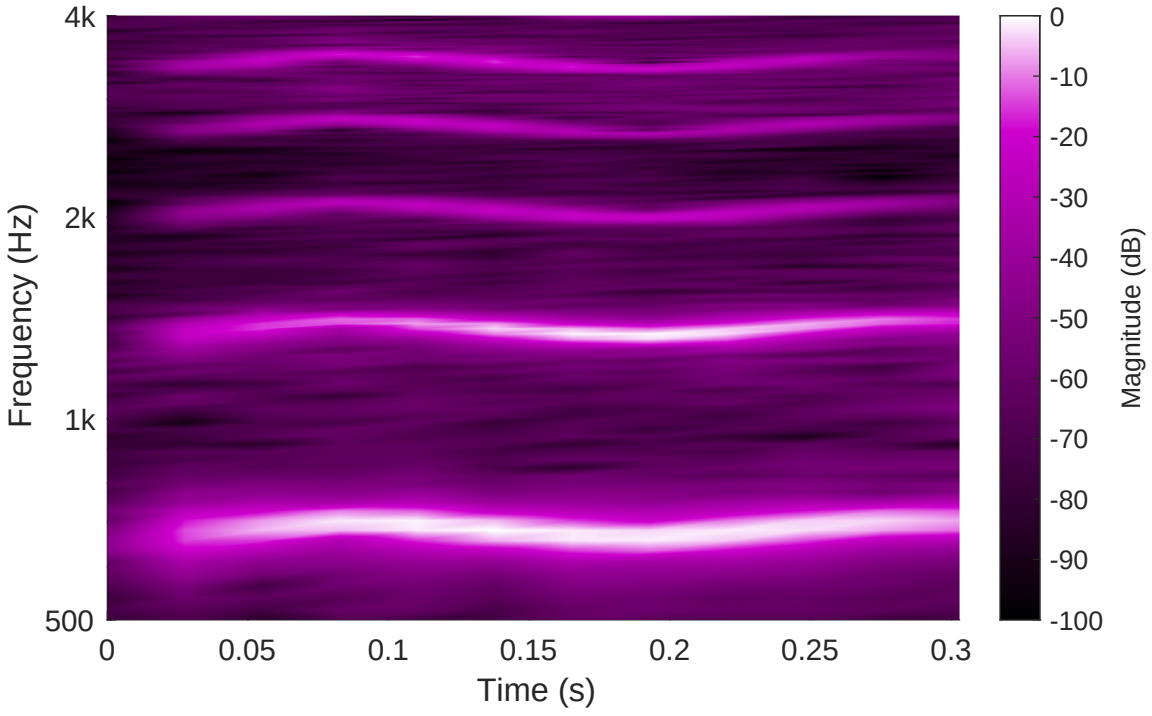

FIGURE A.24: A spectrogram of an anechoic singing note at approximately 680 Hz.

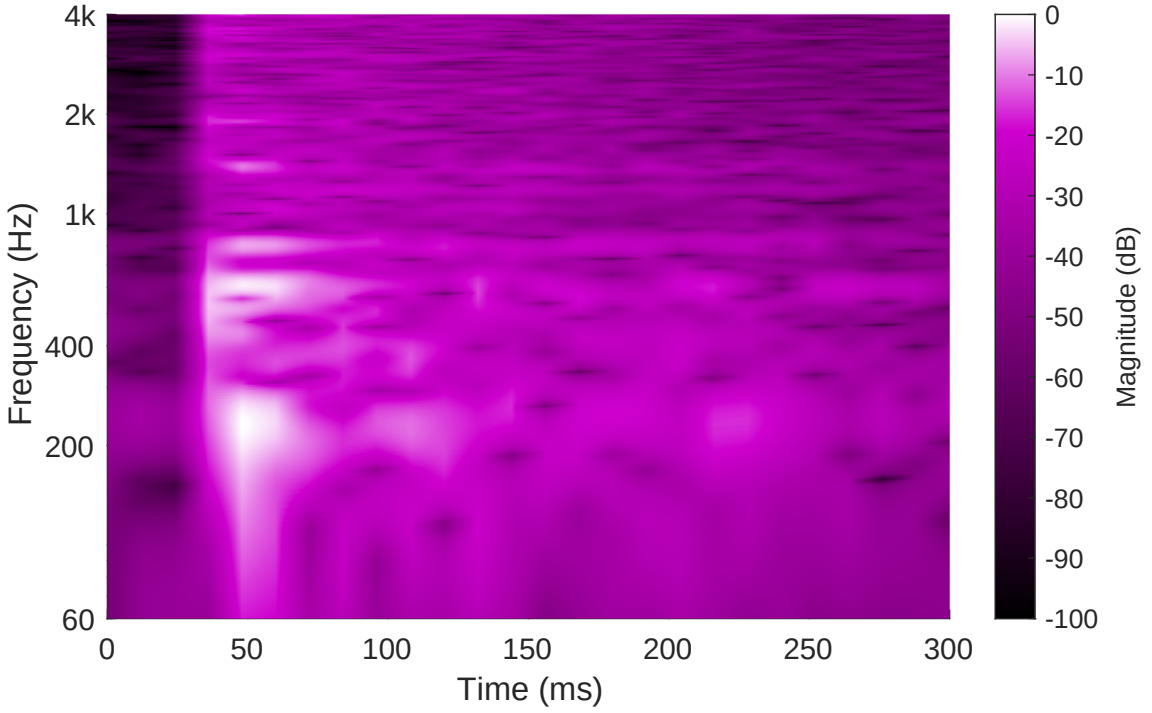

FIGURE A.25: A spectrogram of an auralised snare drum at position S1R2.

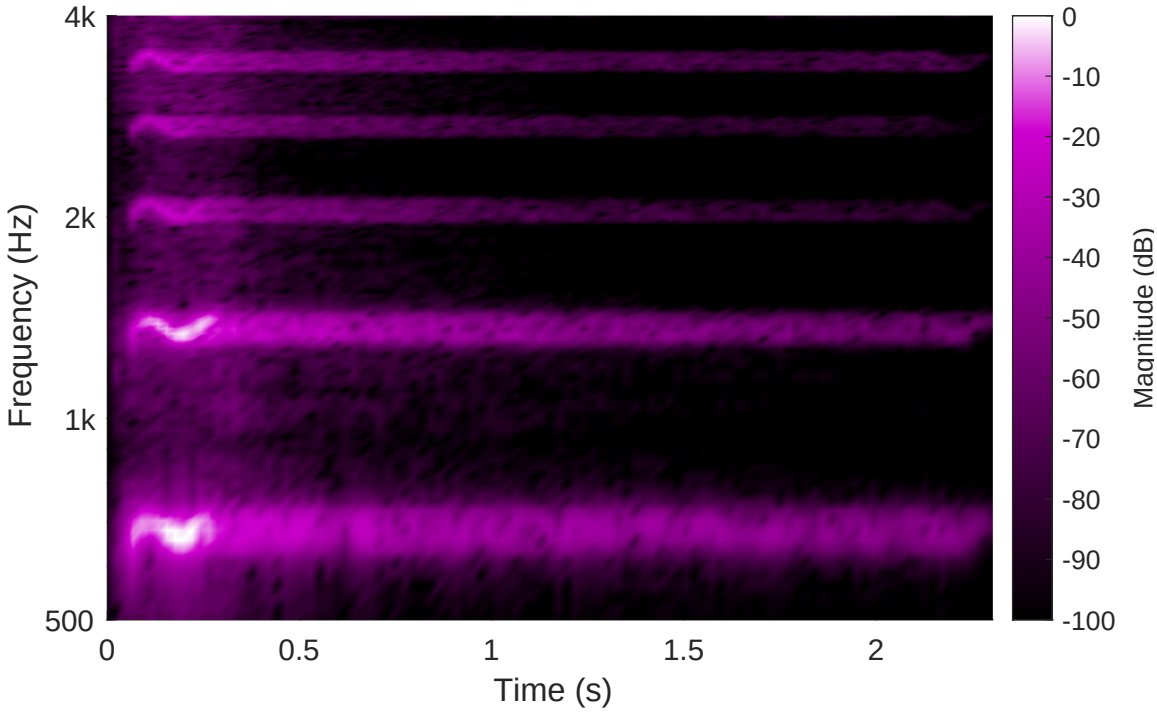

FIGURE A.26: A spectrogram of an auralised singing note at position S1R2.

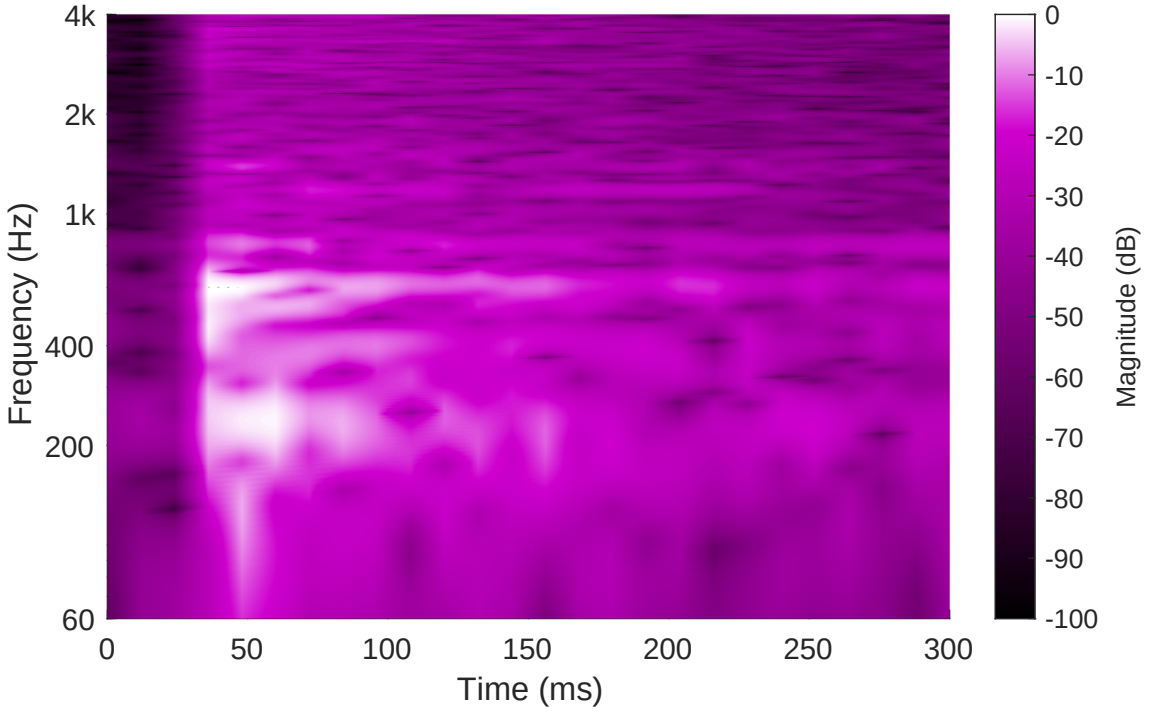

FIGURE A.27: A spectrogram of an auralised snare drum at position S2R1.

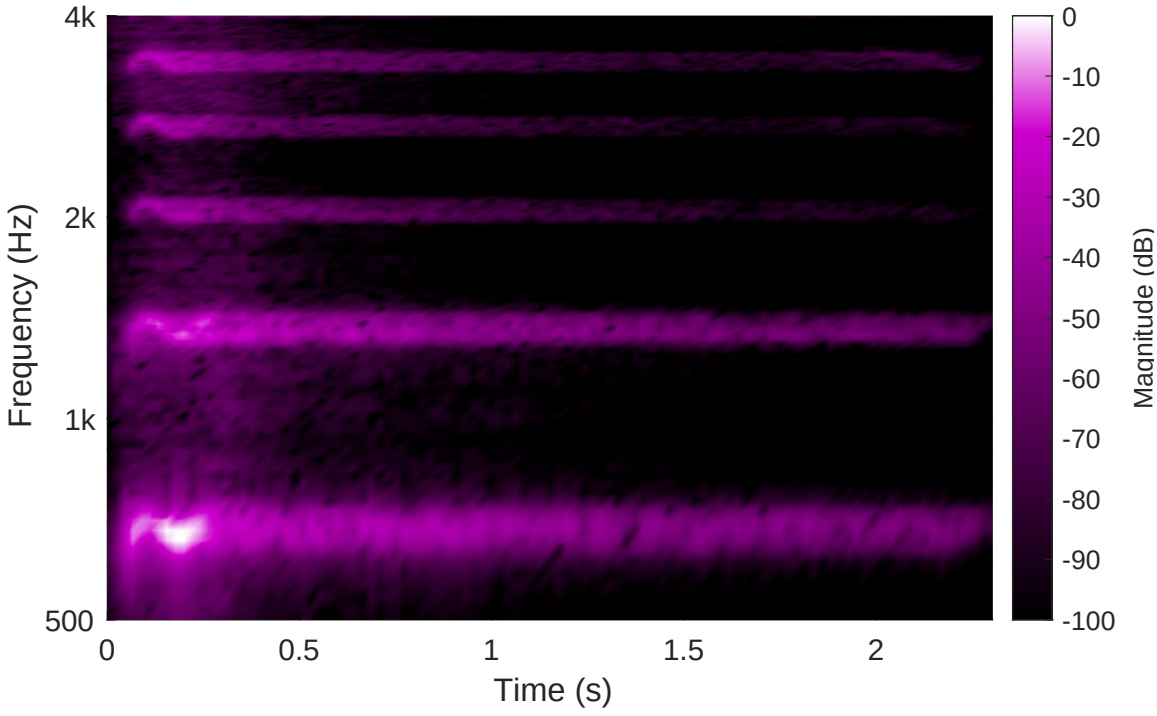

FIGURE A.28: A spectrogram of an auralised singing note at position S2R1.

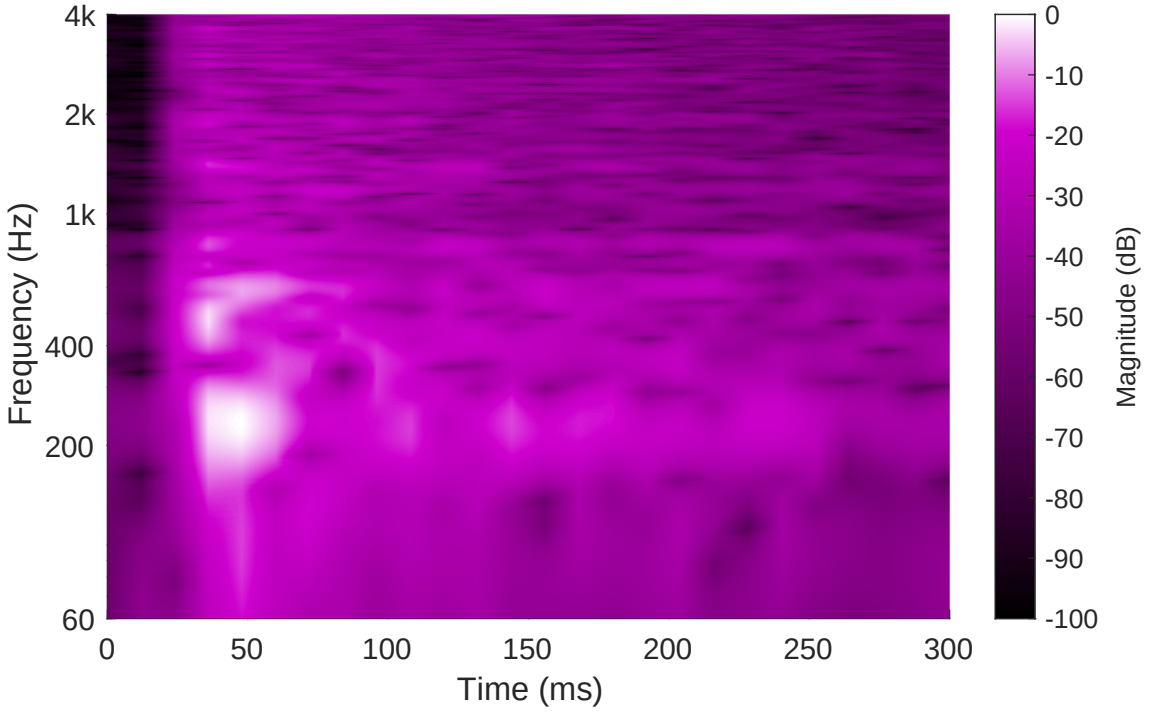

FIGURE A.29: A spectrogram of an auralised snare drum at position S2R2.

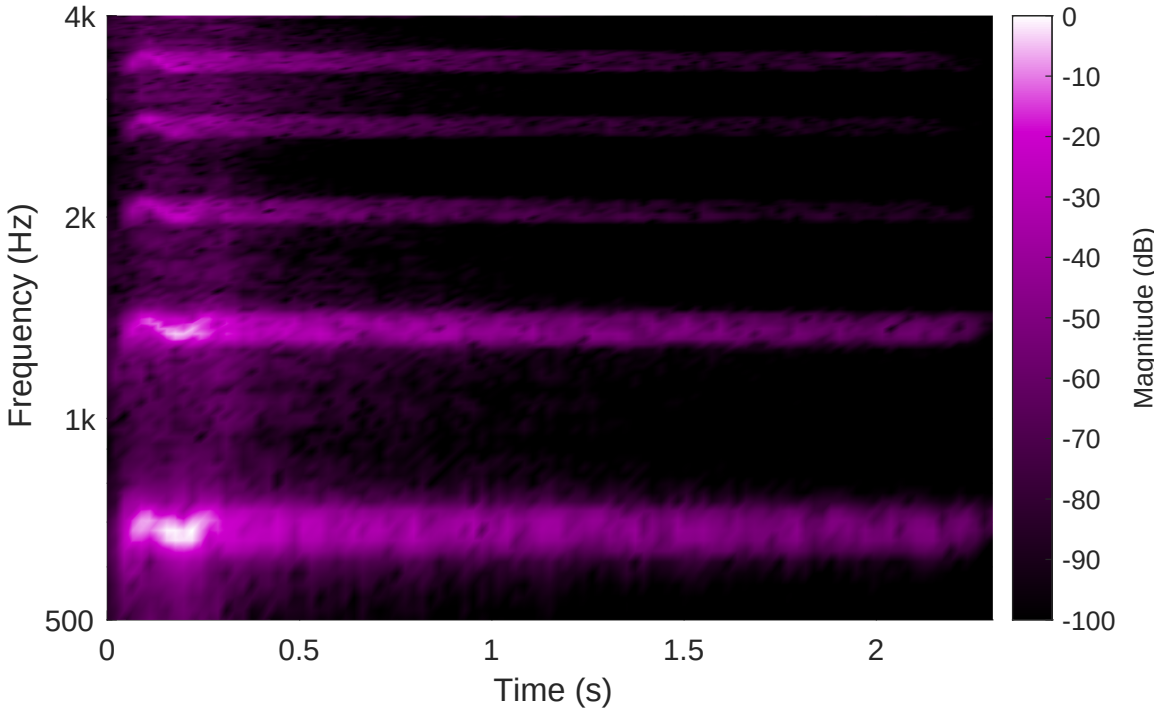

FIGURE A.30: A spectrogram of an auralised singing note at position S2R2.

A.4 Figures of forest scale model measurement

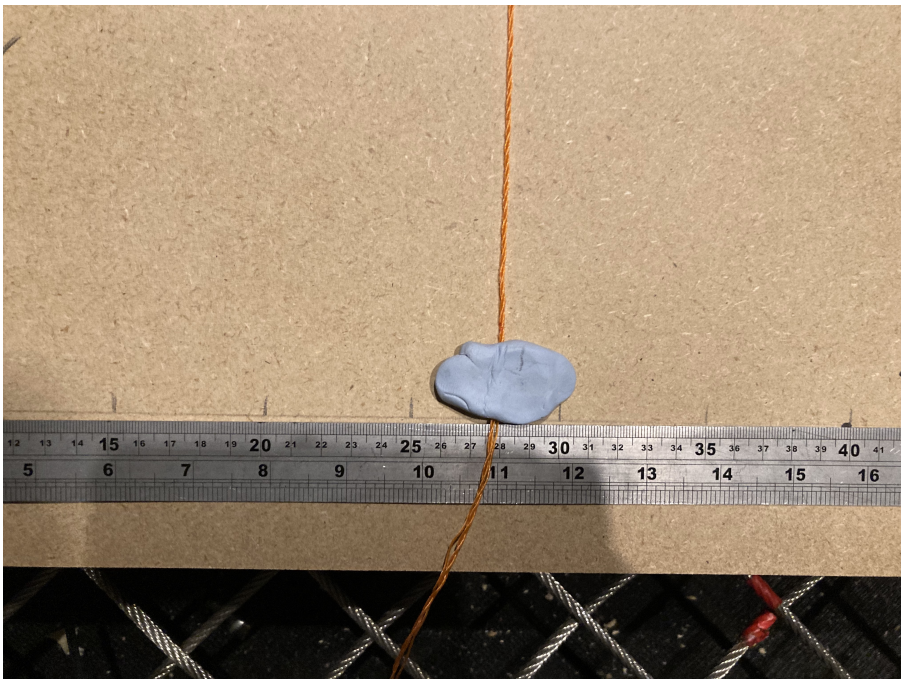

FIGURE A.31: A picture of marking one coordinate on one side of the board. An acoustic string was stabled using the blu tack, and the position was measured using a ruler.

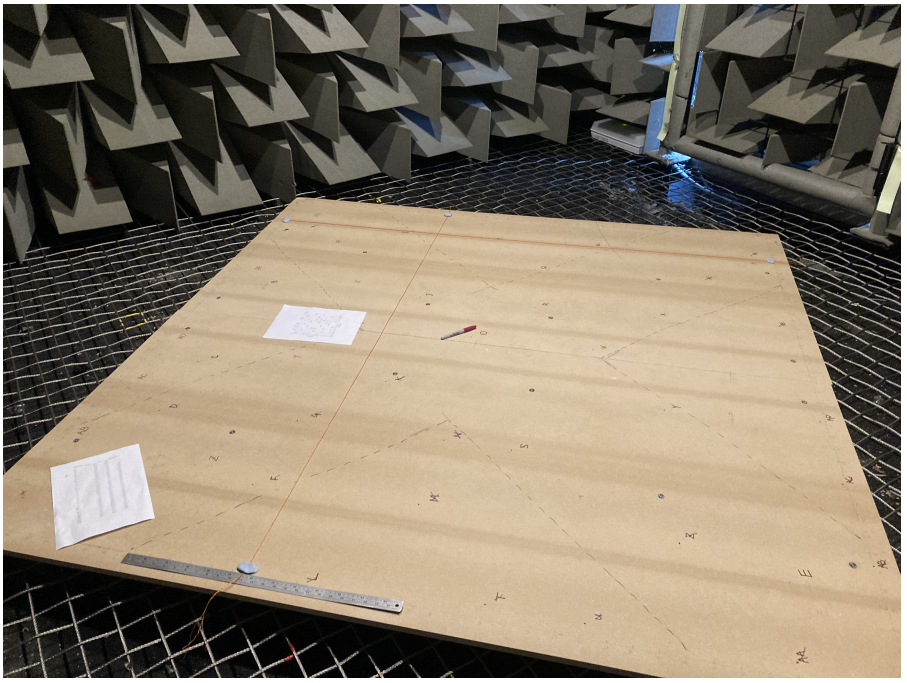

FIGURE A.32: A picture of scale forest layout measurement. Two acoustic strings were positioned on each side of the board, and the intersection was determined as the position.

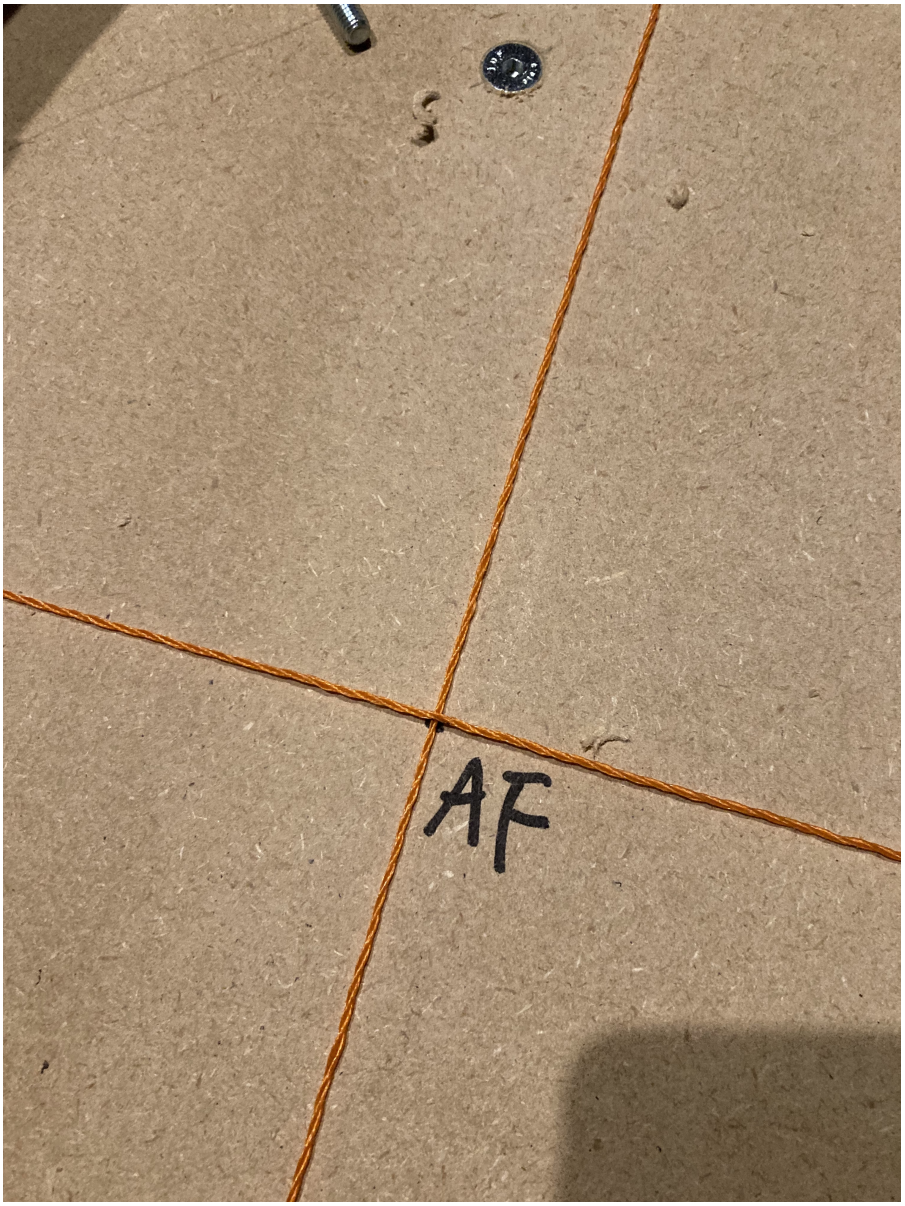

FIGURE A.33: A picture of intersection of *Tree AF*. The intersection was marked as a point, and the tree name was marked on the side.

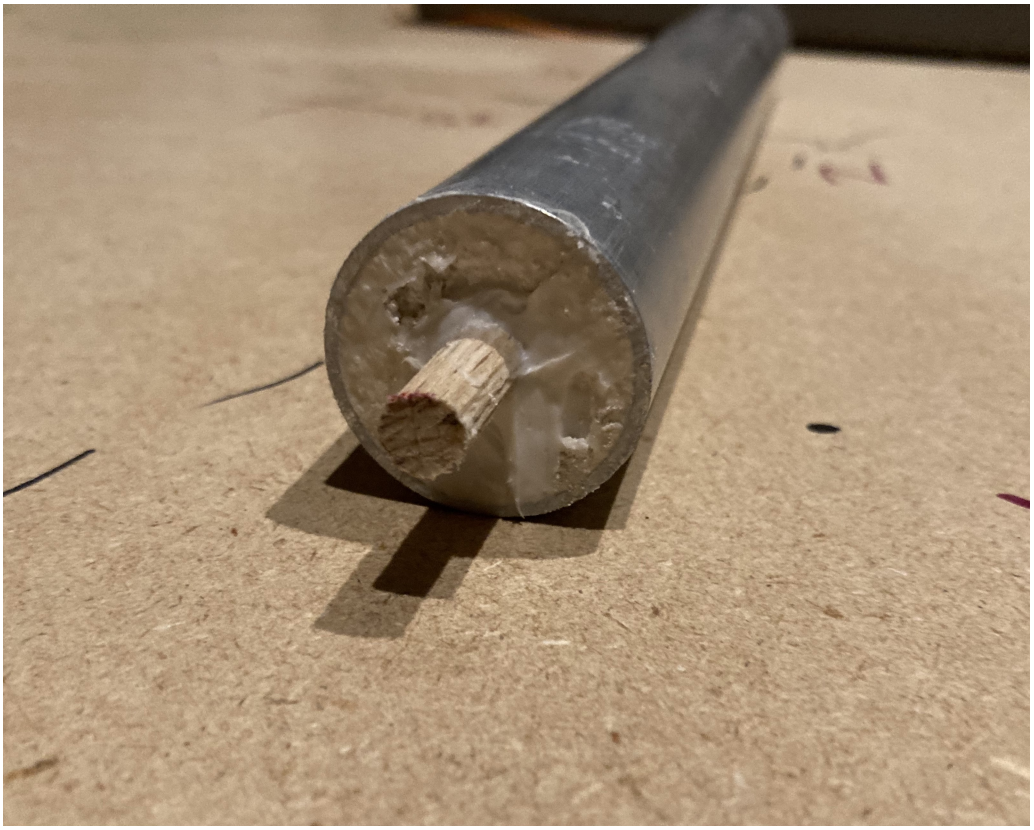

FIGURE A.34: A picture of the bottom of the modelled tree trunk stuck with a dowel. The dowel was half within the plaster and stabilised with glue.

FIGURE A.35: A picture of the modelled tree trunk doweling in the board.

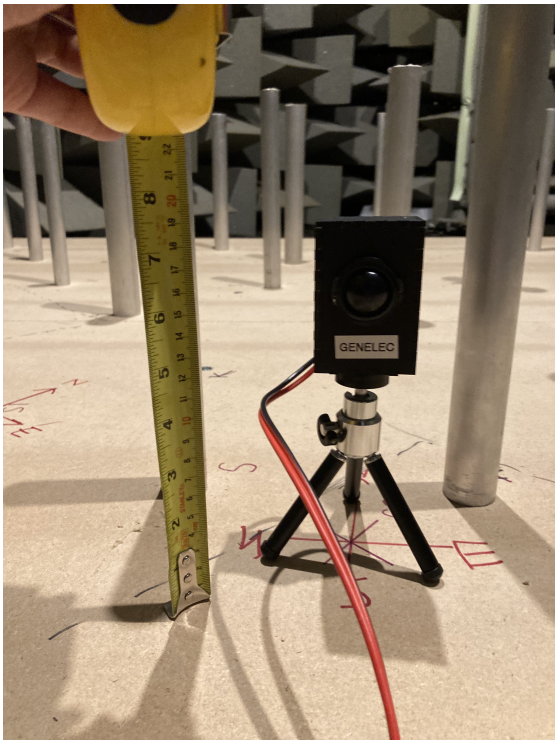

FIGURE A.36: A picture of measuring the height of the tweeter. The centre of the tweeter is situated at a height of 15 cm. Additionally, the tweeter box was designed for this measurement to accurately locate the speaker height.

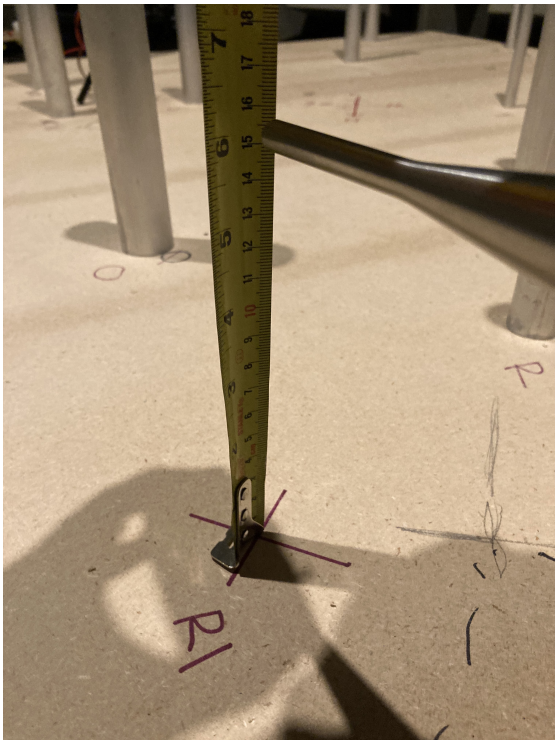

FIGURE A.37: A picture of measuring the height of the M30 measurement microphone. The receiver was situated at a height of 15 cm and the measuring tape was used to locate the receiver position.

FIGURE A.38: A Reference Amplifier A500 preamp (bottom) and a Fireface UCX interface (top) were used in the scale model measurement.

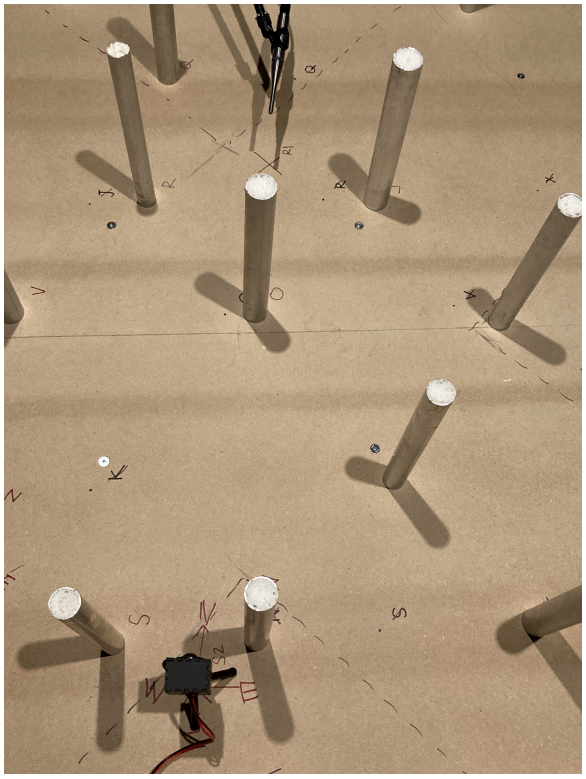

(A) Tweeter facing *North*. Microphone at *Recevier 1*.

(B) Tweeter facing *East*. Microphone at *Recevier 1*.

(C) Tweeter facing *South*. Microphone at *Recevier 1*.

(D) Tweeter facing *West*. Microphone at *Recevier 1*.

FIGURE A.39: Four orientations of the tweeter for the forest scale model IR measurements.

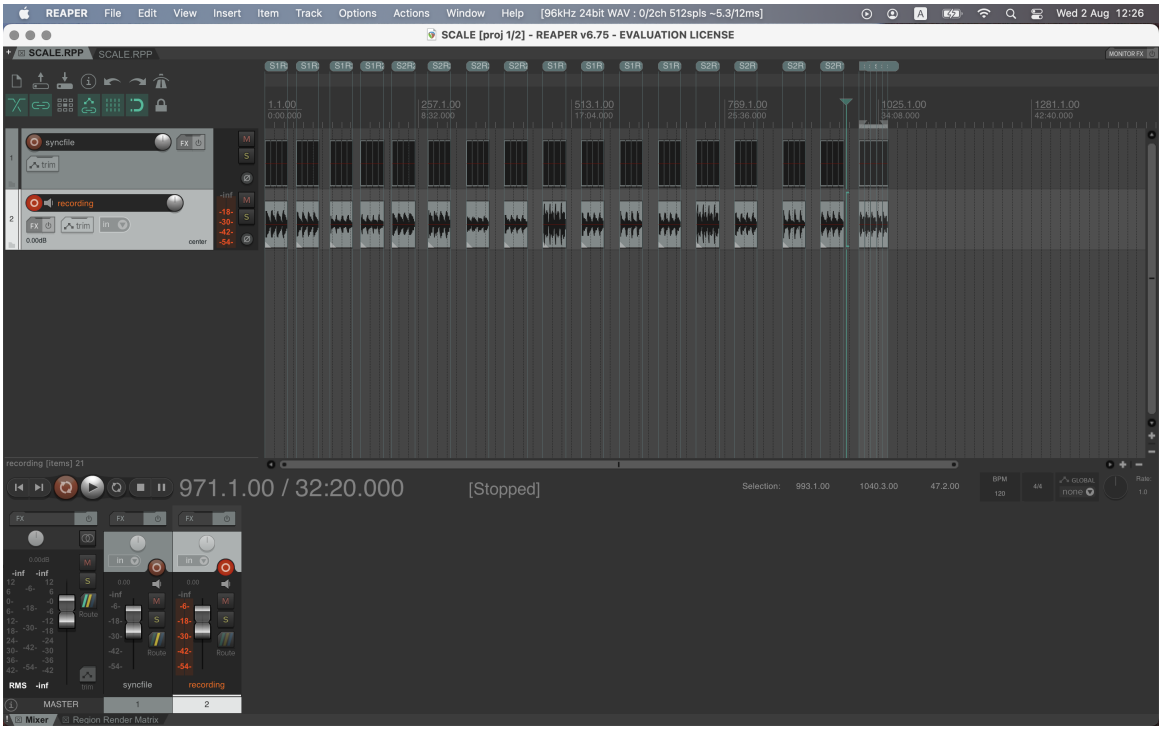

FIGURE A.40: A screenshot of Reaper used as DAW for the forest scale model IR measurement.

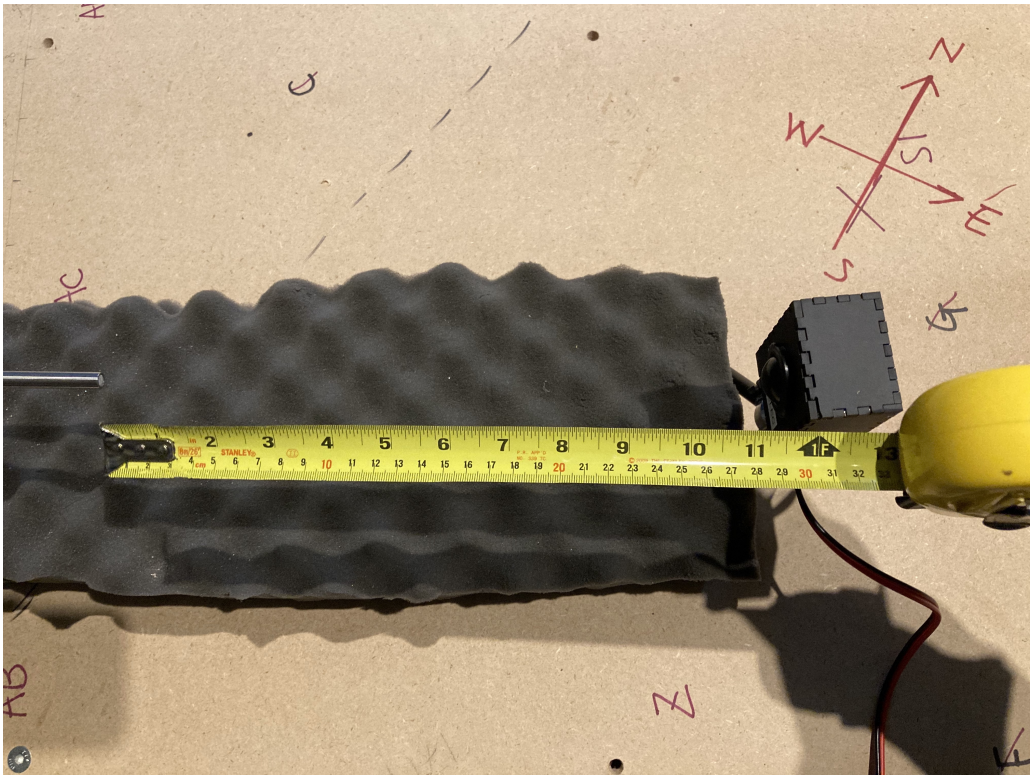

FIGURE A.41: A distance measurement between the tweeter and the microphone. The distance was 30 cm.

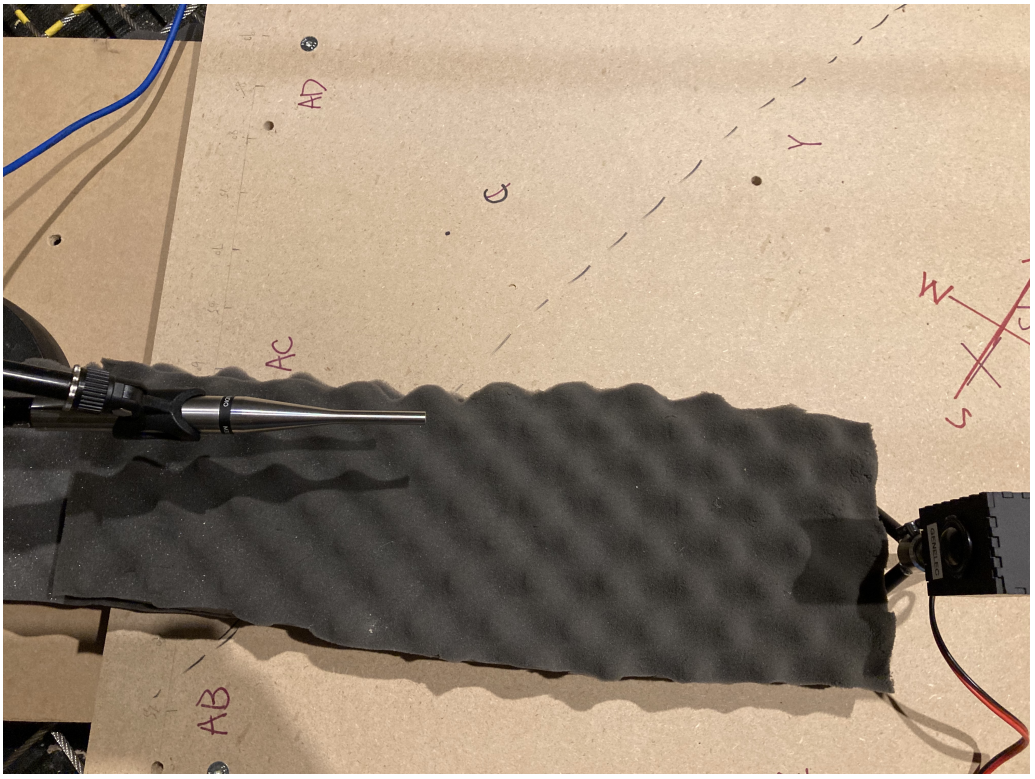

FIGURE A.42: A picture of tweeter response measurement. The M30 microphone was tilted slightly left to capture the responses.

FIGURE A.43: A picture of tweeter response measurement. The M30 microphone was tilted slightly right to capture the responses.

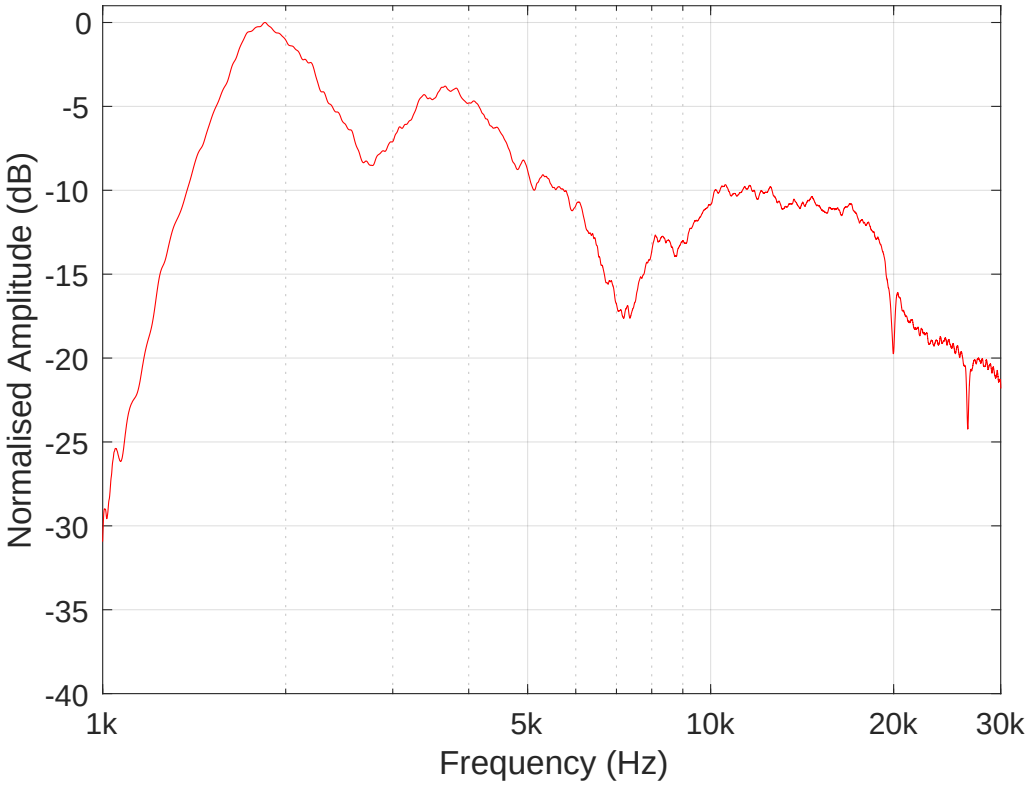

FIGURE A.44: A plot of the tweeter frequency response from 1 to 30 kHz.

Appendix B

Tables

B.1 Tables of forest IR measurement

Position	Distance (m)
S1-S2	3.73
S1-R1	8.65
S1-R2	10.32
S2-R1	9.00
S2-R2	7.91
R1-R2	6.88

Table B.1: Source and receiver layout measurement data. This table documents the distance between two sources and two receivers. For example, S1-S2 documents the distance between *Source 1* to *Source 2* in metres. The Data marked with a green background colour was noted using a tape measure since there is no line of sight.

Tree Name	Circumference (m)	S1 to T (m)	S2 to T (m)	R1 to T (m)	R2 to T (m)
A	0.825	16.9	15.79	8.9	8.7
B	1.14	13.83	11.9	7.77	4.06
C	1.36	12.19	9.19	9.67	2.78
D	1.095	12.12	8.71	11.32	4.62
E	0.77	12.78	9.11	13.35	6.92
F	1.34	8.9	5.16	11.26	6.38
G	1.315	8.13	4.74	8.84	3.98
H	1.285	9.16	7.39	4.85	1.67
I	1	14.28	13.45	5.7	8.4
J	1.425	9.1	8.49	1.85	4.72
K	1.125	6.34	4	6.11	3.72
L	0.635	8.65	5.25	13.45	9.64
M	1.365	5.17	1.74	10.55	8.25
N	1.06	4.19	0.9	8.18	6.71
O	1.31	5.81	5.71	2.91	5.58
P	0.64	12.46	13.17	4.17	10
Q	1.305	9.52	10.76	2.59	9.55
R	0.985	6.77	7.99	2.22	8.16
S	1.045	2.32	1.08	8.48	8.4
T	1.095	6.08	4.19	13.21	11.46
U	0.905	5.75	5.19	13.82	12.97
V	1.325	4.01	6.32	5.08	9.43
W	1.155	11.5	13.39	5.85	12.71
X	0.955	6.62	9.4	6.11	11.91
Y	0.52	2.18	5.83	8.54	11.58
Z	1.015	3.66	9.4	12.34	13.14
AA	1.065	6.88	8.22	15.58	16.15
AB	0.67	6.55	9.25	14.73	16.78
AC	1.07	5.69	9.05	13.01	15.95
AD	0.975	5.87	9.57	11.64	15.55
AE	0.85	8.6	12.09	10.12	15.72
AF	1.03	10.1	13.01	8.25	14.8
AG	1.465	12.89	15.9	10.83	17.57

TABLE B.2: Trees layout measurement data. Columns 3 to 6 marked the distance from a source or receiver to the edge of the tree. For example, *S1 to T* marked the distance from *Source 1* to each edge of the trees in metres. The Data marked with a green background colour was noted using a tape measure since there is no line of sight. The data marked with a yellow background colour was noted as an error measurement, which was found later in the conversion of the layout.

Tree	radius (m)	S1 to T (m)	S2 to T (m)	R1 to T (m)	R2 to T (m)
A	0.13	17.03	15.92	9.03	8.83
B	0.18	14.01	12.08	7.95	4.24
C	0.22	12.41	9.41	9.89	3.00
D	0.17	12.29	8.88	11.49	4.79
E	0.12	12.90	9.23	13.47	7.04
F	0.21	9.11	5.37	11.47	6.59
G	0.21	8.34	4.95	9.05	4.19
H	0.20	9.36	7.59	5.05	1.87
I	0.16	14.44	13.61	5.86	8.56
J	0.23	9.33	8.72	2.08	4.95
K	0.18	6.52	4.18	6.29	3.90
L	0.10	8.75	5.35	13.55	9.74
M	0.22	5.39	1.96	10.77	8.47
N	0.17	4.36	1.07	8.35	6.88
O	0.21	6.02	5.92	3.12	5.79
P	0.10	12.56	13.27	4.27	10.10
Q	0.21	9.73	10.97	2.80	9.76
R	0.16	6.93	8.15	2.38	8.32
S	0.17	2.49	1.25	8.65	8.57
T	0.17	6.25	4.36	13.38	11.63
U	0.14	5.89	5.33	13.96	13.11
V	0.21	4.22	6.53	5.29	9.64
W	0.18	11.68	13.57	6.03	12.89
X	0.15	6.77	9.55	6.26	12.06
Y	0.08	2.26	5.91	8.62	11.66
Z	0.16	3.82	9.56	12.50	13.30
AA	0.17	7.05	8.39	15.75	16.32
AB	0.11	6.66	9.36	14.84	16.89
AC	0.17	5.86	9.22	13.18	16.12
AD	0.16	6.03	9.73	11.80	15.71
AE	0.14	8.74	12.23	10.26	15.86
AF	0.16	10.26	13.17	8.41	14.96
AG	0.23	13.12	16.13	11.06	17.80

TABLE B.3: Converted layout measurement data. Columns 3 to 6 marked the distance from a source or receiver to the centre of the tree. For example, *S1 to T* marked the distance from *Source 1* to the centre of the trees in metres. The Data marked with a green background colour was noted using a tape measure since there is no line of sight. The data marked with a yellow background colour was noted as an error measurement, which was found in the conversion of the layout.

	X axis (m)	Y axis (m)
R1	0	0
R2	-4.52	-5.22
S1	-7.22	4.77
S2	-8.92	1.4
A	3.79	-8.21
B	-1.2	-7.87
C	-6.29	-7.61
D	-8.75	-7.46
E	-11.17	-7.54
F	-10.9	-3.59
G	-8.32	-3.5
H	-3.36	-3.76
I	4.03	-4.27
J	-0.86	-1.89
K	-6.07	-1.65
L	-13.47	-1.37
M	-10.68	0.63
N	-8.31	0.53
O	-3.09	0.39
P	4.26	-0.28
Q	2.05	1.87
R	-0.8	2.21
S	-8.28	2.5
T	-13.11	2.64
U	-13.13	4.71
V	-3.03	4.31
W	4.43	3.84
X	-0.63	6.19
Y	-5.72	6.42
Z	-10.57	6.63
AA	-13.08	8.67
AB	-10.34	10.64
AC	-7.77	10.58
AD	-5.36	10.48
AE	-0.38	10.17
AF	2.47	8.03
AG	4.85	9.86

TABLE B.4: Coordinates of the forest layout.

B.2 Tables of forest IR analysis

	DD of S1-T-R1	DD of S1-T-R2	DD of S2-T-R1	DD of S2-T-R2
A	17.41	15.54	15.95	16.84
B	13.31	7.93	11.03	8.41
C	13.64	5.08	10.29	4.49
D	15.14	6.77	11.38	5.77
E	17.73	9.63	13.71	8.37
F	11.94	5.39	7.85	4.06
G	8.74	2.21	5.00	1.23
H	5.77	0.92	3.65	1.56
I	11.65	12.68	10.47	14.26
J	2.75	3.95	1.79	5.75
K	4.16	0.10	1.47	0.17
L	13.65	8.17	9.90	7.18
M	7.50	3.53	3.72	2.51
N	4.06	0.92	0.42	0.04
O	0.49	1.49	0.04	3.80
P	8.18	12.34	8.54	15.46
Q	3.88	9.17	4.77	12.82
R	0.65	4.92	1.52	8.55
S	2.48	0.73	0.89	1.90
T	10.99	7.57	8.75	8.09
U	11.21	8.69	10.30	10.54
V	0.86	3.54	2.82	8.26
W	9.07	14.26	10.61	18.56
X	4.38	8.51	6.81	13.70
Y	2.24	3.61	5.54	9.67
Z	7.67	6.80	13.06	14.95
AA	14.15	13.05	15.14	16.80
AB	12.84	13.22	15.19	18.33
AC	10.39	11.66	13.40	17.43
AD	9.17	11.41	12.52	17.52
AE	10.34	14.27	13.48	20.17
AF	10.03	14.91	12.59	20.23
AG	15.54	20.61	18.20	26.03

TABLE B.5: Distance difference between source-receiver and source-tree-receiver. For example, *S1-T-R1* noted the distance difference between *Source 1 to Receiver 1* and *Source 1 to Tree to Receiver 1*.

Type of music	Reverberation time (seconds)
Organ	≥ 2.5
Romantic classical	1.8 – 2.2
Early classical	1.6 – 1.8
Opera	1.3 – 1.8
Chamber	1.4 – 1.7
Drama	0.7 – 1.0

TABLE B.6: Recommended reverberation time for an occupied room for different musical performances. From [54].

B.3 Tables of forest scale model IR measurement

Tree Name	Ideal Tube Diameter (mm)	Actual Tube Diameter (mm)	Error (%)
Y	16.56	15.87	4.17
L	20.22	20	1.09
P	20.38	20	1.86
AB	21.32	22.23	4.27
E	24.5	25	2.04
A	26.26	25	4.80
AE	27.06	28.57	5.58
U	28.8	28.57	0.80
X	30.4	28.57	6.02
AD	31.04	31.75	2.29
R	31.36	31.75	1.24
I	31.84	31.75	0.28
Z	32.3	31.75	1.70
AF	32.78	31.75	3.14
S	33.26	31.75	4.54
N	33.74	34.92	3.50
AA	33.9	34.92	3.01
AC	34.06	34.92	2.52
D	34.86	34.92	0.17
T	34.86	34.92	0.17
K	35.8	34.92	2.46
B	36.28	38.1	5.02
W	36.76	38.1	3.65
H	40.9	38.1	6.85
Q	41.54	41.27	0.65
O	41.7	41.27	1.03
G	41.86	41.27	1.41
V	42.18	41.27	2.16
F	42.66	41.27	3.26
C	43.3	41.27	4.69
M	43.44	44.45	2.33
J	45.36	44.45	2.01
AG	46.64	44.45	4.70

TABLE B.7: A table of the sizes of aluminium tubes selected for modelled tree trunks. The error of each modelled tree trunk is also listed in the table.

Appendix C

Lists of audio and MATLAB script

C.1 List of audio

C.1.1 Forest IRs recorded with M30 microphone

- Folder: Appendix - RealForest - IRaverage_M30
- Audio files are mono in 48 kHz 24-bit format:
    1. S1R1.wav
    2. S1R2.wav
    3. S2R1.wav
    4. S2R2.wav

C.1.2 Forest IRs recorded with SoundField microphone

- Folder: Appendix - RealForest - IRaverage_SF
- Audio files are four channels in 48 kHz 24-bit format:
    1. S1R1_SF.wav

2. S1R2_SF.wav
3. S2R1_SF.wav
4. S2R2_SF.wav

- four channel IRs are converted to mid-side stereo in 48 kHz 24-bit format:

1. S1R1_MS.wav
2. S1R2_MS.wav
3. S2R1_MS.wav
4. S2R2_MS.wav

C.1.3 Anechoic audio

- Folder: Appendix - RealForest - Audio
- Audio files are mono in 48 kHz 24-bit format (From [51]):

1. drum.wav
2. drumNote.wav
3. singing.wav
4. SingNote.wav

C.1.4 Auralisation generated with forest IRs mid-side stereo

- Folder: Appendix - RealForest - Auralisation
- Audio files are stereo in 48 kHz 24-bit format:

1. S1R1_drum.wav
2. S1R1_drumNote.wav
3. S1R1_singing.wav

4. S1R1_SingNote.wav
5. S1R2_drum.wav
6. S1R2_drumNote.wav
7. S1R2_singing.wav
8. S1R2_SingNote.wav
9. S2R1_drum.wav
10. S2R1_drumNote.wav
11. S2R1_singing.wav
12. S2R1_SingNote.wav
13. S2R2_drum.wav
14. S2R2_drumNote.wav
15. S2R2_singing.wav
16. S2R2_SingNote.wav

C.1.5 Scale model IRs recorded with M30 microphone

- Folder - Appendix - ScaleForest - ScaleModelIR
- Audio files are mono in 96 kHz 24-bit format:

1. S1R1_ScaleModel.wav
2. S1R2_ScaleModel.wav
3. S2R1_ScaleModel.wav
4. S2R2_ScaleModel.wav

C.1.6 Scale model IRs stretched 10 times longer

- Folder - Appendix - ScaleForest - StrechIR

- Audio files are mono in 96 kHz 24-bit format:

  1. S1R1.wav
  2. S1R2.wav
  3. S2R1.wav
  4. S2R2.wav

C.1.7 Auralisation generated with scale model stretched IRs

- Folder - Appendix - ScaleForest - AuralisationScale
- Audio files are mono in 96 kHz 24-bit format:

  1. S1R1_drum_Scale.wav
  2. S1R1_singing_Scale.wav
  3. S1R2_drum_Scale.wav
  4. S1R2_singing_Scale.wav
  5. S2R1_drum_Scale.wav
  6. S2R1_singing_Scale.wav
  7. S2R2_drum_Scale.wav
  8. S2R2_singing_Scale.wav

C.2 List of MATLAB script

C.2.1 Generate real forest results

- Folder: Appendix - RealForest
  - Generate M30 IRs

1. callM30.m
2. M30AverageIR.m
3. deconvolve.m

– Generate SoundField IRs and auralisation

1. callSF.m
2. SFaverageIR.m
3. deconvolve.m
4. convertBFormToMSStereo.m
5. auralisation.m
6. convolutionIR.m

– Generate M30 waveform results

1. waveformS1R1.m
2. waveformS1R2.m
3. waveformS2R1.m
4. waveformS2R2.m
5. printFigureToPdf.m

– Generate spectrogram results

1. callSpectrogram.m
2. spectrogramComplete.m
3. printFigureToPdf.m

– Generate ISO 3382 acoustic parameters results

1. callAPcompare.m
2. APcompare.m
3. acousticParams.m
4. bandFilter.m
5. energyCalc.m
6. intlinear.m

7. parseArgs.m
8. reverberationCalc.m
9. subaxis.m
10. printFigureToPdf.m

- Generate Schroeder curve results
  1. Tvalue.m
  2. curveCompare.m
  3. printFigureToPdf.m
- Geberate SIRR analysis results
  1. callSIRR.m
  2. sirranalysis_Azimuth.m
  3. printFigureToPdf.m
- Generate spectrum results
  1. callSpectrum.m
  2. dBFS.m
  3. printFigureToPdf.m

C.2.2 Generate forest scale model results

- Folder - Appendix - ScaleForest
  - Generate scale model IR results
    1. callAverageIR.m
    2. AverageIR.m
  - Generate scale model stretched IR auralisation
    1. callAuralisation.m
    2. auralisation.m
    3. convolutionIR.m

- Generate waveform results
  1. S1R1waveform.m
  2. S1R2waveform.m
  3. S2R1waveform.m
  4. S2R2waveform.m
  5. printFigureToPdf.m
- Generate spectrogram results
  1. callSpectrogram.m
  2. spectrogramComplete.m
  3. printFigureToPdf.m
- Generate ISO 3382 acoustic parameters results
  1. callAPcompare.m
  2. APcompare.m
  3. acousticParams.m
  4. bandFilter.m
  5. energyCalc.m
  6. intlinear.m
  7. parseArgs.m
  8. reverberationCalc.m
  9. subaxis.m
  10. printFigureToPdf.m
- Generate Schroeder curve results
  1. Tvalue.m
  2. curveCompare.m
  3. printFigureToPdf.m
- Generate spectrum results
  1. callSpectrum.m

2. dBFS.m
3. printFigureToPdf.m

C.2.3 Generate sound attenuation in a forest and an open field results

- Folder - SPLOpenForest
- Generate SPL in both environments at different distances (A-weighting)
    1. SPLAdistance.m
    2. printFigureToPdf.m
- Generate SPL in both environments in different octave bands
    1. SPLoctave.m
    2. printFigureToPdf.m

References

[1] F. Stevens, D. T. Murphy, L. Savioja, and V. Välimäki, "Modeling sparsely reflecting outdoor acoustic scenes using the waveguide web," *IEEE/ACM Transactions on Audio, Speech, and Language Processing*, vol. 25, no. 8, pp. 1566–1578, 2017.

[2] C.-F. Fang and D.-L. Ling, "Investigation of the noise reduction provided by tree belts," *Landscape and urban planning*, vol. 63, no. 4, pp. 187–195, 2003.

[3] S. B. Shelley, D. T. Murphy, and A. J. Chadwick, "B-format acoustic impulse response measurement and analysis in the forest at koli national park, finland," in *Proceedings of the 16th International Conference on Digital Audio Effects (DAFx13)*. York, 2013, pp. 351–355.

[4] P. Chobeau, "Modeling of sound propagation in forests using the transmission line matrix method," Ph.D. dissertation, Université du Maine, 2014.

[5] K. Spratt and J. S. Abel, "A digital reverberator modeled after the scattering of acoustic waves by trees in a forest," in *Audio Engineering Society Convention 125*. Audio Engineering Society, 2008.

[6] J. H. Rindel, "Modelling in auditorium acoustics. from ripple tank and scale models to computer simulations," *Revista de Acústica*, vol. 33, no. 3-4, pp. 31–35, 2002.

[7] M. Ismail and D. Oldham, "A scale model investigation of sound reflection from building façades," *Applied Acoustics*, vol. 66, no. 2, pp. 123–147, 2005.

[8] J. Y. Jeon, J. K. Ryu, Y. H. Kim, and S.-i. Sato, "Influence of absorption properties of materials on the accuracy of simulated acoustical measures in 1: 10 scale model test," *Applied Acoustics*, vol. 70, no. 4, pp. 615–625, 2009.

[9] T. J. Cox, B. M. Fazenda, and S. E. Greaney, "Using scale modelling to assess the prehistoric acoustics of stonehenge," *Journal of Archaeological Science*, vol. 122, p. 105218, 2020.

[10] H. Kuttruff and E. Mommertz, "Room acoustics," in *Handbook of engineering acoustics*. Springer, 2012, pp. 239–267.

[11] ISO3382-1, *3382, Acoustics–Measurement of room acoustic parameters–Part 1: Performance spaces, 2009*. ISO, 2009.

[12] F. Stevens, "Strategies for environmental sound measurement, modelling, and evaluation," Ph.D. dissertation, University of York, 2018. [Online]. Available: http://etheses.whiterose.ac.uk/22661/

[13] D. M. Howard and J. Angus, *Acoustics and psychoacoustics*. Taylor & Francis, 2017.

[14] B. F. Day, "A tenth-scale model audience," *Applied Acoustics*, vol. 1, no. 2, pp. 121–135, 1968.

[15] J. S. Abel, N. J. Bryan, P. P. Huang, M. Kolar, and B. V. Pentcheva, "Estimating room impulse responses from recorded balloon pops," in *Audio Engineering Society Convention 129*. Audio Engineering Society, 2010.

[16] H.-S. Yang, J. Kang, C. Cheal, T. V. Renterghem, and D. Botteldooren, "Quantifying scattered sound energy from a single tree by means of reverberation time," *The Journal of the Acoustical Society of America*, vol. 134, no. 1, pp. 264–274, 2013.

[17] F. Stevens, "Source localisation using early reflection information," Master's thesis, University of York, 2015.

[18] J. Vanderkooy, "Aspects of mls measuring systems," *Journal of the Audio Engineering Society*, vol. 42, no. 4, pp. 219–231, 1994.

[19] A. Farina, "Simultaneous measurement of impulse response and distortion with a swept-sine technique," in *Audio engineering society convention 108*. Audio Engineering Society, 2000.

[20] ——, "Advancements in impulse response measurements by sine sweeps," in *Audio engineering society convention 122*. Audio Engineering Society, 2007.

[21] F. Stevens and D. T. Murphy, "Acoustic source localisation in an urban environment using early reflection information," *Proc. EuroNoise 2015*, pp. 257–262, 2015.

[22] J. Merimaa and V. Pulkki, "Spatial impulse response rendering i: Analysis and synthesis," *Journal of the Audio Engineering Society*, vol. 53, no. 12, pp. 1115–1127, 2005.

[23] C. F. Eyring, "Jungle acoustics," *The Journal of the Acoustical Society of America*, vol. 18, no. 2, pp. 257–270, 1946.

[24] T. Embleton, "Sound propagation in homogeneous deciduous and evergreen woods," *The Journal of the Acoustical Society of America*, vol. 35, no. 8, pp. 1119–1125, 1963.

[25] D. Aylor, "Noise reduction by vegetation and ground," *The Journal of the Acoustical Society of America*, vol. 51, no. 1B, pp. 197–205, 1972.

[26] D. I. Cook and D. F. Van Haverbeke, "Trees and shrubs for noise abatement," *[s.l.]*, 1971.

[27] F. Fricke, "Sound attenuation in forests," *Journal of Sound and Vibration*, vol. 92, no. 1, pp. 149–158, 1984.

[28] M. A. Price, K. Attenborough, and N. W. Heap, "Sound attenuation through trees: Measurements and models," *The Journal of the Acoustical Society of America*, vol. 84, no. 5, pp. 1836–1844, 1988.

[29] G. Reethof and G. Heisler, "Trees and forests for noise abatement and visual screening." *USDA Forest Service General Technical Report NE*, 1976.

[30] R. Bullen and F. Fricke, "Sound propagation through vegetation," *Journal of sound and Vibration*, vol. 80, no. 1, pp. 11–23, 1982.

[31] J. Kragh, "Road traffic noise attenuation by belts of trees," *Journal of Sound and Vibration*, vol. 74, no. 2, pp. 235–241, 1981.

[32] F. A. Everest and K. C. Pohlmann, *Master handbook of acoustics*. McGraw-Hill Education, 2022.

[33] H. Sakai, S. Shibata, and Y. Ando, "Orthogonal acoustical factors of a sound field in a bamboo forest," *The Journal of the Acoustical Society of America*, vol. 109, no. 6, pp. 2824–2830, 2001.

[34] M. Padgham, "Reverberation and frequency attenuation in forests—implications for acoustic communication in animals," *The Journal of the Acoustical Society of America*, vol. 115, no. 1, pp. 402–410, 2004.

[35] M. Li, T. Van Renterghem, J. Kang, K. Verheyen, and D. Botteldooren, "Sound absorption by tree bark," *Applied Acoustics*, vol. 165, p. 107328, 2020.

[36] P. H. Raven, R. F. Evert, S. E. Eichhorn *et al.*, *Biology of plants*. Macmillan, 2005.

[37] G. Reethof, L. Frank, and O. McDaniel, *Absorption of sound by tree bark*. US Department of Agriculture, Forest Service, Northeastern Forest Experiment, 1976, vol. 341.

[38] S. Sağlam, F. Güzelçimen, D. Bingöl, U. Y. Özkan, and B. Ekici, "An evaluation on acoustic behavior of untreated tree trunks depending on bark physical properties and fiber cell structure," *Journal of Natural Fibers*, vol. 19, no. 4, pp. 1507–1521, 2022.

[39] C. M. Harris, "Absorption of sound in air versus humidity and temperature," *The Journal of the Acoustical Society of America*, vol. 40, no. 1, pp. 148–159, 1966.

[40] M. A. W. Price, *Sound propagation in woodland*. Open University (United Kingdom), 1986.

[41] P. M. Morse, A. S. of America, and A. I. of Physics, *Vibration and sound*. McGraw-Hill New York, 1948, vol. 2.

[42] J. Brooks-Park, "Investigating cylinder scattering solutions for frequency dependant scattering nodes," Master's thesis, University of York, 2021.

[43] F. Spandöck, "Akustische modellversuche," *Annalen der Physik*, vol. 412, no. 4, pp. 345–360, 1934.

[44] A. Burd, "Acoustic modelling–design tool or research project? chapter 7 in "auditorium acoustics" r. mackenzie," 1975.

[45] J.-D. Polack, X. Meynial, G. Dodd, and A. H. Marshall, "The midas system for all scale room acoustics measurements," in *Audio Engineering Society Conference: 11th International Conference: Test & Measurement*. Audio Engineering Society, 1992.

[46] M. Barron and C. Chinoy, "1: 50 scale acoustic models for objective testing of auditoria," *Applied Acoustics*, vol. 12, no. 5, pp. 361–375, 1979.

[47] T. Cox, "How reverberant was stonehenge?" 2020, accessed: 2023-05-25. [Online]. Available: http://trevorcox.me/how-reverberant-was-stonehenge

[48] T. Embleton, "Scattering by an array of cylinders as a function of surface impedance," *The Journal of the Acoustical Society of America*, vol. 40, no. 3, pp. 667–670, 1966.

[49] K. B. Rasmussen, "How to take absorptive surfaces into account when designing outdoor sound reinforcement systems," in *Audio Engineering Society Convention 100*. Audio Engineering Society, 1996.

[50] F. Stevens, "Creswell crags - recording report," 2016.

[51] D. Murphy and F. Stevens, "Ir data - heslington church," 2019, accessed: 2023-07-18. [Online]. Available: https://www.openair.hosted.york.ac.uk/?page_id=508

[52] A. Kuusinen and T. Lokki, "Wheel of concert hall acoustics," *Acta Acustica united with Acustica*, vol. 103, no. 2, pp. 185–188, 2017.

[53] C. Cooper, "The sound of debate in georgian england: Auralising the house of commons," *Parliamentary History*, vol. 38, no. 1, pp. 60–73, 2019.

[54] M. Barron, *Auditorium acoustics and architectural design*. Routledge, 2009.